Utilizing process waters from conversion processes based on regenerative resources for microbial production of platform chemicals

Dissertation to obtain the doctoral degree of
Natural Sciences (Dr. rer. nat.)

Faculty of Natural Sciences
University of Hohenheim

Institute of Food Science and Biotechnology

submitted by
Manuel Josef Merkel

from *Gernsbach*
2023

Dean: Prof. Dr. Jan Frank

1st reviewer: Prof. Dr.-Ing. Rudolf Hausmann
2nd reviewer: Prof. Dr.-Ing. Marius Henkel
3rd examiner: Prof. Dr.-Ing. Reinhard Kohlus

Submitted on: 15.11.2023
Oral examination on: 24.06.2024

"Nothing in life is to be feared, it is only to be understood. Now is the time to understand more, so that we may fear less."

Marie Curie

Acknowledgements

I would like to thank the following people who accompanied me during my doctoral studies for their guidance and support:

First, my greatest gratitude goes to **Prof. Dr.-Ing. Rudolf Hausmann**, my doctoral supervisor for the opportunity to be part of his research group. I would like to thank him for his excellent scientific supervision, the fruitful discussions, and his support.

Furthermore, I would like to thank our Postdocs **Dr.-Ing. Marius Henkel**, who recently was appointed to the **Professorship of Cellular Agriculture** at the **Technical University of Munich**, and **Dr. Lars Lilge** for sharing their expertise in designing experiments and evaluating data, for their advices and words of encouragement in moments where it was needed.

I also would like to thank my dear **colleagues** at the Department of Bioprocess Engineering, for the mutual support, the friendly atmosphere, and the fun times together in and outside of the lab: Dr. Philipp Noll, M. Sc. Till Hennecke, M. Sc. Peter Klausmann, Dr. Mareen Hoffmann, M. Sc. Chantal Treinen, M. Sc. Dirk Kiefer, M. Sc. Maliheh Vahidinasab, M. Sc. Lennart Biermann, M. Sc. Holger Dittmann, M. Sc. Jakob Grether, Eike Grunwaldt and Dipl.-Biol. Anja Sander.

Moreover, I am very grateful for all the motivated **students** that were working on this research project under my supervision to complete their project work, internship, bachelor thesis or master thesis: M. Sc. Maximillian Bolle, M. Sc. Vinayak Chabria, B. Sc. Jonas Flierl, B. Sc. Alexander Martens, B. Sc. Stefanie Konz, B. Sc. Lorena Colotta, M. Sc. Abhilash Konda, B. Sc. Maximillian Krämer.

My gratitude also goes to **Prof. Dr. Thomas Schwartz** for their participation as member of my Thesis Advisory Committee and their recommendations and support.

It further goes to the **project partners** and **academic partners** for the trusting and productive cooperation: Prof. Dr. Nicolaus Dahmen, Dr. Axel Funke, Dr.-Ing. Katrin Ochsenreither, M. Sc. Christin Kubisch, M. Sc. Aline Kövilein, Prof. Dr. rer. Nat. Christoph Syldatk, Prof. Dr. Bastian Blombach, M. Sc. Marc Schmollack

I would also like to thank **Prof. Dr. Thomas Rausch**, **Dr. Tanja Peskan-Berghoefer** and **Hanni Truong** as well as the other **members of the graduate program BBW ForWerts** for organizing and participating in all the interesting and fun workshops and courses.

Finally, I would like to thank my **family and friends** for their continuous support and encouragement and sometimes for necessary, but fun distractions.

List of peer-reviewed articles and scientific contributions

Original research articles

Merkel, M.; Kiefer, D.; Schmollack, M.; Blombach, B.; Lilge, L.; Henkel, M.; Hausmann, R. (2022): Acetate-based production of itaconic acid with *Corynebacterium glutamicum* using an integrated pH-coupled feeding control. In: Bioresource Technology, S. 126994. DOI: 10.1016/j.biortech.2022.126994.

Merkel, M.; Noll, P.; Lilge, L.; Hausmann, R.; Henkel, M. (2023): Design and evaluation of a 3D-printed, lab-scale perfusion bioreactor for novel biotechnological applications. In: Biotechnology Journal, e2200554. DOI: 10.1002/biot.202200554.

Kiefer, D.; **Merkel, M.**; Lilge, L.; Hausmann, R.; Henkel, M. (2021): High cell density cultivation of *Corynebacterium glutamicum* on bio-based lignocellulosic acetate using pH-coupled online feeding control. In: Bioresource Technology 340, S. 125666. DOI: 10.1016/j.biortech.2021.125666.

Schmollack, Marc; Werner, Felix; Huber, Janine; Kiefer, Dirk; **Merkel, Manuel**; Hausmann, Rudolf et al. (2022): Metabolic engineering of *Corynebacterium glutamicum* for acetate-based itaconic acid production. In: Biotechnology for Biofuels and Bioproducts 15 (1), S. 139. DOI: 10.1186/s13068-022-02238-3.

Reviews

Kiefer, D., **Merkel, M.**, Lilge, L., Henkel, M., Hausmann, R. (2021): From acetate to bio-based products: Underexploited potential for industrial biotechnology. Trends Biotechnol. 39 (4), 397–411.

Poster presentations

Merkel, M., Arnold, S., Henkel, M., Hausmann, R. Towards the utilization of process waters from thermochemical conversion for continuous production of biosurfactants. Konferenzbeitrag (Poster), Biosurfactants International Conference, September 2019, Stuttgart.

Merkel, M., Henkel, M., Hausmann, R. Utilizing process waters from thermochemical conversion processes for microbial production. Konferenzbeitrag (Poster), DECHEMA Himmelfahrtstagung, Mai 2019, Hamburg.

Author contribution statement

Parts of this cumulative doctoral thesis are based on peer-reviewed research articles. These articles are based on work accompanying this dissertation between January 2019 and June 2022. A list of published papers related to this work with the respective authors contribution, is provided below. Parts of this work have been previously published with the knowledge and approval of the supervisor Prof. Dr.-Ing. Rudolf Hausmann. Parts of the scientific work shown in this thesis was carried out in cooperation with co-authors.

Chapter 2.1: 1st publication

Merkel, M.; Kiefer, D.; Schmollack, M.; Blombach, B.; Lilge, L.; Henkel, M.; Hausmann, R. (2022): Acetate-based production of itaconic acid with *Corynebacterium glutamicum* using an integrated pH-coupled feeding control. In: Bioresource Technology, S. 126994. DOI: 10.1016/j.biortech.2022.126994.

MM: Conceptualization, Methodology, Formal analysis, Validation, Investigation, Writing – original draft, Visualization. **DK**: Conceptualization, Methodology, Formal analysis, Investigation, Writing – review & editing. **MS**: Conceptualization, Methodology, Investigation, Writing – review & editing. **BB**: Conceptualization, Resources, Writing – review & editing, Supervision, Project administration, Funding acquisition. **LL**: Conceptualization, Validation, Formal analysis, Writing – review & editing. **MH**: Conceptualization, Validation, Methodology, Formal analysis, Writing – review & editing, Supervision, Funding acquisition. **RH**: Conceptualization, Validation, Formal analysis, Writing – review & editing, Supervision, Project administration, Funding acquisition.

Place, date

Signature of the supervisor

Chapter 2.2: 2nd publication

Merkel, M.; Noll, P.; Lilge, L.; Hausmann, R.; Henkel, M. (2023): Design and evaluation of a 3D-printed, lab-scale perfusion bioreactor for novel biotechnological applications. In: Biotechnology Journal, e2200554. DOI: 10.1002/biot.202200554.

MM: Conceptualization, Methodology, Formal analysis, Validation, Investigation, Writing - Original Draft, Visualization. **PN**: Conceptualization, Methodology, Formal analysis, Investigation, Review & Editing. **LL**: Conceptualization, Validation, Formal analysis, Review & Editing. **RH**: Conceptualization, Validation, Formal analysis, Review & Editing, Supervision, Funding acquisition. **MH**: Conceptualization, Validation, Methodology, Formal analysis, Review & Editing, Supervision, Project administration, Funding acquisition.

Place, date

Signature of the supervisor

Abstract

A future bioeconomy relying on biotechnological production processes makes it necessary to find a replacement for sugars as microbial carbon source to prevent ethically questionable competition with the food and feed sector. An attractive alternative is acetic acid, as it is inexpensive, available in high quantities and utilized equally well as glucose by some bacteria. Still, the application of acetic acid as sole carbon source in bioproduction processes offers several challenges. In its protonated form acetic acid leads to medium acidification, when applied in high concentrations, while as salt it leads to salinization causing osmotic stress for the production organisms. As such, established process strategies are difficult to apply with acetic acid, making specialized strategies necessary for production processes.

Therefore, an efficient fed-batch strategy was developed and is presented in the **1st publication** utilizing acetic acid as sole carbon source for production of itaconic acid with a genetically modified strain *C. glutamicum* ICD^{R453C} (pEKEx2-*malE*cad$_{opt}$). An earlier published pH-coupled feeding strategy for addition of glacial acetic acid was adapted to obtain the nitrogen limited conditions necessary for itaconic acid production. It was found that the consumption of ammonia at high carbon to nitrogen ratios of the feeds, which was necessary to achieve nitrogen limited conditions, caused acidification of the medium. This countered the increase of pH-value caused by acetic acid consumption and led to early acetate depletion. Thus, an additional DO-coupled feeding of sodium acetate was started once acetic acid in the medium was depleted. Sodium acetate did not directly effect the pH-value, but its consumption again led to an increase of the pH-value and continuation of the pH-coupled feeding. With this combined strategy an itaconic acid production process was developed with separate growth and production phases. In the end a titer of 29.2 g/L and a volumetric productivity of $0.63\,\mathrm{g\,L^{-1}h^{-1}}$ were achieved. These were comparable to bacterial production processes using glucose as sole carbon source, with the only drawback being a lower yield. Still, the results demonstrated that *C. glutamicum* is suited as production organism on acetate as alternative carbon source.

Another challenge is, that biobased acetic acid, for example produced by thermochemical conversion of lignocellulose, is often available only in dilute concentrations up to 50 g/L or in complex solutions containing potentially harmful substances. Therefore, conventional fed-batch processes are not applicable, because of strong dilution of the product and accumulation of inhibitors. Perfusion bioreactors can be a solution to these problems. They allow application of dilute substrate concentrations, as the bacteria are retained in the reactor. Furthermore, the continuous flow through the system prevents accumulation

of inhibitors.

Thus, the **2nd publication** presented a newly developed, lab scale perfusion bioreactor, that was manufactured via 3D-printing using the fused filament fabrication method. Hydrophilic flat sheet membranes in the main bioreactor module were used for cell retention. A circulation flow was applied for diffusive oxygen supply via an oxygen transfer module that contained hydrophobic membranes and for temperature control via a heat exchanger module. The bioreactor system was characterized regarding oxygen transfer rates and mixing time. Finally, a proof-of-concept cultivation with *C. glutamicum* ATCC13032 on glucose utilizing a dilute feed solution resulted in 18.4 g/L biomass after 53 h of cultivation and a maximum specific growth rate of 0.34 1/h. Until the end of the process no membrane blockage occurred. This showed that the reactor system was suited for bacterial cultivation as well as for application of dilute substrates.

To sum it up, it was shown that acetic acid can be efficiently used as alternative carbon source for bioproduction with *C. glutamicum* as model organism. Still, in case of itaconic acid production further genetic modifications are necessary in future works to increase the product yield. Regarding process strategies for utilization of biobased acetic acid in dilute solutions, a new 3D-printed perfusion bioreactor was successfully developed, and its function proven. Future works can focus on the application of the perfusion system for production processes and evaluate its suitability for bioprocesses with sustainably produced acetic acid

Zusammenfassung

Für eine zukünftige Bioökonomie, die sich auf biotechnologische Prozesse für die Herstellung von Produkten verlässt, ist es notwendig einen Ersatz für Zucker als mikrobielle Kohlenstoffquelle zu finden, um eine ethisch fragwürdige Konkurrenz zu Lebens- und Futtermittel zu vermeiden. Essigsäure ist dabei eine attraktive Alternative, da sie günstig ist, in großen Mengen verfügbar und bei manchen Bakterien ähnlich gut verstoffwechselt wird, wie Glucose. Dennoch bietet die Anwendung von Essigsäure als einzige Kohlenstoffquelle einige Herausforderungenin für Bioprozesse. In ihrer protonierten Form führt Essigsäure zur Versauerung des Mediums. Als Salz führt sie aufgrund der Zufuhr des nicht-verstoffwechselten Co-Ions zu einer Versalzung, die osmotischen Stress bei den Bakterien auslöst. Dadurch lassen sich konventionelle Prozessstrategien nur schwer anwenden. Stattdessen müssen spezialisierte Prozessführungsstrategien für Essigsäure entwickelt werden.

Deswegen war das Ziel der **ersten Publikation**, einen Fed-Batch Prozess zu entwickeln, mit dem eine effiziente Umwandlung von Essigsäure durch den genetisch modifizierten Stamm *C. glutamicum* ICD^{R453C} (pEKEx2-*malE*cad$_{opt}$) zu Itakonsäure erreicht werden konnte. Mit diesem Stamm war eine Limitierung an Stickstoff für die Produktion von Itakonsäure notwendig, weshalb ein bereits veröffentlichter pH-gekoppelter Fed-Batch Prozess an diese Bedingung angepasst wurde. Dabei trat das Problem auf, dass bei hohen Kohlenstoff- zu Stickstoffverhältnissen der Feeds, wie sie zum Erreichen der Stickstofflimitierung notwendig waren, der Verbrauch von Ammoniak durch die Bakterien zu einer Versäuerung des Mediums führte. Diese wirkte dem pH-Anstieg durch den Verbrauch von Essigsäure entgegen und resultierte in einen frühen Essigsäuremangel. Als Lösung wurde der Prozess um eine zusätzliche an den pO2 gekoppelte Zufütterungsstrategie für Natriumacetat erweitert. Natriumacetat beeinflusst bei der Zugabe den pH-Wert nicht direkt. Stattdessen führt erst der erneute Verbrauch von Acetat zu einem pH-Anstieg und zu einer Fortsetzung der pH-gekoppelten Zufütterung von Essigsäure. Mit dieser kombinierten Zufütterungsstrategie konnte ein Prozess für die Itakonsäureproduktion entwickelt werden, bei dem Biomassezunahme und Itakonsäureproduktion zeitlich getrennt werden konnten. Es wurden ein Titer von 29.2 g/L und eine volumetrische Produktivität von 0.63 g $L^{-1}h^{-1}$ erreicht. Diese waren vergleichbar mit bakteriellen Produktionsprozessen mit Glucose als Kohlenstoffquelle, wobei der einzige Nachteil ein geringerer Ertrag war. Die Ergebnisse belegten, dass *C. glutamicum* ein geeigneter Modellorganismus für die Produktion mit Essigsäure als einziger Kohlenstoffquelle ist.

Eine weitere Herausforderung ist die Verfügbarkeit von biobasierter Essigsäure zumeist

in Lösungen mit geringen Konzentrationen oder in komplexen Lösungen mit potenziell schädlichen Komponenten. Die geringe Konzentration führt bei konventionellen Fed-Batch Prozessen zu einer starken Verdünnung des Produkts sowie zu einer Akkumulation von Inhibitoren, weshalb sie nicht geeignet sind. Eine mögliche Lösung bieten Perfusionsbioreaktoren. Diese erlauben die Verwendung von geringen Substratkonzentrationen, da die Zellen im Reaktor zurückgehalten werden und bei erhöhten Flussraten nicht ausgeschwemmt werden. Zudem vermeidet der kontinuierlich Feed-Strom die Akkumulation der Inhibitoren.

Deswegen wurde in der **zweiten Veröffentlichung** ein Perfusionsbioreaktor entwickelt, der mittels des additiven Herstellungsverfahrens *fused filament fabrication* hergestellt wurde. Hierbei wurden hydrophile Membranscheiben im Hauptbioreaktormodul für die Zellrückhaltung eingesetzt. Ein Kreislaufstrom wurde für die diffusive Sauerstoffversorgung mittels hydrophober Membranen in einem Sauerstoff-Transfer Modul sowie für die Temperaturkontrolle mit einem Wärmetauscher-Modul angelegt. Das Bioreaktorsystem wurde anhand der Sauerstofftransferrate sowie anhand der Mischzeit charakterisiert. Zuletzt wurde eine Kultivierung von *C. glutamicum* ATCC13032 mit Glucose sowie unter Verwendung einer niedrigkonzentrierten Feedlösung als Proof-of-Concept durchgeführt. Diese resultierte in eine maximale Biomassekonzentration von 18.4 g/L nach 53 h und einer maximalen spezifischen Wachstumsrate von 0.34 1/h. Bis zum Ende des Prozesses trat keine Blockade der Membran ein. Damit wurde gezeigt, dass sich das Reaktorsystem für die Kultivierung von Bakterien sowie für die Anwendung dünner Substrate eignet.

Zusammengefasst wurde gezeigt, dass Essigsäure effizient als alternative Kohlenstoffquelle für die mikrobielle Produktion mit *C. glutamicum* als Modellorganismus eingesetzt werden kann. Dennoch sind für die Produktion von Itakonsäure weitere genetische Anpassungen nötig, um den Ertrag zu erhöhen. Für die Biokonversion von biobasierter, niedrigkonzentrierter Essigsäure wurde erfolgreich ein 3D-gedruckter Perfusionsbioreaktor entwickelt und seine Funktion bewiesen. Zukünftige Arbeiten können sich auf die Anwendung des Perfusionssystems für Produktionsprozesse fokussieren und dessen Eignung für Bioprozesse zum Beispiel mit Lignocellulose-basierter Essigsäure evaluieren.

Table of Contents

List of Figures

List of Tables

Abbreviations and symbols

AAB	Acetic acid bacteria
ABS	Acrylonitrile butadiene styrene
ACN	Aconitase
ACS	Acetyl-CoA synthetase
ADH	alcohol dehydrogenase
AK	Acetate-kinase
ALDH	aldehyde dehydrogenase
A. pasteurianus	*Acetobacter pasteurianus*
AR	Acid resistance systems
ATF	Alternating tangential flow
ATP	Adenosine triphosphate
B. cereus	*Bacillus cereus*
CAD	Computer-aided design
CH_3	Methyl
C. necator	*Cupriavidus necator*
C-N ratio	Molar carbon to nitrogen ratio
C. glutamicum	*Corynebacterium glutamicum*
CO	Carbon monoxide
CO_2	Carbon dioxide
Co/Fe-S Pr	Corrinoid iron-sulphur protein
CS	Citrate synthase
CoA	Coenzyme A
CPE	Co-polyester
CRP	Catabolite repressor protein
DNA	Deoxyribonucleic acid
DO	Dissolved oxygen concentration
E. coli	*Escherichia coli*
EU	European union
FBPase	Fructose bisphosphatase
GPI	Glucose-6-phosphate isomerase
GRAS	Generally regarded as save
GTP	Guanosine triphosphate
$[H]$	Reduction equivalent
H_2	Hydrogen
H_2O	Wasser
H. bluephagensis	*Halomonas bluephagensis*

ICD	Isocitrate dehydrogenase
ICL	Isocitrate lyase
MBR	Membrane bioreactor
ME	Malic enzyme
MES	Microbial electrosynthesis
MS	Malate synthase
NAD^+/NADH	Nicotinamide adenine dinucleotide
$NADP^+$/NADPH	Nicotinamide adenine dinucleotide phosphate
O_2	Oxygen
OD	Optical density
ODx	Oxaloacetate decarboxylase
P	Phosphate
PCR	Polymerase chain reaction
PEP	Phophoenol pyruvate
PEPCk	Phosphoenolpyruvate carboxykinase
PEPS	Phosphoenolpyruvate synthase
PES	Polyethersulfone
PHA	Polyhydroxyalkanoates
PHB	polyhydroxy butyrate
PP	Pyrophosphate
PPase	Pyrophosphatase
P. putida	*Pseudomonas putida*
Pt	Platin
PTA	Phosphotransacetylase
PTFE	Polytetrafluoroethylene
PVDF	Polyvinylidene fluoride
R	Recycle ratio
RpoS	Sigma factor
SCACT	Succinyl-CoA-acetate-CoA transferase
TCA	Tricarboxylic acid
THF	tetrahydrofolic acid
WJP	Wood-Ljungdahl pathway
$Y_{P,S}$	Product yield
μ_{max}	Maximum specific growth rate

Chapter

1 Introduction

1.1 General introduction

During the last years global challenges like the supply security of finite resources, the climate change, as well as global hunger and nutrition have increased the awareness for the importance of environmental protection as well as sustainable approaches for production and energy generation (Dieken et al. 2020). This enticed the EU and its member states to declare research strategies related to bioeconomy, with the goal to reduce carbon dioxide emissions and usage of fossil resources by using biomass as feedstock (Bell et al. 2018; Dieken et al. 2020). Biotechnology plays an important role on the way to a biobased economy. Products like plastics or certain chemicals that normally are produced solely from non-renewable resources, can at least partially be replaced by more sustainable biotechnological production routes with lesser CO_2-emissions that rely on renewable resources (Lokko et al. 2018). Still, many biotechnological production processes rely on sugars like glucose or sucrose won from starch-rich plants and molasses as substrate for production (Wendisch et al. 2016). At the same time, global food production needs to be doubled until 2050 to be able to satisfy the nutritional needs of the growing world population according to prognoses (Woźniak et al. 2021). This sets the utilization of plants, that are of nutritional value, for conversion into technical products into direct competition to their use for human nutrition or animal feed and causes an ethical problem. Therefore, it is important to find alternative substrates that do not compete with food to achieve a biobased economy. One example for such a substrate is acetic acid (from now on called acetate, since most often it exists in its dissociated form in the aqueous solutions used in this study).

Acetate was estimated to be produced at high quantities of 17.88 million tons in 2023 (Mordor Intelligence 2023) and is additionally rather inexpensive (461 – 1019 $ per ton in 2023, Chemanalyst 2023, with the prices decreasing again after a spike caused by the recent crises). Currently, it is still mostly produced from fossil resources. The dominant production route is carbonylation of methanol using syngas and metal-organic catalysts based on cobalt or iridium (Martín-Espejo et al. 2022). The carbonylation process takes place at a temperature between 150 – 300°C under elevated pressure of 60 bar. Another petrochemical production route is direct oxidation of ethane. Besides petrochemical production routes, biobased routes for sustainable production of acetate also exist, providing 10% of the total acetate produced in 2015 (Spekreijse et al. 2021). Biobased production routes of acetate include fermentation of ethanol (Hutkins 2007b), anaerobic digestion (Luo et al. 2016), conversion of lignocellulose via hydrolysis (Kiefer et al. 2021a) or pyrolysis (Sarchami et al. 2021; Arnold et al. 2017), bacterial fixation of carbon dioxide (Braun et al. 1981) and microbial electro synthesis (Jourdin et al. 2015), the latter two processes being still mostly under research.

Industrially acetate is mainly used for synthesis of cellulose acetate and vinyl acetate monomers, which are used as precursor or additive for plastics production but also in paints, coating, and textiles (Pal et al. 2017). Besides applications in the polymer or chemical industry, fermentative produced acetate also has applications as food conservative or condiment in the form of vinegar. Still, only a small share of the acetate produced annually is used for food applications (Martín-Espejo et al. 2022). Hence, utilization of acetate for microbial conversion to products like speciality chemicals does not compete with applications for food.

1.2 Fermentative production processes for acetate

Traditionally acetic acid is produced in the form of vinegar via fermentation of ethanol containing solutions like wine. Acetic acid bacteria (AAB) from the genera *Acetobacter*, *Gluconobacter* and *Gluconoacetobacter* convert ethanol to acetate via incomplete oxidation (Hutkins 2007b). The reaction includes two oxidation steps of ethanol with the enzymes alcohol dehydrogenase and aldehyde dehydrogenase (Pal et al. 2017). In general, three processes are used for production of vinegar: The Orleans Process or open vat process, the trickling generator process and submerged fermentation (Deshmukh et al. 2021). The Orleans process is most likely the oldest and is mostly used for premium vinegar today (Hutkins 2007a). A horizontal barrel with holes for aeration on top is filled two third with wine or a similar alcoholic solution and inoculated with AAB. The bacteria form a biofilm on the liquid surface and slowly convert the ethanol. To increase the ethanol conversion rate, the trickling generator process was developed (Deshmukh et al. 2021). Here, the already inoculated substrate is trickled onto a solid bed made from wood chips, which enables continuous production of vinegar. The most modern process is the submerged fermentation which utilizes distilled ethanol and controlled production parameters resulting in acetic acid concentrations up to 140 g/L (Andrés-Barrao et al. 2016).

While vinegar is mostly used as conservative, condiment or cleaning agent and is produced with ethanol fermented from glucose, novel fermentative production processes for biobased acetic acid targeting industrial applications are under research. Examples are C1-gas fixation or electrosynthesis.

1.2.1 Fermentation of C1-gasses

Bacteria exist that can convert CO_2 or CO to acetate by using H_2 as electron donator. These bacteria are called homoacetogenic and are mostly obligate anaerobic (Diekert et al. 1994). Homoacetogenic bacteria transform CO_2 and H_2 to acetate with a conserved pathway called the reductive acetyl-CoA pathway or Wood-Ljungdahl pathway (WJP), named after the persons who decrypted it. An overview of the pathway is shown in Figure 1.

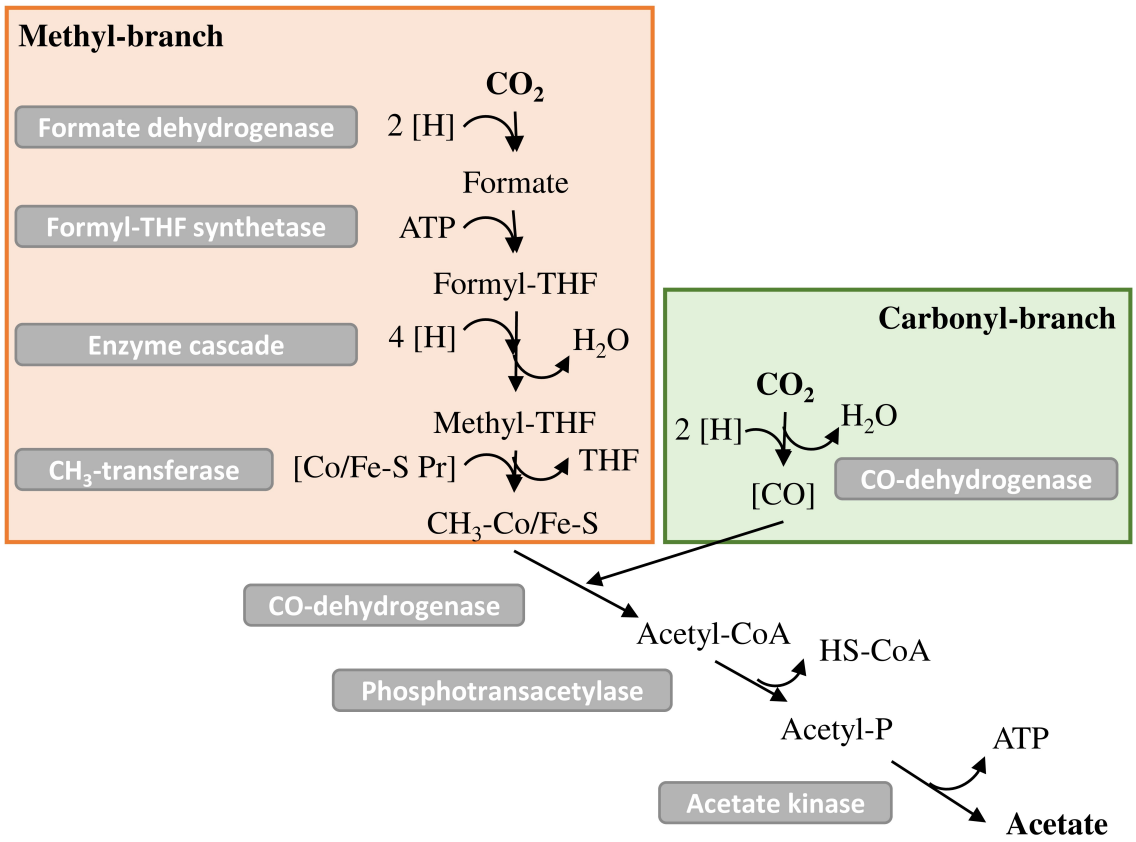

Figure 1: Reductive acetyl-CoA pathway or Wood-Ljungdahl pathway which is used by some acetogenic bacteria for acetate formation from C1-gases like CO_2. Abbreviations used in the figure: ATP = adenosine triphosphate, CH_3 = methyl, CO = carbon monoxide, CO_2 = carbon dioxide, Co/Fe-S Pr = corrinoid iron-sulphur protein, [H] = reduction equivalent, (HS-)CoA = coenzyme A, THF = tetrahydrofolic acid.

Summarized, the WJP consists of two branches (Diekert et al. 1994). The methyl branch is responsible for forming the methyl group of acetate, while the carbonyl branch is responsible for the carboxyl-group. The first reaction step in the methyl branch is the

reduction of CO_2 to formate by formate dehydrogenase, followed by binding to tetrahydrofolic acid (THF) via the enzyme formyl-THF synthetase. This reaction is catalysed under consumption of one molecule adenosine triphosphate (ATP). What follows is an enzyme cascade resulting in the dehydration and reduction of formyl-THF to methyl-THF. Last step for formation of the ready methyl group is its transfer to corrinoid iron-sulphur protein as carrier by the enzyme methyltransferase.
The carbonyl-branch only consists of the reduction of CO_2 to CO by the enzyme carbon monoxide dehydrogenase, which additionally is responsible for the formation of acetyl CoA by combining CO with the methyl-group. Acetyl-CoA is then further converted to acetate by the two enzymes phosphotransacetylase and acetate kinase with acetyl phosphate as intermediate. Here one molecule ATP is regenerated.
As can be seen by the WJP, homoacetogenic bacteria are interesting for production of acetate, as it is their natural main product and formation of side products is low owing to the low formation of ATP as energy carrier (Stark et al. 2022).
To date the highest acetate titer of 59.2 g/L and highest productivity of 146.8 g L^{-1} h^{-1} were achieved by Kantzow et al. (2015).

1.2.2 Electrobiosynthesis

Microbial electrosynthesis (MES) is another novel method for acetate production first described in 2010 by Nevin et al. (2010) as a way to store energy generated from renewables like solar or wind power. In this method electroautotrophic bacteria, that can directly use electrons from a cathode for product formation, are used for reduction of CO_2 as a carbon source to products like acetate or methane. For acetate production with MES bacteria from the genera *Acetobacterium* (Ma et al. 2021), *Acetoanaerobium* (Sleat et al. 1985) *Sporomusa* (Aryal et al. 2018; Nevin et al. 2010), *Clostridium* (Nevin et al. 2011) or the termophillic *Moorella* (Yu et al. 2017) are reported. Typically, MES is performed in H-cells, which is a system consisting of two chambers filled with electrolyte that are are separated by an ion exchange membrane in the middle (T.-S. Song et al. 2017). The cathode consists mostly of carbon-based materials like carbon cloth, carbon felt or graphite with high surface areas for the biofilm to adhere on (Aryal et al. 2018). To date, one of the highest acetate productivities per electrode surface area was achieved by Jourdin et al. (2015) with an acetic acid production rate of 685 g m^{-2} d^{-1} and a CO_2 and electron recovery of close to 100% using a novel reticulated vitreous carbon cathode covered by multiwalled carbon nanotubes and the highest volumetric productivity of 1.04 g L^{-1} d^{-1} was achieved by Marshall et al. (2013), who used bacterial strains that were adapted to MES in 150 days of cultivation. While promising, this technology is still at an early

stage of development and further improvements of productivity must be made to achieve commercialisation.

1.3 Lignocellulose-based production of acetate

Globally, lignocellulose biomass is one of the largest renewable resources with a yearly production capacity of up to 181.5 billion tonnes (state 2018, Singh et al. 2022). It forms the cell wall of plants, and its content is especially high in leaves, grass, or wood. Thus, lignocellulose biomass includes non-food sources like agricultural residues or forestry wastes (Himmel et al. 2007; Oasmaa et al. 2010). Lignocellulose consists of the three biopolymers cellulose, hemicellulose and lignin. The first polymer, cellulose, consists of glucose monomers that are bound via (β 1-4)-glycosidic bonds. It forms crystalline strains, that are interconnected by hydrogen bonds and are covered by the second polymer, hemicellulose (W. Zhang et al. 2013). Hemicellulose is a heterogenous biopolymer that is formed by different monomers like glucose, xylose, mannose, arabinose, galactose and acidic saccharides like glucuronic acid. In opposite to cellulose, it has an amorphous and branched structure (Mosier et al. 2005). The combination of cellulose and hemicellulose form the plant's skeleton. The last polymer, lignin, is an aromatic polymer consisting of phenylpropanoid precursors. Typical phenyl-groups are syringyl, guaiacyl or hydroxy-phenyl (Haghighi Mood et al. 2013). It stabilizes the plants cell wall and makes the cellulose and hemicellulose structures inaccessible for enzymes or microbes.
Cellulose is the main constituent of lignocellulose with 35 – 50% followed by hemicellulose with 20 - 35% and lignin with 15 – 20% (Haghighi Mood et al. 2013). The exact composition varies from plant to plant and is dependent on factors like type of plant, growth conditions and age.
In order to make lignocellulose biomass available for biotechnological processes its recalcitrance has to be overcome, which describes the strong resistance against hydrolysation by enzymes or decomposition by microbes (Himmel et al. 2007). The insolubility of lignocellulose, the lignin content, wax layers and the heterogenous composition are factors contributing to the recalcitrance. Thus, methods are necessary to convert lignocellulose to a substrate that is available for bacterial consumption (Haghighi Mood et al. 2013; Mosier et al. 2005). Two common methods for converting lignocellulose are hydrolysis and pyrolysis, which result in substrates that contain acetate as major component.

1.3.1 Conversion of lignocellulose biomass via hydrolysis or pyrolysis

One property of lignocellulose biomass that makes its depolymerization or conversion challenging, is its resistance to hydrolysis via enzymes or to decomposition by microorganisms. To make lignocellulose available for bacterial conversion the recalcitrance must be overcome. Two methods have been established for this purpose: hydrolysis and pyrolysis (Lange 2007).
Hydrolysis describes a process during which the cellulose and hemicellulose fractions of lignocellulose are converted into their monosaccharides via a combination of chemical and enzymatic degradation. Pyrolysis is a process that relies mostly on heating to high temperatures in the absence of oxygen (Bridgwater 2012). Through the heat treatment the energy-rich products biochar, a liquid fraction, often called pyrolysis oil or bio-oil, and non-condensable gases called syngas are generated. These have high heating values and thus can be used for energetic purposes like fuels. Both methods have in common, that a pretreatment of the biomass in the form of drying and grinding is necessary. In the case of hydrolysis, this pretreatment is often followed by dilute acidic or alkaline hydrolysis (W. Zhang et al. 2013), auto-hydrothermal treatment, or solvation with organic solvents like ethanol (Ko et al. 2020) at modest temperatures around 120°C to 200°C. As a result, hydrogen bonds connecting cellulose, hemicellulose, and lignin are degraded, thus making the different polymers soluble and available for enzymatic degradation. The final step is enzymatic hydrolysis of the polysaccharides with cellulases, hemicellulases and accessory enzymes like phenolic acid esterase into monomeric sugars (Himmel et al. 2007). The treatment with acids or bases at elevated temperatures can already lead to formation of small concentration of acetate around 1 to 15 g/L from strongly acetylated hemicellulose (Ko et al. 2020). To achieve higher concentrations, hydrolysis can be followed up by microbial conversion of the sugar monomers (Lange 2007).
For pyrolysis the pretreatment is directly followed by heat treatment, leading thermochemical decomposition and fragmentation of lignocellulose to smaller organic and inorganic substances. Literature distinguishes between three different categories of pyrolysis by the temperature and heating rate applied: Carbonization, gasification, and fast pyrolysis (Bridgwater 2012). Carbonization is characterized by slow heating rates and modest temperatures around 290 – 400°C with biochar or charcoal as the main product. For gasification, also slow heating rates are employed, but to high temperatures around 750 – 900°C. This results in syngas as the main product. The last category is fast pyrolysis. Compared to the others, fast pyrolysis applies fast heating rates of a few seconds (around 2 s) to a temperature of around 500°C (Bridgwater 2012). This leads to formation of pyrolysis oil as the main product with ratios of up to 75% (S. Wang et al. 2017).
Pyrolysis of lignocellulose leads to formation of acetate as a major component with concen-

trations of up to 17wt% mainly through hydrolysis of acetyl side chains from hemicellulose (Xinhua Shi et al. 2014). Other reactions leading to acetate formation are fragmentation of anhydrosugars stemming from cellulose and their degradation products like hydroxy acetaldehyde and 5-hydroxymethylfurfural (Stefanidis et al. 2014), or the Diels-Alder cycloaddition of conjugated diene and furanone (Demirbas 2007). Highest concentrations of acetate were found at temperatures around 350°C, which is the initial decomposition temperature of cellulose and hemicellulose. Increasing the pyrolysis temperature is reported to lead to a reduction in acetate concentration, probably because of the heat labile nature of acetate (Sarchami et al. 2021).
In comparison to hydrolysis, an advantage of pyrolysis is that all types of biomasses can be converted, from plant biomass to animal residues and kitchen waste (Ghodake et al. 2021). Furthermore, the achievable acetate concentrations without follow-up processing steps are 10-times higher (Xinhua Shi et al. 2014; Ko et al. 2020).
Both conversion methods can lead to formation of complex substrates, that contain organic substances which are potentially harmful for microorganisms (Jönsson et al. 2016). Still, this problem is more acute for pyrolysis (Horlamus et al. 2019; Arnold et al. 2017). Pyrolysis leads to a complex composition of organic compounds like different ketones, organic acids, and alcohols like methanol, because of the high temperature. The degradation of lignin also leads to release of phenolic components like guaiacol or syringol (Xinhua Shi et al. 2014), which also have strong inhibiting potential.
For hydrolysis elevated temperatures, and the application of acids or bases can lead to formation of side products like furfural or 5-hydroxymethyl furfural, which inhibit bacterial growth, but mostly in less complex compositions (Jönsson et al. 2016; Horlamus et al. 2019). Because of these inhibiting components, pyrolysis oils need to be treated, if they are intended for direct microbial conversion (Arnold et al. 2017).

1.4 Bacterial utilization of acetate

1.4.1 Metabolic pathways for acetate utilization

The tricarboxylic acid (TCA) cycle is the central and most important metabolic pathway of most aerobes. Its main purpose is formation of redox equivalents like $NADH+H^+$ that are used for generating a proton motive force in the respiratory chain, which is then used by the enzyme ATP-synthase to synthesize energy-rich ATP. Besides formation of redox equivalents, the TCA cycle also serves the purpose of supplying cells with amino acids for synthesis of new cell components. To keep the cycle running, oxaloacetate

needs to be continuously replenished. With glucose or other sugars as sole carbon source, oxaloacetate is mostly formed from pyruvate generated through glycolysis (Gerstmeir et al. 2003). As acetate cannot enter the central metabolism through glycolysis, different pathways and anaplerotic reactions are necessary. Figure 2 shows an overview of the central metabolism with acetate as sole carbon source.

The first step of acetate metabolism is the transport into the cell. In most cases transport happens passively, as protonated acetate can freely permeate through the lipid bilayer of the cellular membrane (Roe et al. 2002). Nonetheless, some bacteria like *Corynebacterium glutamicum* are reported to possess transporter molecules for acetate anions (Jolkver et al. 2009). Once acetate entered the cell, it is activated to acetyl-CoA via two pathways under consumption of ATP. The first pathway involves the enzymes acetate-kinase (AK) and phosphotransacetylase (PTA). AK catalyses the phosphorylation of acetate to acetyl-phosphate by transferring one phosphate group from ATP, yielding ADP as a result (Veit et al. 2009). Next PTA catalyses the transacetylation reaction to acetyl-CoA during which reaction the phosphate group of acetyl-phosphate is replaced by coenzyme A (CoA).

The second pathway involves only one enzyme, namely acetyl-CoA synthetase (ACS), that binds acetate to CoA in a two-step reaction (Renilla et al. 2012). In the first step ATP is consumed to form acetyl-AMP and pyrophosphate (PP) is released, while in the second step AMP is replaced by CoA to form acetyl-CoA, thereby releasing AMP. The activation of acetate via AK-PTA is reversible and less energy-demanding than the activation via ACS, since ATP is only consumed to ADP instead of AMP (Lin et al. 2006). For many bacteria the AK-PTA pathway is mainly used for recycling CoA from acetyl-CoA by forming acetate, while at the same time generating a small amount of ATP during excess of carbon sources like glucose (Wolfe 2005). The acetate activation reaction via ACS is irreversible invivo due to the presence of pyrophosphatases inside the cell, that split pyrophosphate to single phosphates (Wolfe 2005, Lin et al. 2006).

After activation to acetyl-CoA, the next step is the TCA-cycle where acetyl-CoA is converted to amino acids or used for generation of ATP. As mentioned before oxaloacetate needs to be replenished to keep the TCA-cycle going. To form the C4-molecule oxaloacetate from the C2-molecule acetyl-CoA, the glyoxylate cycle (Krebs-Kornberg cycle) is used as anaplerotic pathway (Gerstmeir et al. 2003; Kornberg et al. 1957). It involves the two enzymes isocitrate lyase (ICL) and malate synthase (MS) and bypasses the two decarboxylation steps of isocitrate. As a result, one molecule of succinate and one molecule of malate are formed from two molecules of acetyl-CoA with glyoxylate as intermediate product. Both can then be converted to oxaloacetate through the TCA-cycle.

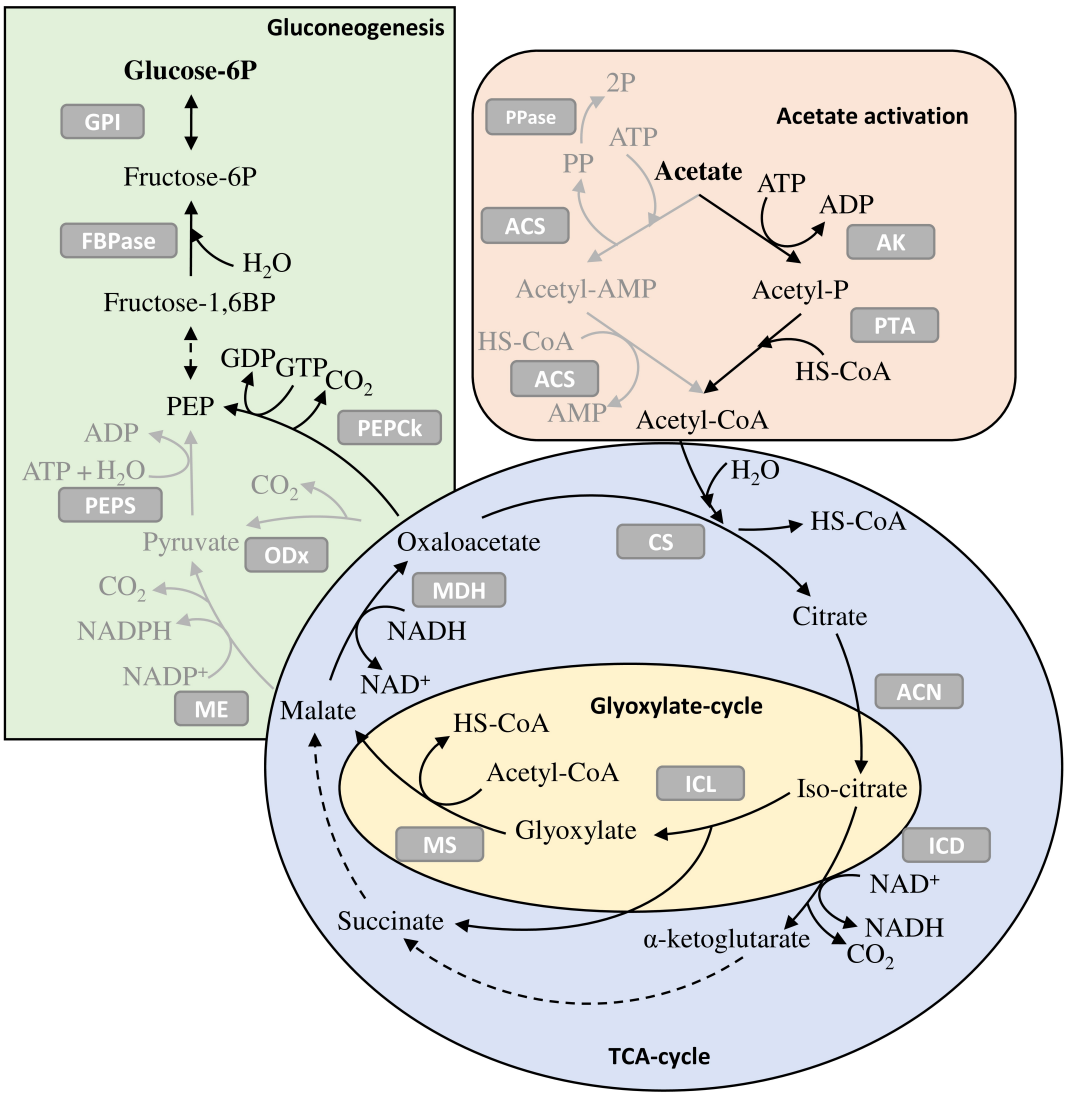

Figure 2: Metabolic pathways for bacterial acetate consumption and gluconeogenesis (Kiefer et al. 2021a, Gerstmeir et al. 2003). Black arrows depict the metabolic pathways specific for *C. glutamicum*, while the grey lines show general pathways. Abbreviations used in the figure: ACN = aconitase, ACS = acetate synthase, AK = acetate kinase, ATP = adenosine triphosphate, CO_2 = carbon dioxide, CS = citrate synthase, FBPase = fructose bisphosphatase, GPI = glucose-6-phosohate isomerase, GTP = guanosine triphosphate, HS-CoA = coenzyme A, ICD = isocitrate dehydrogenase, ICL = isocitrate lyase, ME = malic enzyme, MS = malate synthase, NAD^+/NADH = nicotinamid adenine dinucleotide, $NADP^+$/NADPH = nicotinamid adenine dinucleotide phosphate, ODx = oxaloacetate decarboxylase, P = phosphate, PEP = phosphoenolpyruvate, PEPCk = phosphoenolpyruvate carboxykinase, PEPS = phosphoenolpyruvate synthase, PP = pyrophosphate, PPase = pyrophosphatase, PTA = phosphotransacetylase, TCA = tricarboxylic acid.

Besides replenishing oxaloacetate, another important step is the formation of sugar molecules, that are necessary for synthesis of nucleotides and other cell components. This

process is called gluconeogenesis and consists of different pathways starting at malate or oxaloacetate that lead either to formation of pyruvate or phosphoenol-pyruvate (PEP) (Netzer et al. 2004; Sauer et al. 2005). Both are further converted to fructose-6-phophate or glucose-6-phosphate via reversed glycolysis, with the enzyme fructose bisphosphatase bypassing an irreversible glycolysis step.

1.4.2 Inhibiting effect of acetate and tolerance mechanisms

Although acetate has potential as inexpensive and environmentally friendly substrate, it is harmful to most bacteria in concentrations above 0.5% (Trček et al. 2015). Also, since acetate is a side product as consequence of overflow metabolism, for many bacteria its conversion rates are often low.

Acetate exerts inhibition on bacterial growth in several ways. First, acetic acid in the protonated form can freely diffuse across the cell membrane into the cytosol (Booth 1985). Because acetic acid has a pKa of 4.75 and most bacterial cytosols have a regulated pH value of 7.5 - 7.6 (Booth 1985; Wilks et al. 2007), it dissociates after diffusing into the cytosol, thus acidifying the intracellular pH-value. The accumulation of acetate inside the bacterial cell increases the osmotic pressure (Roe et al. 1998), while the accumulation of protons is believed to disturb the proton-motive force necessary for generation of ATP (Axe et al. 1995; Herrero et al. 1985). Acetate also directly effects metabolic pathways, especially the methionine-synthesis pathway, leading to accumulation of toxic homocysteine and depletion of methionine as important cellular building block (Roe et al. 2002).

Because of these effects, bacteria developed mechanisms to prevent or soften the harmful effects of acids like acetate. Theses mechanisms are similar in the basic principle for different bacteria even though different amino acids may be involved (Senouci-Rezkallah et al. 2011; Tanaka et al. 2008). Because of this, the four acid resistance systems (AR) of *Escherichia coli* (Zhao et al. 2018) will be explained as example. Only few is known about the first system, AR1. It is a ATP consuming system that is active when the availability of amino acids like glutamate is limited (Sun et al. 2011). A sigma factor RpoS (Price et al. 2000) and the catabolite repressor protein CRP (Castanie-Cornet et al. 2001) are involved in its function. The remaining three systems follow the principle of binding a proton by decarboxylation of certain amino acids and secretion the decarboxylated product into the surrounding medium (Lu et al. 2013; Zhao et al. 2018). For the excretion antiporters are used that simultaneously transport new amino acids into the cell. In this regard AR 2 utilizes glutamate, which is decarboxylated to γ-amino butyric acid, AR 3 decarboxylates arginine to agmatine and AR 4 lysine to cadaverine. Each system comes with their own set of decarboxylases and antiporters (Zhao et al. 2018). The release of

ammonia by deamination of amino acids is another way to counter lowered cytoplasm pH for some bacteria (Lu et al. 2013).
Besides these resistance systems against acids in general, a class of bacteria exists that has developed resistance mechanisms especially for acetate, which allow them to cope even with high acetate concentrations of 6% to over 10% (Trček et al. 2015; B. Wang et al. 2015a).
Acetobacteracea or so-called AAB, are well known for their ability to oxidize ethanol to acetic acid via alcohol dehydrogenase (ADH) and aldehyde dehydrogenase (ALDH). The three genera *Acetobacter*, *Gluconoacetobacter* and the reclassified *Komagateibacter* are commonly applied in industry for vinegar production. Two transport systems were reported, that aim to reduce the intracellular acetate concentration. The first one is a proton motive force driven efflux system for acetate (Matsushita et al. 2005) and the second a putative ABC-transporter that is able to actively transport acetate out of the cell (Nakano et al. 2006). Furthermore, AAB can change the composition of their cell membrane to counter passive diffusion of acetic acid. Trcek and colleagues (2007) researched changes in lipid content and composition of *Komagateibacter europaeus*. They observed a decrease of overall lipid content with a lower phospholipid ratio and increased glycolipid and neutral lipid ratios as reaction to acetic acid availability. The authors concluded that these changes serve to reduce the cell surface and to make the cell membrane more hydrophobic (Trcek et al. 2007). Several authors also found ADH and ALDH to be important for acetic acid resistance by deletion experiments and comparison of different versions of the enzymes. High activity ADH and ALDH provide the energy necessary for morphological changes of the cell membrane and for the active excretion of acetate (Trcek et al. 2006; Nakano et al. 2008; B. Wang et al. 2015b). Dissimilation of acetate is another way to cope with its toxicity. For most bacteria acetate is converted to acetyl-CoA via ACS or via PTA and AK with acetyl-phosphate as intermediate. Some strains of *Acetobacter aceti* can dissimilate acetic acid via a third pathway with a changed TCA-cycle depending on the gene cluster *aar* (Mullins et al. 2013). *AarA* encodes a citrate synthase, *aarC* a succinyl-CoA-acetate-CoA transferase (SCACT) and *sixA* encodes a phosphoprotein phosphatase, a regulator for the *aar* complex. SCACT catalyses the conversion of acetate and succinyl-CoA to acetyl-CoA and succinate, thereby replacing the missing succinyl-CoA synthetase. Other resistance mechanisms include general stress response to acids like production of special chaperones (Andrés-Barrao et al. 2012) or acid resistant versions of certain proteins and enzymes like aconitase (Nakano et al. 2008; Okamoto-Kainuma et al. 2011). Deamination or decarboxylation of certain amino acids is a way to adjust intracellular pH by binding protons through replacement of the carboxyl-group with a proton or by release of ammonia (B. Wang et al. 2015b).

1.4.3 Strategies for improving acetate tolerance

Because acetate is produced as side product by many organisms, ways of improving the resistance against acetate as inhibitor, but also on improving acetate consumption were researched. As many of the natural resistance systems were related to the availability of amino acids, one approach was to add amino acids to the culture broth to relief acetate stress (Han et al. 1993; Sandoval et al. 2011; Roe et al. 2002). Of the amino acids tested, addition of methionine led to a strong release of inhibition by acetate. As mentioned in section 1.4.2, acetate inhibits enzymes of the methionine biosynthesis branch leading to accumulation of toxic homocysteine. One theory connects the addition of methionine to downregulation of the methionine biosynthesis pathway and thus to less production of homocysteine (Roe et al. 2002). Other attempts to prevent the accumulation of growth-inhibiting homocysteine due to the presence of acetate targeted genes of the pathway. Mordukhova and colleagues (2008) experimented on improving heat tolerance of *E. coli* by modifying homoserine o-succinyltransferase (MetA) via random mutagenesis. MetA is the first enzyme in methionine synthesis and was proven to slowly denature at temperatures above 25°C. They succeeded by replacing five amino acids and found that the modified MetA not only improved growth up to a temperature of 44°C, but also increased acetic acid resistance (Mordukhova et al. 2008). In a later work the authors created a mutated version of MetE and combined it with the mutated MetA. MetE is a cobalamin independent methionine synthetase and is responsible for the conversion of homo cysteine to methionine (Mordukhova et al. 2013). The resulting mutant showed an increased growth rate from 0.16 1/h for the wildtype to 0.21 1/h in presence of 20 mM sodium acetate. Further methods for improving acetic acid tolerance included adaptive evolution with identification of mutations, that had beneficial effects on acetic acid resistance (Rajaraman et al. 2016). Utilizing this approach, it was discovered by the authors that a point mutation in the gene *rpoA* increases growth of *E. coli* ATCC8739 from 0.41 1/h to 0.52 1/h with 85 mM acetate as carbon source. The gene *rpoA* includes the code for the alpha subunit of a RNA polymerase core enzyme. Modifying a cAMP receptor protein via error prone PCR (Chong et al. 2013) or overexpressing ATP-dependant helicase gene *recG* from *A. aceti* in *E. coli* also led to improved growth on acetic acid (Steiner et al. 2003). For the latter case the authors assumed the helicase to be responsible for stress related DNA-repair.

1.4.4 Genetically and metabolically enhanced consumption of acetic acid

Improving consumption of acetic acid is another way to enhance resistance against the acid's stress, while at the same time increasing productivity. Overexpression of the *acs* pathway is a common method for enhancing consumption of acetate (Lin et al. 2006; Noh et al. 2018; H.-S. Song et al. 2018), while different reports on the effectiveness of overexpressing the *pta-ackA* pathway are available. Xiao and colleaques (2013) reported increased growth for *E. coli* on pure acetate up to 100 mM with overexpressed *acs*, but reduced growth for overexpressed *pta-ackA* (Xiao et al. 2013). Zhang and colleagues (2019) reported opposite findings with reduced biomass formation, when overexpressing *acs* in comparison to *pta-AckA* (S. Zhang et al. 2019). Li and colleagues (2016) also found reduced growth, when overexpressing *acs* and referred this effect to the higher energy demand. Another way to improve consumption of acetate is engineering the regulatory system (Castaño-Cerezo et al. 2015). *Acs* is transcriptionally regulated by cAMP and post-transcriptionally by acetyltransferase *patZ* and by deacetylase *cobB* in presence of glucose. Acetylation of a lysine-side group of ACS lead to its inactivation. In this regard deletion of *patZ* was tested to prevent downregulation of ACS and increase acetate co-consumption with glucose, which was successful for *E. coli* BL21 and another strain (Peebo et al. 2014). In other cases deletion of the transacetylase gene did not lead to changed growth behaviour (Castaño-Cerezo et al. 2015; Starai et al. 2004). A point mutated *acs* gene was insensitive to acetylation, so that a 2.7 fold increase in acetate consumption could be achieved in one study (Novak et al. 2018b). Other methods, that directly affected the pathways for acetic acid conversion to acetyl CoA included replacement of the promotors of *acs* or *pta-ackA* with stronger, unregulated versions (Huang et al. 2018; Peebo et al. 2014; H. Yang et al. 2019) and in one case replacement of *acs* with the gene from *A. pasteurianus* (J. Yang et al. 2016). Redistribution of intracellular acetyl-CoA fluxes to the TCA-cycle, glyoxylate shunt and gluconeogenesis can also have an influence on acetate consumption and growth on acetate. Increasing flux through the glyoxylate shunt can be achieved by deleting the *AceBAK* regulator iclR, thus leading to higher acetate consumption (Li et al. 2016; Noh et al. 2018). This can be further modulated by overexpression of single genes of the *AceBAK* operon or *gltA*, a gene coding for citrate synthase (Noh et al. 2018). A reduction of the flux to gluconeogenesis by deleting *maeB*, an enzyme responsible for conversion of malate to pyruvate, was reported to lead to higher acetate consumption and growth (H. Yang et al. 2019; Li et al. 2016).

It is also possible to introduce acetic acid catabolism in bacteria, that are not able to utilize it naturally. Kabisch and colleagues (2013) engineered *Bacillus subtilis* for growth on acetic acid by transferring the genes *aceA* and *aceB* of the glyoxylate shunt from *Bacillus licheniformis*. The addition of the glyoxylate shunt genes led to diauxic growth

with consumption of acetic acid and to a lower degree also acetoin after the main carbon source glycerol was depleted. The authors also reported increased OD values for the transformed bacterium (Kabisch et al. 2013).

1.4.5 Overview over bacterial production processes with acetate as sole carbon source

As mentioned in section 1.4.2, acetate has an inhibiting effect on many microorganisms. Because of this, only few exceptions and special strains were used in actual production processes. Besides fungi, where bioproduction processes utilizing acetate as sole carbon source have been published for lipid synthesis with yeasts (Salsabila et al. 2021) or organic acid synthesis with filamentous fungi like *Aspergillus oryzae* (Kövilein et al. 2021), only a few bacteria were found to be suited for bioproduction on acetate as sole carbon source. A summary of bacterial processes using acetate is shown in Table 2.
Most reported processes rely on *E. coli* as production host, with only few mentions of other bacteria like *Cupriavidus necator* (Garcia-Gonzalez et al. 2018; Vlaeminck et al. 2022) or *Pseudomonas putida* (Arnold et al. 2019b; S. Yang et al. 2019). Both bacteria are model organisms for production of polyhydroxyalcanoates (PHA), a class of polymer that can be used as bioplastics and that can be synthesized from acetyl CoA as precursor. Products derived from acetyl CoA are beneficial for using acetate as substrate, because it is directly converted to acetyl CoA. Thus, ideally carbon loss is minimized. Other products are derived from the TCA cycle, like succinate (Huang et al. 2018) or itaconate (Noh et al. 2018), which is a C5 dicarboxylic acid that was listed as one of the twelve most important products derived from biomass by the US Department of Energy. Genetic modifications and metabolic engineering even enabled production with novel synthetic pathways using acetate as sole carbon source (Novak et al. 2020; H. Yang et al. 2019). The broad spectrum of different products listed in table 1 and the increasing product titers, especially during recent years, show the great potential of using acetate as alternative to sugars for bioproduction.

Table 2: Overview over a selection of bacterial production processes using acetate as sole carbon source.

Bacterium	Process-Type	Product	Titer	Reference
E. coli				
	Fed-Batch	β-caryophyllene	1.1 g/L	(J. Yang et al. 2016)
	Fed-Batch	Mevalonate	1.1 g/L	(X. Xu et al. 2018)
	Resting cells	Acetone	6.6 g/L	(H. Yang et al. 2019)
	Batch	3-hydroxypropionate	3.0 g/L	(J. Lee et al. 2018)
	Whole cell catalysis	3-hydroxypropionate	15.8 g/L	(Lai et al. 2021)
	Fed-Batch	Phloroglucinol	1.2 g/L	(X. Xu et al. 2017)
	Fed-Batch	Itaconic acid	3.6 g/L	(Noh et al. 2018)
	Batch	Tyrosine	0.7 g/L	(Jo et al. 2019)
	Resting cells fed-batch	Succinic acid	22.9 g/L	(Huang et al. 2018)
	Fed-Batch	2,3-butanediol and acetoin	1.2 g/L	(Novak et al. 2020)
P. putida				
	Batch	Rhamnolipids	0.3 g/L	(Arnold et al. 2019b)
	Fed-Batch	PHA	0.7 g/L	(S. Yang et al. 2019)
C. necator				
	Fed-Batch	Poly-3-hydroxy(butyrate-co-valerate)	48.0 g/L	(Garcia-Gonzalez et al. 2018)
	Fed-Batch	PHB	58.5 g/L	(Vlaeminck et al. 2022)
B. cereus				
	Batch	Polyhydroxybutrate (PHB)	1.5 g/L	(P. Wang et al. 2019)
H. bluephagensis				
	Fed-Batch	PHB	49.8 g/L	(J. Zhang et al. 2022)

1.5 *Corynebacterium glutamicum* as model bacterium for acetate utilization

Corynebacterium glutamicum is a gram-positive, aerobic and non-pathogenic bacterium, that was first isolated from soil in 1957 during the search for a natural glutamate producing organism (Kinoshita et al. 1957). It is a well-known industrial producer of amino acids like glutamate or lysine, with annual production capacities of over 2.5 million tons/year and over 1.5 million tons/year, respectively (J.-Y. Lee et al. 2016). Titer of up to 120 g/L and high productivities of 4 – 5 g $L^{-1}h^{-1}$ are reported for both amino acids (D. Zhang et al. 2014; Becker et al. 2011). This effective production capability led to a high research interest for *C. glutamicum* as production organism for other valuables. In 2003 the complete genome of *C. glutamicum* was deciphered, leading to better understanding of the organism and to development of better tools for strain engineering (Kalinowski et al. 2003). Regarding products, *C. glutamicum* has been used or modified for production of a selection of chemicals. Other amino acids produced included for example L-alanine, L-methionine (J.-Y. Lee et al. 2016), or L-valin (Blombach et al. 2014). Regarding organic acids, *C. glutamicum* was also found to be an efficient producer of acids like succinic acid or lactate under oxygen deprived conditions, achieving titer of up to 100 g/L and higher (Briki et al. 2020; Okino et al. 2005). Further products include alcohols like ethanol (J.-Y. Lee et al. 2016) or isobutanol (Blombach et al. 2014). A low protease activity and the existence of two pathways for protein secretion even spurred interest for using *C. glutamicum* as production host for recombinant proteins (M. J. Lee et al. 2018).

Besides the aptitude for producing a selection of different chemicals, another advantage of *C. glutamicum* is its broad substrate spectrum. Besides glucose and fructose this includes carboxy acids like lactate, acetate, pyruvate and propionate (Wendisch et al. 2000), alcohols like ethanol (Jolkver et al. 2009) and even aromatic compounds (Shen et al. 2012). During growth on mixtures of different substrates, *C. glutamicum* shows no sign for diauxic growth or preference for one specific substrate. Instead, the substrates are metabolized simultaneously. Only for glutamate and glucose diauxic growth was reported, where glucose was consumed first (Wendisch et al. 2000).

Regarding acetate as alternative carbon source, *C. glutamicum* was reported to be able to grow on acetate concentrations of up to 10 g/L without signs of inhibition and to tolerate even higher concentrations (Arnold et al. 2019a). For growth on acetate as sole carbon source, the bacterium uses the glyoxylate cycle described in section 1.4.1 as anaplerotic reaction for replenishing the TCA-cycle with C4-moelcules (Black lines and descriptors in Figure 2 show metabolic pathways for utilization of acetate specific for *C. glutamicum*). Opposite to *E. coli*, which can activate acetate to acetyl-CoA via the PTA-AK and the

ACS pathways, *C. glutamicum* is reported to only use the PTA-AK pathway (Veit et al. 2009). The genes *pta* and *ackA* of the acetate activation pathway as well as the genes *aceA* and *aceB* of the glyoxylate cycle enzymes are essential for growth on acetate as sole carbon source. They are strictly controlled by transcriptional regulators, mainly by RamA and RamB (Cramer et al. 2007; Gerstmeir et al. 2004). RamA is an activator protein, that increases expression of all enzymes involved in acetate metabolism in presence of acetate and RamB acts as repressor in absence of this substrate. It has been reported that only RamA is essential for growth on acetate as sole carbon source, while deletion of RamB leads to a reduction in a slight reduction in activity of the glyoxylate cycle (Cramer et al. 2007).

For gluconeogenesis during growth on acetate *C. glutamicum* specifically uses the PEP-carboxykinase pathway for conversion of oxaloacetate to PEP under consumption of GTP as cofactor, making the enzyme essential for growth on acetate as carbon source (Netzer et al. 2004). While the bacterium possesses genes for malic enzyme, its activity is too low to sustain growth.

1.6 Perfusion bioreactors

1.6.1 General information

Commonly bioreactors and bioprocesses are assigned to three categories depending on their operation mode (Chmiel 2011). These are batch fermentation, fed-batch fermentation, and continuous fermentation. The three categories are differentiated by the presence of medium streams entering or leaving the bioreactor system. In batch mode no substance streams are added or removed from the bioreactor after its inoculation. All substrates are added from the beginning in high enough concentrations for formation of the target product. The only substances added are gases like air or O_2, because of the low solubility of O_2 and to remove excess CO_2 formed during the cultivation, gases like CO_2 or NH_3 that have an impact on the pH value of the medium and pH-correction solutions. In fed-batch mode, the bioreactor is only filled with medium to a small percentage of the total working volume and a feed solution is added during the process. This allows better control over the bacterial culture and prevents substrate inhibition or overflow metabolism, which is the production of side products at high substrate concentrations. The last mode is continuous mode, in which a feed solution is continuously added to the bioreactor and culture broth is continuously removed, which leads to dilution of the culture broth. The rate at which the culture broth is diluted is called the dilution rate, which is the ratio between medium flow rate and bioreactor volume. Generally, the goal of continuous processes is to achieve a steady state, at which productivity and growth rate can be controlled to a constant value by controlling the availability of a limiting substrate. At this steady-state the dilution rate equals the growth rate of the culture, because the same amount of cells is removed from the culture as is produced by cell growth. In that way the dilution rate can be used to control the availability of a limiting nutrient and the growth rate of the cell population. The dilution rate is typically set below the maximum achievable specific growth rate, since a higher dilution rate would mean that more cells are removed from the process than the population can produce by growing and that the cells are ultimately washed out of the reactor (Chmiel 2011). The advantages of a continuous process at steady state is stable product formation over a long time, while product inhibition is prevented. Furthermore, cost can be reduced, because smaller reaction vessels are needed in comparison to the other modes of fermentation. A disadvantage is the increased risk of contamination.

A special form of continuous mode is the perfusion strategy. Processes run in perfusion mode utilize bioreactors, which are supplied with a cell retention or cell recycle system (Sieck et al. 2017). The complete or partial retention and recycling of cells, allows for high cell density and therefore increased productivities at smaller reactor volumes in compar-

ison to the other process modes. Furthermore, it allows the application of dilution rates higher than the maximum specific growth rate of the bacterial culture, that would lead to wash out of cells at common continuous process mode (Chmiel 2011). Higher dilution rates can be advantageous for example when substrates with dilute carbon concentrations are applied or when the substrate contains toxic substances. On the opposite, the main disadvantage is the high medium consumption combined with a low concentration of extracellular products, which leads to increased cost for downstream production (Sieck et al. 2017).

Several methods for cell retention have been under use during the last years, that can be sorted into methods that rely on retention by size or retention by density (Voisard et al. 2003). The first category uses physical barriers like membranes or filter systems in different configurations. The second category uses the difference in density between cells and culture broth and focusses on technology that increases the sedimentation velocity. The different methods will be described in more detail in the following subsections. Increased focus will be placed on membrane systems, as they are the most suited for lab and small-scale applications. An important parameter for perfusion processes and the cell retention system is the recycle ratio R (Chmiel 2011). It describes the ratio of cell-free permeate to the medium inflow. With some cell retention devices like membranes full retention of biomass can be achieved, resulting in a recycle ratio of 1. Other devices and configurations can be partially permeable for biomass or include a deliberate biomass bleed stream out of the bioreactor and result in a recycle ratio lower than 1. Both complete retention and partial retention can have advantages and disadvantages. A complete cell retention can lead to higher cell densities, but also dead cells and cell fragments are retained potentially lowering the cell viability (Voisard et al. 2003). A partial retention leads to expulsion of cell fragments and therefore to better cell viability and ultimately longer process times. On the other hand, process control is more complex, and an additional biomass removal step must be included in downstream processing (Gagnon et al. 2018). Furthermore, cell density and volumetric productivity are limited in this case.

1.6.2 Devices for cell retention based on density

As mentioned before, one way to retain cells is by using the difference in density between cells and the surrounding liquid. Their main advantage over membrane-based retention devices, is that they can principally run indefinitely without risk of clogging or fouling (Voisard et al. 2003). Furthermore, density-based retention devices mostly do not retain the complete biomass but are permeable for dead cells and cell fragments. Thus, increasing cell viability and product quality. A challenge is the low difference in densities

between cells and their surrounding fluid. This leads to low sedimentation rates and long residence times in the cell retention device. Therefore, most cell retention technologies based on density difference enhance the sedimentation velocity by increasing gravitational forces or increasing the particle size through formation of agglomerates.
An example of a simple device that uses normal gravity for cell retention is the cell settler (Choo et al. 2007). This is a device that offers a large surface area with low liquid height and low perfusion rates to enhance settling time. Enhanced versions are the inclined settlers that offer several plates that are orientated in an angle to the vertical direction (Coronel et al. 2020). This improves the separation of living cells from cell debris.
Acoustic settlers are another example for an enhanced cell settling device. Here an acoustic resonance filed is applied that causes cells to form agglomerates (Trampler et al. 1994). The increased size of these agglomerates in comparison to single cells leads to higher sedimentation velocity. The high effect of cell size on sedimentation velocity is also what makes application of cell settlers for production processes with bacteria or yeasts challenging as they are mainly designed for mammalian cells with more than 10 times larger cell size. The long sedimentation velocity of bacterial cells leads to low perfusion rates (Freeman et al. 2017).
A technology that does not depend on normal gravity is the continuous centrifuge (Johnson et al. 1996). Continuous centrifugation is a cell retention method, that utilizes high centrifugal forces for separation of biomass from spent culture broth. While the culture broth is collected, the cells are drawn back into the bioreactor system. The centrifuge has the advantage of achieving high separation efficiency and being reliable, in comparison to other methods, where pore clogging or fouling can occur (Choo et al. 2007; Kim et al. 2007). Centrifuges also have a high separation efficiency for dead cells. Those are mostly transported out of the bioreactor in the supernatant, as they have a lower density than viable cells (Johnson et al. 1996). Disadvantages of continuous centrifuges are high shear forces as well as temperature and nutrient fluctuations, that put the biomass under increased stress that can lead to lowered cell viability (Kim et al. 2007).

1.6.3 Devices for cell retention based on size

The second category for cell retention devices relies mostly on size differences to separate biomass from the culture broth using membranes as physical barrier. Bioreactors that utilize membranes for cell retention are often referred to as membrane bioreactors (MBR) (Akkoyunlu et al. 2021). The main advantages of membranes for cell retention, in comparison to density based devices, are simple operation and scale up, full retention of biomass at lower energy consumption and shorter residence times in the retention device (Coutte

et al. 2017). Membranes can either consist of ceramic materials like aluminium, circonium or titanium oxide or of organic polymers like polyethersulfone (PES), polyvinylidene fluoride (PVDF), Polypropylene and more (Akkoyunlu et al. 2021; Coutte et al. 2017). Depending on their pore size they are categorized as macrofiltration, microfiltration, ultrafiltration or reverse osmosis membranes. The selection of the required material and pore size depends on following criteria:
- Size of the cells to be retained.
- Size of products and unwanted contaminants.
- Potential interaction between cells, their side products or medium components with the membrane material.
- Substance parameters like viscosity and density of the medium.
For bacteria typically microfiltration membranes with a pore size of 0.1 µm to 0.45 µm are used (Y. Wang et al. 2007). Membrane based cell retention systems can be operated either externally of the bioreactor vessel with a recycle loop or internally submersed in the culture broth. Both modes of operation have their advantages and disadvantage (Akkoyunlu et al. 2021). When the cell retention module is applied externally, often higher specific membrane areas can be achieved, and the membrane can be exchanged during operation in case of pore clogging. At the same time the circulation flow can lead to increased shear stress for cells and introduces inhomogeneities into the process. In comparison, internal cell retention devices are more limited in the achievable membrane area, but they reduce energy requirements, because no additional pump is needed for a circulation flow, and they lead to a more homogenous medium.
The main drawback of membranes in general is the tendency of pore clogging to occur after some time, which reduces permeate flux, increases transmembrane pressure and can even lead to complete blockage of the membrane (Akkoyunlu et al. 2021). This effect, which is referred to as membrane fouling, has several causes (H. Xu et al. 2020). It can be caused by the formation of a filter cake on the membrane surface, which consists of retained particles and substances and that leads to increased filter resistance. Adsorption of solutes or dispersed molecules either inside the pores or at the pore orifice, because of interactions like Van-der-Waals forces, electrostatic forces or chemical bonding can be other causes (Xiafu Shi et al. 2014). The adsorbed molecules constraint the effective pore size and therefore reduce the liquid flux. Furthermore, particulates or macromolecules can completely block a pore, when they have a high enough size (Slimane et al. 2019). For biological solutions the most common components leading to membrane fouling are proteins, polysaccharides (H. Xu et al. 2020) and nucleic acids (Esclade et al. 1991). But also cells themselves can lead to pore clogging if they start to form biofilms on the membrane surface or inside the pores. To remove or prevent membrane fouling sheer is often generated at the membrane surface either through stirring, bubble aeration or by using

high liquid velocities in cross flow mode (Su et al. 2021; Xiafu Shi et al. 2014). Cross flow refers to an application of membranes, where the main flow passes the membrane tangentially and is split into an orthogonal permeate flow and a retentate flow, that is recycled back into the bioreactor (Su et al. 2021). The high liquid velocity and the shear forces generated prevent the formation of a filter cake as well as adsorption of particulates. This is opposed to the typical dead-end filtration mode, where all the filtrate flow passes through the membrane and retained substances collect on the membrane. Another way to prevent membrane fouling is backflushing, where liquid is pumped through the membrane from the permeate side to remove particles from the pores (Xiafu Shi et al. 2014). Because these methods often are effective only for a certain amount of time or are difficult to control, specialized membrane devices have been developed that are less prone to fouling.

Spin filters

Spin filters are cell retention devices that have been used in perfusion cultures for a long time (Brennan et al. 1987). They consist of a cylindrical filter membrane or a wired mesh, that is closed on both sides and immersed into the culture broth (Vallez-Chetreanu et al. 2007). For rotating the filter, it can be attached either to the stirrer shaft or to a separate rotating shaft. The attachment to a separate shaft was shown to be beneficial, as too high rotation speed was shown to lead to higher fluid exchange rates and thus lesser retention efficiency (Voisard et al. 2003). A pump is used to remove the permeate from the inside of the spin filter, which generates the transmembrane pressure necessary for filtering the culture broth. Spin filters can be made either from stainless steel (Brennan et al. 1987), from ceramics (Yabannavar et al. 1992) or from synthetic polymers like for example nylon (Brennan et al. 1987). Fouling is prevented by the centrifugal forces of the spinning filter, which also enhances cell sieving in a way, that even higher pore sizes than cell size can be used (Voisard et al. 2003). A main advantage of a spin filter is a high achievable perfusion rate (Vallez-Chetreanu et al. 2007). The main drawback is the tendency for fouling at long process times. It was shown that fouling of spin filters is impacted by rotation speed, perfusion rate and filter material, where metallic filters are more prone to adhesion of proteins and DNA and thus to fouling (Brennan et al. 1987). In literature, usage of spin filters for cell retention is reported for bioreactor volumes of up to 500 L (Deo et al. 1996).

Hollow Fibers and alternating tangential flow (ATF) devices

Hollow fibers are tubular membranes with diameters below 0.5 mm. They are made from similar materials and with similar pore sizes than typical flat sheet membranes, but with

their cylindrical form they offer a high surface to volume ratio as well as more homogenous fluid dynamics (Akkoyunlu et al. 2021). The homogenous flow behaviour makes them especially suited for cross flow applications and the high surface to volume ration allows easy scale up by numbering up the fibers in parallel stacks. In that way high membrane areas can easily be achieved. Hollow fibers are used for several applications. Examples are the bubble-free transfer of oxygen via diffusion (Ahmed et al. 1992), cell retention for suspension cultures as well as nutrient supply and carrier for cells in adhesion culture (Napoli et al. 2014) or biofilms (Ercan et al. 2015). Because of their cylindrical form and usually small diameter high flow velocities and thus shear forces can be achieved, that are able to remove particles and chemicals leading to membrane fouling. Still, fouling is also a drawback of hollow fiber systems, as changes of transmembrane pressure over the length of the fibers and concentration polarisation can hinder permeate flow over time (Weinberger et al. 2022).
One attempt to lower the risk of fouling and increase the process time was the development of an alternating flow system. The ATF is a special device, where the hollow fiber cartridge is not connected to a recirculation line for the retentate. Instead, the module ends at a diaphragm pump that generates a pulsating flow that periodically switches its direction (Weinberger et al. 2022). By this pulsating behaviour fresh culture broth is drawn into the cell retention device and filtered. When the flow changes its direction, retained cells are pushed back into the reactor. At the same time a certain fraction of the permeate is drawn back into the module, thereby removing particles from the inside of the pores thus reducing fouling (Kim et al. 2007). Besides better fouling behaviour, ATF devices have the advantage of lower shear stress in comparison to tangential flow filtration, because of lower flow velocities (Gupta 2017).

1.6.4 Application of perfusion bioreactors for bacterial processes

Perfusion bioreactors and perfusion processes are commonly used in wastewater treatment either by using a sedimentation basin for removal of activated slugde, which is the conventional method, or by using special MBR when higher purity or removal of small contaminants like pharmaceuticals are needed (Bertanza et al. 2017; Al-Asheh et al. 2021). Besides wastewater, perfusion bioreactors are also commonly applied in cell culture applications, for example for production of antibodies or other biopharmaceuticals as well as for tissue engineering (Wong et al. 2022). As mentioned before, utilization of perfusion processes for cell cultures resulted in high cellular viability and product quality, as cell fragments or dead cells are continuously removed from the process (Freeman et al. 2017). Furthermore, protein-based pharmaceuticals often have low stability in the culture broth,

because of which continuous product removal is necessary (Walther et al. 2019). For these reasons most of the cell retention devices described in earlier sections were mainly developed and optimized with cell culture applications in mind.

Still, perfusion bioreactors were also considered for bacterial production processes for example to achieve process intensification (Akkoyunlu et al. 2021). As such, higher cell densities and volumetric productivities can be achieved at lower volumes through cell retention in a perfusion process, because inhibiting side products are continuously removed from the process and the risk of washing out the biomass is prevented. Furthermore, the cost for hardware and for downstream processing can potentially be lowered by integrating the removal of biomass in the production process, which removes the necessity of additional filtration or centrifugation equipment to remove the cells from the culture broth.

Tajarudin et al. (2018) achieved to produce acetate with a high productivity of 37.9 $gL^{-1}h^{-1}$ in a MBR using *Clostridium butyricum* as production organism. Utilization of the MBR allowed removal of the in higher concentrations toxic acetate and butyrate, which led to the productivity increase. Jung and Lovitt (2010) demonstrated the utilization of a 36 L pilot scale MBR for production of lactic acid bacteria, which can be used as food supplement to help digestion or for manufacturing of fermented foods. Because of the formation of inhibitory metabolites like lactate or acetate, productivity in batch mode was low. With a MBR cell concentrations as well as volumetric productivities could be increased by 5.5 – 28.9 times and by 5.5 – 23.7 times, respectively.

Another target for bacterial perfusion processes was the utilization of alternative substrates that originate from waste. Often these substrates contain inhibiting or even toxic substances or only dilute carbon concentrations, that makes their application in conventional fed-batch processes difficult (see sections 1.2 and 1.3). Inhibitors present in the substrate do not accumulate in perfusion processes (Akkoyunlu et al. 2021). Furthermore, lower substrate concentrations can be applied by increasing the feed rate.

The applicability of dilute substrates for bioproduction in MBR was shown in several studies for production of PHA with bacteria like *Bacillus megaterium* (Kacanski et al. 2022), *Cupriavidus necator* (Schmidt et al. 2016; Haas et al. 2017) or *E. coli* (Ahn et al. 2001). For example, Haas et al. (2017) achieved a high productivity of 3.1 g polyhydroxy butyrate (PHB) L^{-1} h^{-1} as well as a high cell density of 148 g/L with 76%wt PHB using a MBR with a dilute feed concentration of 50 g/L glucose.

Regarding the utilization of waste liquids as alternative substrates, Aloui et al. (2022) used crude glycerol as substrate for co-production of PHA and phenazines with *Pseudomonas chlororaphis* subsp *aurantiaca* in a MBR. There they achieved titers of 19.1 g/L PHA, which was 28.4-times higher than in batch culture, and a phenazine titer of 79.4 mg/L.

In another study of the same group Khomlaem et al. (2023) used sugars from lignocellulose

hydrolysis for production of PHA as well as PHA + asaxanthin with *Bacillus megaterium* and *Paracoccus* sp. LL1, respectively, in a MBR. By using a MBR they achieved 9 and 13-fold higher PHA and astaxanthin titers as well as 4 and 10-fold higher productivities of 0.58 and 0.39 g $L^{-1}h^{-1}$, respectively, in comparison to batch cultivations.
These examples demonstrate the suitability and benefits of perfusion cultures also for bacterial production processes.

1.7 Aim of the thesis

As most bacterial production processes rely on sugars as main carbon source (Wendisch et al. 2016), that are in competition with food and feed applications, it is important to find alternative carbon sources to achieve a biobased and sustainable industry (Lokko et al. 2018). As such, acetate has proven to be a suitable candidate, as it can be produced via sustainable means (Kiefer et al. 2021a), can be utilized by bacteria commonly used for bioprocessing (Arnold et al. 2019a) and is readily available (Mordor Intelligence 2023). Still, there are several challenges to its utilization. Acetate is inhibiting for most organisms at concentrations above 5 g/l, thus it must be fed to the process in a strictly controlled manner (Trček et al. 2015). As an acid acetate leads to decreasing pH when added during a fed-batch process, while its addition as salt quickly leads to osmotic stress due to the low solubility of sodium acetate (300 g/L). Furthermore, production of biobased acetate through sustainable means like lignocellulose conversion (Ko et al. 2020; Xinhua Shi et al. 2014; Arnold et al. 2017), C1-gas fixation (Kantzow et al. 2015) or electrosynthesis (Jourdin et al. 2015) results mostly in substrate solutions with dilute acetate concentrations. Thus, it is necessary to find novel process strategies that alleviate these restrictions. Regarding the suitable production organism, *C. glutamicum* was known to be able to utilize acetate as sole carbon source for a long time (Wendisch et al. 2000). Still, while some studies have shown unrestricted growth for acetate concentrations of up to 10 g/L and tolerance for even higher concentrations (Arnold et al. 2019a), no studies were published for bioproduction processes using this organism with acetate as sole carbon source. For these reasons the aim of this study was structured into two main objectives. The first objective was to examine the suitability of *C. glutamicum* for production of valuables using acetate as sole carbon source and to develop a fed-batch process for efficient feeding of acetate using this bacterium. As an exemplary product itaconic acid was selected, a C5 dicarboxylic acid, which can potentially be used for production of bioplastics, as biomedical compound and as additive for paints (Noh et al. 2018; Otten et al. 2015; Merkel et al. 2022). For production of itaconic acid a genetically engineered strain *C. glutamicum* ICD^{R453C} (pEKEx2-*malE*cad$_{opt}$) was used. The requirement for nitrogen limitation to achieve itaconic acid production added an additional difficulty (Otten et al. 2015). Therefore, the impact of different carbon to nitrogen (C-N) ratios on itaconic acid production was examined in shaking flask cultivations. Maximum specific growth rates, biomass, and product yields, itaconic acid titer and volumetric productivity were recorded. Next a fed-batch process with pH-coupled feeding of glacial acetic acid was adapted to the nitrogen limitation conditions necessary for itaconic acid production. As a result, the pH-coupled process was extended with a DO-coupled feeding of sodium acetate to achieve an enhanced production phase.

The second objective was the development of a perfusion bioreactor using 3D-printing as manufacturing method. A perfusion process was selected, because it allows utilization of dilute substrates and prevents accumulation of toxic substances or metabolites (Chmiel 2011). With this, direct utilization of sustainably produced acetate can be achieved. 3D-printing was selected as manufacturing method because it allows fast and inexpensive prototyping and high flexibility regarding design choices (Thompson 2022). As a first step suitable materials were selected depending on their chemical tolerances, mechanical properties, and compatibility with *C. glutamicum*. After the materials were selected, a perfusion bioreactor using hydrophilic membranes for cell retention, an oxygen transfer module based on membrane diffusion and a heat exchanger for temperature control was developed and characterized regarding oxygen transfer rate as well as mixing time. The final step was a proof-of-concept batch-perfusion hybrid cultivation with *C. glutamicum* ATCC 13032.

Chapter

2 Publications

2.1 Acetate-based production of itaconic acid with *Corynebacterium glutamicum* using an integrated pH-coupled feeding control

This article is published as original article:

Merkel, Manuel; Kiefer, Dirk; Schmollack, Marc; Blombach, Bastian; Lilge, Lars; Henkel, Marius; Hausmann, Rudolf (2022):

Acetate-based production of itaconic acid with *Corynebacterium glutamicum* using an integrated pH-coupled feeding control.

In: Bioresource Technology 351, S. 126994.
DOI: 10.1016/j.biortech.2022.126994.

This publication contains supplemental material which can be found at: https://doi.org/10.1016/j.biortech.2022.126994 Additionally, the supplemental material is included on the disc provided with this dissertation under the file-name "Supplementary Materials Publication 1".

Bioresource Technology 351 (2022) 126994

Contents lists available at ScienceDirect

Bioresource Technology

journal homepage: www.elsevier.com/locate/biortech

Acetate-based production of itaconic acid with *Corynebacterium glutamicum* using an integrated pH-coupled feeding control

Manuel Merkel [a], Dirk Kiefer [a], Marc Schmollack [b], Bastian Blombach [b,c], Lars Lilge [a], Marius Henkel [a,*], Rudolf Hausmann [a]

[a] University of Hohenheim, Institute of Food Science and Biotechnology, Department of Bioprocess Engineering, Fruwirthstrasse 12, 70599 Stuttgart, Germany
[b] Microbial Biotechnology, Campus Straubing for Biotechnology and Sustainability, Technical University of Munich, Straubing, Germany
[c] SynBiofoundry@TUM, Technical University of Munich, Straubing, Germany

HIGHLIGHTS

- Itaconate production with *C. glutamicum* on acetate as sole carbon source.
- Itaconate titer of 29.2 g/L was achieved using a pH and DO-coupled feeding strategy.
- Volumetric productivity (0.63 g $L^{-1}h^{-1}$) on acetate is competitive to glucose.
- Low buildup of salt concentration because base titration for pH-control is omitted.

GRAPHICAL ABSTRACT

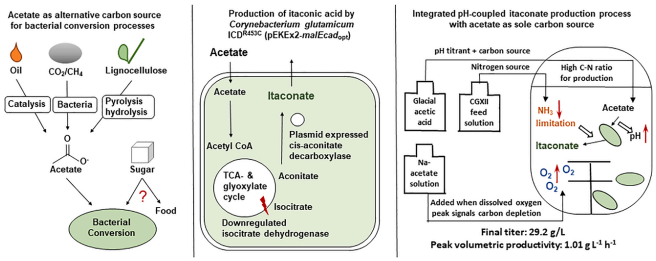

ARTICLE INFO

Keywords:
Itaconic acid
Bioeconomy
Corynebacterium glutamicum
Acetic acid
Fed-batch cultivation
Process control

ABSTRACT

To date, most bio-based products of industrial biotechnology stem from sugar-based carbon sources originating from food and feed competing resources. Exemplary for bioproducts converted from glucose, the potential C5 platform chemical itaconic acid is presently produced by the filamentous fungus *Aspergillus terreus*. Here, an engineered strain of the industrial platform organism *Corynebacterium glutamicum* ATCC 13032 was used for acetate-based production of itaconic acid to overcome current production difficulties. For this purpose, *C. glutamicum* ICD^{R453C} (pEKEx2-*malEcad*$_{opt}$) with a mutated *icd* variant for reduced isocitrate dehydrogenase activity was constructed harbouring pEKEx2-*malEcad*$_{opt}$, that includes a *cis*-aconitate dehydrogenase gene originating from *A. terreus*. Overall, a peak volumetric productivity of 1.01 g $L^{-1}h^{-1}$ was achieved resulting in an itaconate titer of 29.2 g/L, by using an integrated pH-coupled acetate feeding control in a fed-batch process without base titration. The results support the high potential of acetate as alternative substrate for bioproduction.

* Corresponding author.
E-mail address: Marius.Henkel@uni-hohenheim.de (M. Henkel).

https://doi.org/10.1016/j.biortech.2022.126994
Received 11 January 2022; Received in revised form 8 March 2022; Accepted 9 March 2022
Available online 11 March 2022

1. Introduction

With the growing awareness for sustainability and the shift to green production processes with lower impact on environment, biotechnological processes for conversion of renewable substrates increase in relevance. However, one drawback of most bioprocesses is the predominant use of carbon sources, which are generated from starch or sugar containing plants (e.g. sucrose or glucose). Usually, these plants are used for human nutrition or as animal feed, which results in an ethical problem (Philp, 2018). For this reason, utilizing alternative substrates that do not possess this problem but result in similar production capabilities has become an important research area. As such, acetate is one alternative substrate that offers advantages for application in biotechnology. Examples include the relatively low price and lack of competition in feed and food as discussed in detail by several authors (Blombach et al., 2021; Kiefer et al., 2021b; Novak and Pflügl, 2018). It is still mostly generated from fossil resources via processes like metal-catalyzed methanol carbonylation (Yoneda et al., 2001). However, a large number of alternative acetate production routes with higher sustainability do already exist or are currently under investigation. Pyrolysis (Arnold et al., 2017) or hydrolysis (Gong et al., 2016) of lignocellulosic biomass and fixation of CO_2 or CO via the acetogenic Wood-Ljundahl pathway are a few examples (Hu et al., 2013).

In recent years, utilization of acetate has gained attention in research as replacement for glucose as microbial carbon source, when several authors achieved high product yields for exemplary production of polyhydroxybutyrate (PHB) (Garcia-Gonzalez and De Wever, 2018) or succinate (Yuan Liu et al., 2011). However, microbial acetate conversion is challenging, as most microorganisms are already inhibited at low acetate concentrations (Trček et al., 2015).

The industrial platform bacterium *Corynebacterium glutamicum* is an example for a promising acetate-converting organism, that demonstrated high growth rates on moderate concentrations of acetate as sole carbon source (Arnold et al., 2019). Furthermore, high cell densities could be achieved with the wild-type strain *C. glutamicum* ATCC 13032 on acetate by using a novel pH-coupled fed-batch strategy, that was demonstrated in a previous work (Kiefer et al., 2021a). Continuing from there, the next goal was to investigate the effectiveness of this process strategy for production of value-added chemicals. Therefore, a genetically engineered strain of *C. glutamicum* was constructed, with the ability to convert acetate into the C5 chemical itaconic acid.

Under production conditions, itaconic acid is present in its dissociated form. As such, the term itaconate will subsequently be used.

Itaconate is a potential platform chemical that was considered to be between the twelve most promising biobased products, as its properties allow high value applications (Werpy and Petersen, 2004). It can be used as precursor for bioplastics (Ali and Kaneko, 2021), especially as bio-based replacement of acrylic acid, resins or coatings (Robert and Friebel, 2016; Trotta et al., 2019). Further applications exist in the textile industry (Boondaeng et al., 2021) and in the medical area as drug carrier or carrier with antimicrobial characteristics (Chiloeches et al., 2021). Currently, around 40.000 t of itaconate are produced annually mainly from glucose with the filamentous fungus *Aspergillus terreus*. It is produced by conversion of citric acid from the tricarboxylic acid (TCA) cycle first to *cis*-aconitate with the enzyme aconitase (ACO) followed by transformation to itaconate by *cis*-aconitate dehydrogenase (CAD) (Klement and Büchs, 2013). Although a volumetric productivity (P_V) of 0.99 g $L^{-1}h^{-1}$ can be achieved using this microorganism, resulting in a high titer of 160.0 g/L (Krull et al., 2017), it offers some drawbacks causing increased production costs. It is sensitive to shear stress and to fluctuations in oxygen supply, where even short-time oxygen depletion can lead to production stop for several hours (Saha, 2017). Furthermore, as an opportunistic human pathogen, *A. terreus* belongs to risk group 2 in some countries and requires special safety precautions (Schlembach et al., 2020). For this reason, different production hosts have been examined for their capability to produce itaconate: fungi like *Ustilago maydis* (Becker et al., 2020; Demir et al., 2021; Hosseinpour Tehrani et al., 2019) and bacteria such as *Escherichia coli* (Harder et al., 2018, 2016; Okamoto et al., 2014) and *Corynebacterium glutamicum* (Otten et al., 2015). Until now, the highest bacterial itaconate titer was achieved with *E. coli*. Harder et al. (2018) developed a temperature-controlled production strain and process achieving a titer of 46.9 g/L. In case of *C. glutamicum*, the potential of itaconate production was proven by Otten et al. (2015), who achieved a titer of 7.9 g/L in a batch cultivation with glucose as carbon source.

In this work, a genetically engineered strain of *C. glutamicum* ATCC 13032 was used for the first time to produce itaconate from the alternative carbon source acetate. The performance of the newly constructed strain *C. glutamicum* ICD^{R453C} (pEKEx2-$malEcad_{opt}$) was evaluated in shaking flask cultivations with different carbon to nitrogen (C-N) ratios. Insights from these experiments were used to adapt a previously published high cell density pH-stat process (Kiefer et al., 2021a) to achieve highest possible itaconate production. Further optimization led to a novel fed-batch process, that integrates pH and DO-coupled feeding strategies for production of itaconate under nitrogen limited conditions. Using glacial acetic acid for both pH-control and as carbon source eliminated the need for bases for pH titration, which potentially leads to reduced salt waste. With this process setup a maximum itaconate titer of 29.2 g/L could be achieved after 46.0 h, which is comparable to bacterial production processes on glucose (Harder et al., 2016). The results further support the potential of acetate as alternative substrate for microbial production processes, with *C. glutamicum* being a major candidate as industrial production organism.

2. Materials and methods

2.1. Chemicals and materials

If not stated otherwise, the chemicals used in this work were obtained from Carl Roth GmbH (Karlsruhe, Germany). Morpholino propanesulfonic acid (MOPS, order number 1081) as buffering agent was obtained from GERBU Biotechnik GmbH (Heidelberg, Germany). The antifoam agent was gifted by Zschimmer & Schwarz GmbH & Co KG (Lahnstein, Germany). Enzymatic assay kits from R-biopharm AG (Darmstadt, Germany) were obtained for analysis of ammonia (Cat No. 11112732035) and acetate (Cat. No. 10148261035).

2.2. Bacterial strain and strain engineering

Escherichia coli strains were cultured in 2xYT medium (16 g/L tryptone, 10 g/L yeast extract, 5 g/L NaCl; (Green and Sambrook, 2012) at 37 °C for 16.0 – 20.0 h and supplemented with 50 µg/L kanamycin sulfate as needed. *Corynebacterium glutamicum* was grown in 2xYT medium or BHIS medium (37 g/L BHI, 91 g/L sorbitol) at 30 °C for 16.0 – 20.0 h in liquid medium or 2–3 days on agar-plates. Solid medium was prepared by addition of 18 g/L agar to liquid medium. *E. coli* DH5α (Hanahan, 1983) was used for maintenance of plasmids. Plasmid DNA from *E. coli* was prepared using the "NucleoSpin® Plasmid" kit purchased from MACHEREY-NAGEL GmbH & Co. KG (Düren, Germany). Genomic exchange of isocitrate dehydrogenase (ICD) to the mutated variant ICD^{R453C} in *C. glutamicum* ATCC 13032 was achieved by a double cross-over event followed by positive–negative selection on BHIS plates supplemented with kanamycin and 2xYT plates supplemented with 10% (w/v) sucrose, respectively (Schäfer et al., 1994). Therefore, electrocompetent *C. glutamicum* ATCC 13032 were prepared according to Tauch et al. (2002) and transformed with pK19*mobsacB*-ICD^{R453C} (Schwentner et al., 2018) by electroporation (van der Rest et al., 1999). Successful mutation was analyzed by colony PCR using "Q5® High-Fidelity DNA Polymerase" purchased from New England Biolabs GmbH (Frankfurt, Germany) including the primers oMS-ICD1 (5′-TTACTTCTTCAGTGCGTCAACG-3′) and oMS-ICD2 (5′-ATGGCTAA-GATCATCTGGACC-3′). A "NucleoSpin® Gel and PCR Clean-up" kit

purchased from MACHEREY-NAGEL GmbH & Co. KG (Düren, Germany) was used for purification of PCR products. The subsequent sequencing was performed with the sanger-sequencing method by Eurofins Genomics GmbH (Ebersberg, Germany) with oMS-ICD3 (5'-TGTAGTCACGCAGAACGTTACC-3') using "TubeSeq Service". A positive clone was used to produce electrocompetent *C. glutamicum* ICD^{R453C} as described above, followed by transformation with pEKEx2-*malEcad*$_{opt}$ (Otten et al., 2015). Generally, all kits listed in this section were used according to the manufacturer's protocols.

2.3. Cultivation media

The bacterial strain was stored as 25% (v/v) glycerol stocks at −80 °C. 2xYT medium supplemented with 5 g/L Na-acetate was generally used for first precultures. Acetate was added sterile from an autoclaved stock solution containing 277 g/L Na-acetate. For consecutive cultures modified CGXII minimal medium based on the composition of Keilhauer et al. (1993) was used. Kanamycin sulfate (25 µg/mL) was generally used as a selection marker.

Modified medium composition $CGXII_{Fl}$ was used (pH 6.8) for shaking flask cultivations to investigate the influence of different molar C-N ratios on growth and itaconate production:

13.7 g/L Na-acetate, 1 g/L KH_2PO_4, 1 g/L K_2HPO_4, 0.25 g/L $MgSO_4 \times 7\ H_2O$, 0.01 g/L $CaCl_2 \times 2\ H_2O$, 21 g/L MOPS, 0.2 mg/L D-biotin, 0.06 g/L protocatechuic acid (PCA) and 1 mL/L trace element solution (TES). TES was composed of 10 g/L $FeSO_4 \times 7\ H_2O$, 10 g/L $MnSO_4{\cdot}H_2O$, 1 g/L $ZnSO_4 \times 7\ H_2O$, 0.2 g/L $CuSO_4$ and 0.02 g/L $NiCl_2 \times 6\ H_2O$ (pH acidified with HCl). Different concentrations of $(NH_4)_2SO_4$ (10 g/L, 2.2 g/L, 1.1 g/L, 0.56 g/L, 0.37 g/L) resulting in C-N ratios of 2, 10, 20, 40 and 60 mol/mole were added as nitrogen source. The second preculture medium was prepared with 5 g/L $(NH_4)_2SO_4$. For fed-batch bioreactor cultivations the medium composition was further modified, resulting in modified $CGXII_{BR}$ minimal medium (pH 6.8): 13.7 g/L Na-acetate, 1 g/L KH_2PO_4, 1 g/L K_2HPO_4, 2.8 g/L $(NH_4)_2SO_4$, 1.25 g/L $MgSO_4 \times 7\ H_2O$, 0.01 g/L $CaCl_2 \times 2\ H_2O$, 21 g/L MOPS, 0.2 mg/L D-biotin, 0.06 g/L PCA and 2 mL/L TES. Additionally, 1 mL/L antifoam was added to the main bioreactor cultivations. Modified $CGXII_{BR}$ medium was always freshly prepared, as it tends to precipitate after prolonged storage.

During the fed-batch phase, a total number of three different feed solutions were used. Feed solution 1 contained pure glacial acetic acid serving as pH control titrant and acetate supply, simultaneously. For addition of nitrogen source and replenishment of salts, CGXII feed solutions consisting of 10 g/L KH_2PO_4, 10 g/L KH_2PO_4, 2 mg/L D-biotin and either 105.0 g/L (C-N ratio of 10 mol/mole) or 26.3 g/L urea (C-N ratio of 40 mol/mole) were prepared. Feed solution 3 was composed of 300 g/L Na-acetate. The complete feeding strategy is described in more detail in chapter 2.4.3. During medium preparation, the components $CaCl_2 \times 2\ H_2O$, $MgSO_4 \times 7\ H_2O$, $(NH_4)_2SO_4$, PCA, biotin, isopropyl-β-D-thiogalactopyranosid (IPTG), kanamycin sulfate and TES were always added aseptically from stock solutions.

2.4. Cultivation conditions

2.4.1. Inoculum preparation

Two consecutive precultures were performed in baffled shaking flasks filled with 10% (v/v) medium for preparation of the inoculum. Shaking flask cultivations were generally performed at 30 °C and 120 rpm in an incubator shaker (New Brunswick™/Innova® 44, Eppendorf AG, Hamburg, Germany). 100 µL bacterial glycerol stock were used for inoculation of first precultures of *C. glutamicum* ICD^{R453C} (pEKEx2-*malEcad*$_{opt}$) in 250 mL baffled shaking flasks with 25 mL of 2xYT medium + 5 g/L Na-acetate. After 24.0 – 25.0 h of incubation, 2% ($v/v_{2nd\ preculture}$) were used to inoculate 25 mL of the second preculture with respective modified $CGXII_{FL}$ minimal medium composition in a shaking flask followed by incubation for another 24.0 – 25.0 h. For bioreactor cultivations the medium volume was increased to 700 mL separated to two 3 L shaking flasks.

2.4.2. Cultivations in shaking flasks

Cultivations in 500 mL shaking flasks with 10% (v/v) medium were performed to examine growth and production capabilities of *C. glutamicum* ICD^{R453C} (pEKEx2-*malEcad*$_{opt}$) at different C-N ratios. Therefore, modified $CGXII_{Fl}$ minimal media with a constant acetate concentration of 10 g/L and varying C-N ratios (2, 10, 20, 40 and 60 mol/mol) were prepared. To induce itaconate production, 1 mM IPTG was added at the beginning of the cultivation. Main cultures were inoculated to a starting optical density (OD_{600nm}) of 1 and performed as biological triplicates.

2.4.3. Fed-batch cultivations in bioreactors

Fed-batch experiments were conducted in 42 L custom-built bioreactors (Zeta GmbH, Graz/Lieboch, Switzerland) that were previously described by Hoffmann et al. (2020). They were fitted with probes for online data measurement of pH (EasyFerm Bio HB Arc 120, Hamilton Bonaduz AG, Bonaduz, Switzerland) and dissolved oxygen concentration (DO) (VisiFerm DO ARC 120 Ho, Hamilton Bonaduz AG, Bonaduz, Switzerland). During the growth phase, DO was controlled to 30% by increasing the stirring rate (200 – 900 rpm) and air flow (2 L/min – 20 L/min). At higher cell densities a sufficient supply of oxygen was ensured by enriching the pressurized air with oxygen. When switching to DO-coupled feeding, stirring rate and air flow were fixed to 900 rpm and 20 L/min, respectively. Cultivation temperature was controlled to 30 °C. To start a cultivation, 700 mL of inoculum were transferred to the bioreactor resulting in a starting OD_{600nm} of 1. The experiments were carried out with a starting volume of 10 L including the inoculum. Furthermore, 1 mM IPTG was added to the medium directly at the beginning of the cultivation. Since IPTG is a gratuitous induction molecule and is not metabolized, a concentration of 1 mM should be sufficient to activate the corresponding promotor system throughout the cultivation process. In this way, a strong constitutively active promotor could be simulated. During pH-coupled feeding, glacial acetic acid was added as titrant by the pH-control. A feeding program written in the numerical computing environment MATLAB (release 2020b, The MathWorks, Natick, MA, USA) correlated the addition of CGXII feed solutions to the addition of glacial acetic acid by comparing weight differences of the respective storage bottles, as described before by Kiefer et al. (2021a). The pH control was thus set to 7.2 ± 0.1 and first started, when the pH increased to 7.3. During the additional DO-coupled feeding phase, feed solution 3 with 300 g/L Na-acetate was added in pulses to achieve an acetate concentration of around 5.0 – 6.0 g/L. The rise in DO above 80% signalized the depletion of acetate in the medium. For better demonstration, Fig. 1 shows a flow scheme visualizing the control mechanisms leading to feed additions.

2.5. Sampling and offline analytics

Samples were taken in regular intervals for all cultivations performed. Growth was monitored by measuring the OD_{600nm} using a spectrophotometer (Biochrom WPA CO8000, Biochrom Ltd., Cambrigde, United Kingdom). Saline was used as blank as well as for diluting when necessary. Dry biomass concentrations were correlated to OD_{600nm} using the predetermined correlation factor of 4.3 found in a previous work (Kiefer et al., 2021a). For analysis of substrate and product concentrations, 1 mL cell free culture supernatant was prepared and stored at −20 °C for each sample. Therefore, 1 mL freshly harvested sample was centrifuged for 10 min at 14,000 rpm and 4 °C (5430 R, Eppendorf AG, Hamburg). Acetate and ammonium concentrations were analyzed spectrophotometrically (Genesys 150 UV/Vis, Thermo Fisher Scientific GmbH, Braunschweig, Germany) using enzymatic assay kits from R-Biopharm AG (Darmstadt, Germany), according to the manufacturer's protocols. Itaconate concentration in the supernatant was analyzed using the spectrophotometric method of Hartford (Hartford, 1962)

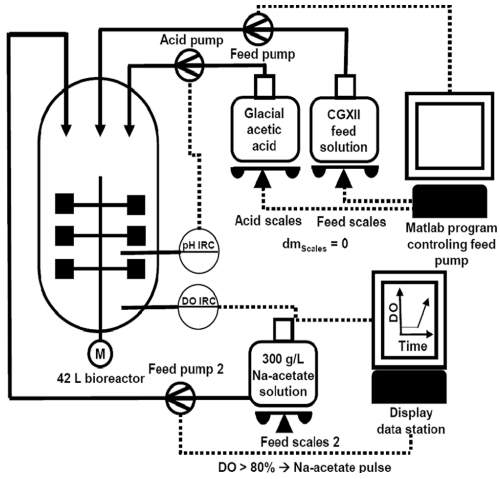

Fig. 1. Flow diagram of the control strategy for pH and DO-coupled feeding of acetate for bacterial conversion to itaconate. Addition of glacial acetic acid is directly coupled to online pH control. A matlab program is used to feed the same amount of CGXII-feed solution as acid, by compensating weight differences (dm_{Scales}). Additional feeding of a Na-acetate solution is coupled to culture DO. Acetate depletion leads to a rise of DO above a threshhold (80%), which is used as signal for pulsed Na-acetate feeding. In that way acetate is replenished, without lowering pH. The availability and consumption of acetate causes a drop in DO and a rise in pH, that continues the pH coupled feeding.

adapted to well plate format. Therefore, 100 µL sample volume was mixed with 130 µL pyridine. Next, 575 µL acetic anhydride was added and the solution incubated at 32 °C and 1500 rpm for 30 min in a thermo shaker (ThermoMixer C, Eppendorf AG, Hamburg, Germany). A colored complex is formed by addition of acetic anhydride and pyridine to itaconate, which absorbs light at 385 nm. In an interval of 0.1 g/L to 0.006 g/L the absorbance has a linear correlation to itaconate concentration. For spectrophotometric analysis 300 µL of each sample was transferred to a well of a 96 well plate. Absorbance was measured in a plate reader (Multiscan GO, Thermo Fisher Scientific Oy, Vantaa, Finland). Itaconate concentrations were calculated using a calibration curve (0.1, 0.075, 0.05, 0.025, 0.0125, 0.006 and 0 g/L itaconate) that was run with each analysis.

2.6. Data analysis

Following growth parameters were determined for evaluation of cultivations and for easier comparison. Linear regression of a semi-logarithmic plot of OD_{600nm} against time was used for determination of maximum specific growth rates μ_{max} [h^{-1}]. Maximum product yield $Y_{P,Smax}$ [$g_{itaconate}/g_{acetate}$] and biomass yield $Y_{X,Smax}$ [$g_{biomass}/g_{acetate}$] were calculated using the mass of itaconate (dm_p) or biomass (dm_x) accumulated and the amount of acetate consumed during the same time (dm_s) using linear regression of a corresponding graph. Final yields were calculated using the maximum mass differences over the course of the complete cultivation. Volumetric productivity over a certain amount of time (P_{Vi}) was determined by linear regression of a plot of product concentration over time, while overall volumetric productivity (P_V) was calculated by dividing the final itaconate concentration with the total process time.

3. Results and discussion

3.1. Effect of different C-N ratios on growth and itaconate production in shaking flask cultivations

C. glutamicum was engineered for the production of itaconate by introducing the ICD variant R453C, which possesses 29% activity in comparison to the wild-type enzyme (Schwentner et al., 2018). Furthermore, expression vector pEKEx2 was used for plasmid-based expression of the codon-optimized *cis*-aconitate dehydrogenase (CAD) gene from *A. terreus* fused to the gene encoding the maltose-binding protein as described in detail by Otten et al. (2015).

To evaluate growth and production capabilities of the newly constructed strain *C. glutamicum* ICD^{R453C} (pEKEx2-$malEcad_{opt}$), shaking flask cultivations were performed with acetate as sole carbon source in modified $CGXII_{FL}$ minimal medium. Nitrogen limitation is necessary for initiating itaconate production, as demonstrated by Otten et al. (2015). For this purpose, varying ammonium concentrations were tested to study the effect of different molar C-N ratios on growth and itaconate production. The C-N ratios tested were C-N 2 mol/mole, which was the ratio of the original medium composition without limitation, as well as C-N 10 to 60 mol/mole. Graphs for biomass and product concentration of each C-N ratio are shown in Fig. 2. A summary of the calculated parameters is given in Table 1.

Under standard conditions without nitrogen limitation, μ_{max} of strain *C. glutamicum* ICD^{R453C} (pEKEx2-$malEcad_{opt}$) on 10 g/L acetate was reduced by around 28% compared to that of wild type strain ATCC 13032 (μ_{max} = 0.45 h^{-1}), as shown in a previous study (Kiefer et al., 2021a). The lowered μ_{max} is most likely an effect of downregulated ICD activity. Although the glyoxylate cycle is highly active during growth on acetate as a way to replenish oxaloacetate and supply precursors for gluconeogenesis, a majority of the accumulated carbon is still metabolized through the TCA cycle (Wendisch et al., 2000). The mutation in the *icd* gene could have led to reduced growth rates due to the decreased flux through the common TCA pathway. With increasing C-N ratio, μ_{max} as well as biomass concentrations were found to decrease from maximum values of 0.34 h^{-1} and 3.7 g/L (C-N ratio of 2 mol/mole) to a minimum of 0.20 h^{-1} and 1.8 g/L (C-N ratio of 60 mol/mole). These results are in line with findings of Otten et al. (2015), who used a similar strain for

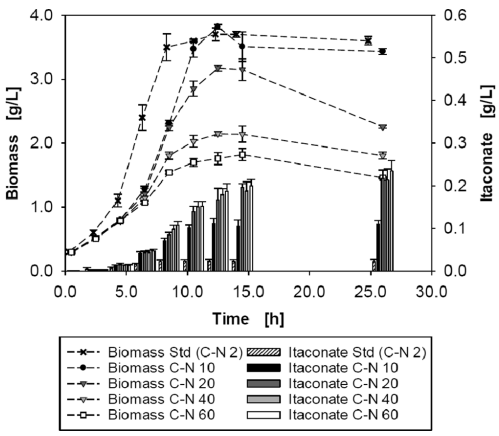

Fig. 2. Time courses of biomass (symbols) and itaconate (bars) concentration during shaking flask cultivations of *C. glutamicum* ICD^{R453C} (pEKEx2-$malEcad_{opt}$) with varying C-N ratios. Acetate was used as sole carbon source and C-N ratios of 2, 10, 20, 40 and 60 mol/mole were tested. Error bars represent the standard deviation of biological triplicates.

Table 1
Overview over cultivation parameters determined in shaking flask cultivations of *C. glutamicum* ICD^{R453C} (pEKEx2-*malEcad*$_{opt}$) on acetate as sole carbon source. The effect of the C-N ratio on itaconate production was investigated by varying the concentration of $(NH_4)_2SO_4$.

C-N ratio [mol/mol]	max. biomass concentration [g/L] [d]	μ_{max} [h^{-1}] [b]	$Y_{X,S}$ [g/g] [a]	$Y_{P,X}$ [g/g] [a]	$Y_{P,S}$ [g/g] [a]	max. productivity [g $L^{-1}h^{-1}$] [c]	titer [g/L]
2 (Standard)	3.7 ± 0.1	0.34 ± 0.00	0.35 ± 0.01	0.01 ± 0.00	0.00 ± 0.00	0.00 ± 0.00	0.0 ± 0.0
10	3.9 ± 0.0	0.25 ± 0.00	0.30 ± 0.00	0.03 ± 0.00	0.02 ± 0.01	0.02 ± 0.00	0.1 ± 0.0
20	3.2 ± 0.1	0.22 ± 0.00	0.28 ± 0.03	0.07 ± 0.00	0.02 ± 0.00	0.02 ± 0.00	0.2 ± 0.0
40	2.2 ± 0.0	0.22 ± 0.00	0.23 ± 0.03	0.09 ± 0.01	0.02 ± 0.00	0.02 ± 0.00	0.2 ± 0.0
60	1.8 ± 0.1	0.20 ± 0.00	0.28 ± 0.02	0.11 ± 0.02	0.03 ± 0.00	0.02 ± 0.00	0.2 ± 0.0

[a] Calculated from maximum concentrations over the course of the cultivation.
[b] Calculated by linear regression of a semi-logarithmic plot of biomass concentration against time.
[c] Determined by linear regression of constant product increase in a plot of itaconate concentration against time.
[d] Calculated from optical densities measured at 600 nm using a predetermined correlation factor of 4.3.

production of itaconate on glucose as carbon source. Under non-limiting conditions they also observed a reduction of growth rate from 0.41 1/h to 0.33 1/h, which was reduced further to 0.19 1/h under nitrogen limited conditions. This confirms that the growth rate reduction observed for *C. glutamicum* ICD^{R453C} (pEKEx2-*malEcad*$_{opt}$) is not caused by the presence of acetate as potentially inhibitory substrate. It is also in accordance with a finding made in an earlier study, that acetate shows no growth inhibiting effect at concentrations of up to 10 g/L (Kiefer et al., 2021a).

According to the elemental biomass composition of *C. glutamicum* ($CH_{1.78}O_{0.68}N_{0.18}$) (Eggeling and Reyes, 2005) a C-N ratio higher than 5 mol/mole should lead to nitrogen limited conditions and lowered biomass formation. Even at the highest nitrogen limitation tested (C-N ratio = 60 mol/mole), a biomass concentration of 1.8 g/L was still reached, which is about half of the concentration at a C-N ratio of 2 mol/mole. This might be explained by the fact, that metabolic pathways are adapted to conserve nitrogen reserves under nitrogen limited or depleted conditions. These adaptations include increased transport of nitrogen sources as well as protein degradation to allow growth even under strong nitrogen limitation or depletion (Burkovski, 2007; Silberbach et al., 2005).

In contrast to biomass formation, volumetric productivity of itaconate as well as its $Y_{P,S}$ were shown to increase with higher C-N ratios, reaching a maximum of 0.02 g $L^{-1}h^{-1}$ and 0.03 g/g at a C-N ratio of 60 mol/mole, respectively.

While $Y_{P,S}$ increased slightly from 0.02 g/g at C-N of 10 mol/mole to 0.03 g/g at C-N 60 and $Y_{P,X}$ from 0.03 g/g to 0.11 g/g, P_V did not increase further for the C-N ratios tested above 20 mol/mole. Surprisingly, the itaconate titer did not change much at C-N ratios of 60 and 40 mol/mole, where 30% of the acetate starting concentration was still available after 14.0 h of cultivation. This could indicate that a certain amount of nitrogen is required to maintain cell viability and product formation. When comparing the itaconate yields on acetate to yields described by Otten et al. (2015) on glucose as carbon source, the latter was drastically higher (0.29 g/g in comparison to 0.02 g/g). However, it must be considered that production on glucose in Otten et al.'s work started first after ~ 10 h of cultivation during stationary phase, due to a high initial glucose concentration of 40 g/L. The higher number of generations might have led to a higher plasmid propagation for CAD overexpression and thus to an increased itaconate biosynthesis. Therefore, the data for both substrates might be more comparable under similar production conditions and longer cultivation times.

3.2. Combined pH and DO-coupled fed-batch process for optimized itaconate production

Next, the aim was to develop an acetate-based itaconate production process in a 42 L bioreactor, based on a previously published high cell density process (Kiefer et al., 2021a). For this, a two-phase fed-batch cultivation strategy containing a biomass formation (C-N ratio of 10 mol/mole) and itaconate production phase (C-N ratio of pH-coupled feed solutions = 40 mol/mole + additional DO-coupled feeding of Na-acetate) was chosen. As demonstrated in the study, acetate feeding during the fed-batch phase was coupled to pH by using glacial acetic acid for online pH control. The C-N ratio of 10 mol/mole was chosen for the growth phase, as it resulted in the highest biomass concentration of 69.8 g/L for *C. glutamicum* ATCC 13032 wildtype (Kiefer et al., 2021a). The C-N ratio between the feeds was increased to 40 mol/mole at a cell density of 19.1 g/L (OD_{600nm} = 80) to initiate nitrogen limitation and the production phase. While productivity and final titer were similar for a C-N ratio of 20 mol/mole in shaking flask cultivations, a ratio of 40 mol/mole was chosen to separate biomass growth and production more than would be possible with a C-N ratio of 20 mol/mole, by providing higher nitrogen limitation. It should be noted that the principle of growth-decoupled production phase is commonly used in biotechnological processes to achieve higher product yields. A ratio of 60 mol/mole, on the other hand, could be insufficient for maintaining cellular activity.

When only a pH-coupled feeding control was used in early experiments (see supplementary materials), the acetate concentration was found to constantly decrease during the itaconate production phase until complete consumption after only 4.0 h of production. The reasons for this might be low ammonia supply and itaconate production, both leading to an acidification of the culture medium. The acidification counteracts the pH increase necessary for acetic acid feeding. Therefore, an additional DO-coupled feeding control was integrated within the production phase after first depletion of acetate. Once acetate was completely consumed and the DO concentration rose, a concentrated Na-acetate solution (300 g/L) was added to the medium. Na-acetate was a way of replenishing the carbon source without effecting pH directly. Consequently, acetate consumption then led to a rising culture pH again and with that to the continuation of the pH-coupled feeding principle. The DO served as a signal for acetate depletion and for pulsed feeding of the additional Na-acetate solution.

Graphs for cultivation parameters are shown in Fig. 3. A summary of the determined process parameters for growth and production phase is given in Table 2.

During the initial batch phase (t = 8.6 h) without pH-control, the biomass concentration of *C. glutamicum* ICD^{R453C} increased to 1.7 g/L (see Fig. 3a). At the same time, consumption of acetate (Fig. 3b) caused an increase in culture pH (Fig. 3c). The pH control was started after the pH increased to 7.3 to initiate the pH-coupled feeding phase for biomass production (C-N ratio between feeds of 10 mol/mole). μ_{max} was at 0.24 h^{-1} until the beginning of the fed-batch phase (t = 10.1 h), where it slowly declined to 0.20 h^{-1}. Opposite to that, the $Y_{x,s}$ was stable at 0.36 g/g during the whole growth phase (t = 20.0 h). Itaconate production was at a minimum during the early biomass production phase with an itaconate concentration of only 0.7 g/L after 16.0 h, as enough nitrogen was supplied (shown in Fig. 3b). In the following time itaconate concentration got tripled to 2.3 g/L after 19.4 h. This increase was

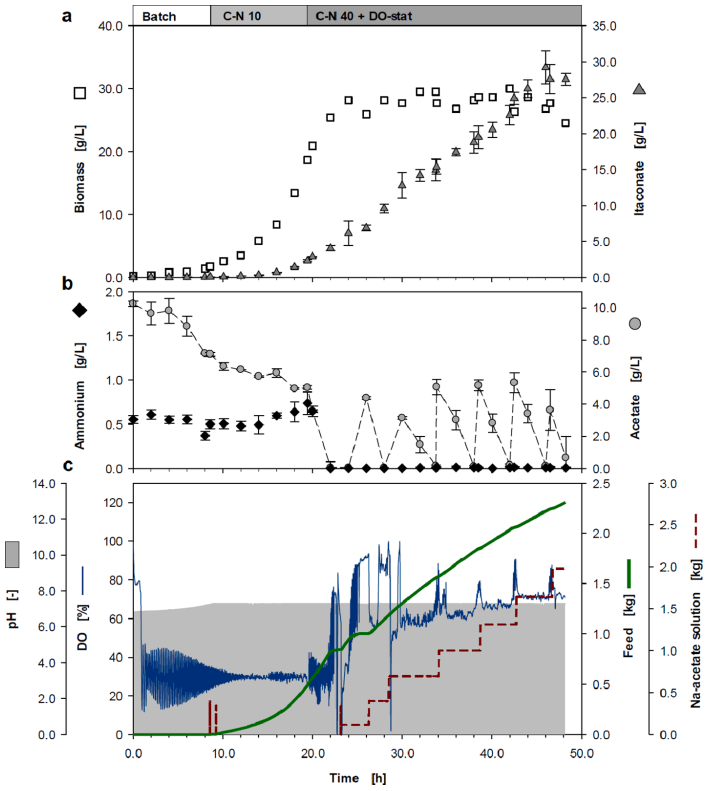

Fig. 3. Plots of cultivation data of a two-phase fed-batch process for acetate-based production of itaconate with *C. glutamicum* ICD^{R453C} (pEKEx2-*malEcad*$_{opt}$) using an integrated pH and DO-coupled strategy for addition of acetic acid and Na-acetate. A pH-coupled fed batch phase with a C-N ratio between the feed solutions of 10 mol/mole was used for initial biomass formation. After 19 g/L of biomass were accumulated, the production phase was started by applying a C-N ratio between the feeds of 40 mol/mole and by starting an additional DO-coupled feeding of a Na-acetate solution. Graph (a) shows the timecourse of biomass (white squares) and itaconate (grey triangles) concentration. Graph (b) shows the timecourse of ammonium (black diamonds) and acetate concentration (grey circle) and (c) plots of pH (grey area), DO (blue line), mass of feed added (green line) and mass of Na-acetate added (red intermittent line). Error bars demonstrate standard deviation for analytical triplicates.

Table 2
Comparison of cultivation parameters determined in a two-phase fed-batch process for acetate-based production of itaconate with *C. glutamicum* ICD^{R453C} (pEKEx2-*malEcad*$_{opt}$) using an integrated pH and DO-coupled strategy for addition of acetic acid and Na-acetate, respectively.

	biomass phase	production phase	overall
process time [h]	19.4	26.6	46.0
$c_{biomass,max}$ [g/L] [a]	19.1	30.7	30.7
μ_{max} [h^{-1}] [a]	0.24	0.07	–
$Y_{X,S}$ [g/g] [a]	0.36	0.06	0.16
IA titer [g/L]	2.3	29.2	29.2
$Y_{P,S}$ [g/g] [a]	0.04	0.21	0.16
productivity [g $L^{-1}h^{-1}$] [a]	0.12	1.01	0.63

[a] See description of footnotes at Table 1.

potentially caused by the increase in biomass from 8.6 to 19.1 g/L combined with a slight nitrogen limitation. After reaching an OD_{600nm} of roughly 80 (19.1 g/L CDW after 19.4 h), the C-N feeding ratio was adjusted from 10 to 40 mol/mole to induce more severe nitrogen limitation and the itaconate production phase. This led to quick consumption of the remaining ammonium concentration of around 0.6 g/L, while the biomass concentration still increased to a maximum of 29.8 g/L. At the same time, the itaconate titer increased to 4.0 g/L and acetate declined from 5.0 g/L (t = 19.4 h) to complete consumption after a process time of 23.0 h.

At that point, an increase in DO above 80% signalized the start of the additional DO-coupled feeding. Therefore, manual feeding of the Na-acetate solution was repeated every time the DO was higher than 80%, as can be seen by the acetate spikes (Fig. 3b) that correlate to the DO spikes (Fig. 3c). After the first addition of acetate salt, nitrogen was depleted, only being added by the C-N 40 CGXII-salt feed. This was sufficient to prevent the biomass from increasing, while keeping the cells active. Thus, the biomass concentration stayed stable between 26.5 and 30.7 g/L with only small fluctuations. Only within the last few hours of process time a tendency of decreasing biomass concentration was detected. This may indicate that an increased ammonia supply might be necessary to sustain the biomass for a longer cultivation time. However, as visible in Fig. 3a, the itaconate titer increased in a seemingly linear manner during the prolonged production phase yielding a final titer of 29.2 g/L after 46.0 h and a maximum volumetric itaconate productivity of 1.01 g $L^{-1}h^{-1}$. During production phase $Y_{P,S\ max}$ of itaconate was at 0.21 g/g, which is 30% of the maximum theoretically possible product yield of 0.73 g/g (Noh et al., 2018). Overall, this process achieved a final itaconate titer of 29.2 g/L with an overall $Y_{P,S}$ of 0.16 g/g and a P_V of 0.63 g $L^{-1}h^{-1}$.

Compared to the only available acetate-based itaconate production process from Noh et al. (2018), which produced 3.6 g/L itaconate using an engineered strain of *E. coli* and a pulsed feeding strategy, the bioprocess presented in this study can be regarded as more efficient. With respect to process performance, using *C. glutamicum* as production host and a fed-batch process with integrated pH and DO-coupled feeding control led to an 8-fold higher titer, 1.8-fold higher final $Y_{P,S}$ (0.16 g/g in

comparison to 0.09 g/g), and more than 10-fold higher P_v (0.63 g $L^{-1}h^{-1}$ in comparison to 0.04 g $L^{-1}h^{-1}$). This already demonstrates the potential of *C. glutamicum* for itaconate production, but also for product conversion of acetate in general.

The achieved titer of 29.2 g/L is also comparable to bacterial itaconate production processes based on glucose as carbon source (see supplementary materials). For instance, Harder et al. (2016) achieved a similar titer of 32.0 g/L on glucose as sole carbon source using a modified strain of *E. coli*. The authors used a model-based approach to genetically enable and improve itaconate production by implementing five interventions. In addition, their more recent thermo switch process achieved a higher final titer of 46.9 g/L using a strain of *E. coli* with temperature-controlled repression of *icd* (Harder et al., 2018).

In both works, Harder et al. achieved $Y_{P,S}$ between 0.45 and 0.49 g/g. These were higher than the $Y_{P,S}$ of 0.16 g/g, observed in this work with *C. glutamicum* ICD^{R453C} (pEKEx2-*malEcad*$_{opt}$) on acetate as carbon source (both carbon sources result in a maximum theoretical yield of ~ 0.7 g/g). However, a 2.3-fold and 1.6-fold higher volumetric productivity of 0.63 g $L^{-1}h^{-1}$ was achieved in the present work, in comparison to their results (P_V = 0.27 g $L^{-1}h^{-1}$ (Harder et al., 2016) and 0.39 g $L^{-1}h^{-1}$ (Harder et al., 2018).

A similar conclusion can be drawn for itaconate production with fungi.

With *U. maydis* a 2.6-fold higher $Y_{P,S}$ of 0.41 g/g was achieved by Demir et al. (2021). However, the P_V of 0.79 g $L^{-1}h^{-1}$ and $P_{V,max}$ of 1.01 g $L^{-1}h^{-1}$ are comparable to the results achieved in this work, especially considering the 2.5-fold longer process time (t = 112.8 h) that led to a titer of 88.4 g/L and thus higher P_V (Demir et al., 2021).

A lower $Y_{P,S}$ was partially expected with this production strain using acetate as carbon source. In comparison to growth on glucose, the glyoxylate cycle is active besides the common TCA pathway during growth on acetate as carbon source. Thus, an inhibition of ICD through mutation, has a lower impact on the aconitate pool as isocitrate is further transformed to glyoxylate (Gerstmeir et al., 2003). Regarding the industrially established production host *A. terreus*, there is still room for improvement, as a P_V of 0.99 g $L^{-1}h^{-1}$ resulting in a titer of 160.0 g/L and a $Y_{P,S}$ of 0.46 g/g and were achieved with this fungus (Krull et al., 2017).

In summary, a drawback of the process is the rather low $Y_{P,S}$, while the main advantage is the high P_V, that seemed to be stable for over 22.0 h and did not decline at the end of the 46-h process time. This suggests that continuing the process for a longer time, might lead to higher product titers as long as the cells can be kept active. A lower accumulation of salt is another promising benefit in comparison to conventional processes, as no base titration is necessary to counter the acidification resulting from itaconate production. With respect to downstream processing, this can reduce cost for salt waste. Furthermore, it can improve itaconate recovery, as itaconate is mainly purified by two consecutive crystallization steps through evaporation and cooling (López-Garzón and Straathof, 2014). Besides lower salt accumulation in the culture medium, the acetate-based process offers another advantage for downstream processing. It is stated in literature that residual glucose from upstream processing leads to reduced itaconate recovery due to interference with itaconate crystallization (Zhang et al., 2009). With the process developed in this work, acetate is quickly depleted, when the DO-controlled feeding is stopped. Furthermore, if acetate is still available after fermentation, it might be evaporated during the crystallization process, as its boiling point of 118 °C is close to water.

Overall, this study marks a first step in establishing *C. glutamicum* as host of itaconate, but also as general producer with acetate as sole carbon source. Until now, only few bacterial acetate-based processes have been published, where product titers higher than 10.0 g/L were achieved (Garcia-Gonzalez and De Wever, 2018; Huang et al., 2018), and none with *C. glutamicum*. The itaconate titer of 29.2 g/L shows the potential of bacterial processes with acetate to achieve a performance comparable to their glucose-based counterparts. It must be considered that most of the other bacterial strains already underwent several steps of genetic optimization, while the strain *C. glutamicum* ICD^{R453C} (pEKEx2-*malEcad*$_{opt}$) was engineered with mostly basic modifications necessary for itaconate production. Genetic adjustments potentially lead to better overall performance. Thus, a strain engineering approach might target several aspects like improving acetate consumption under nitrogen limited conditions. During the experiments a reduction in specific acetate consumption from 0.5–0.6 g $g^{-1}h^{-1}$ to 0.2–0.3 g $g^{-1}h^{-1}$ could be observed after nitrogen was depleted. A reduction of active acetate uptake is a known reaction to nitrogen limitation, in order to conserve energy and nitrogen reserves (Silberbach et al., 2005). In that regard, a release of active acetate transport from metabolic regulation might be a starting point for further genetic engineering approaches targeting productivity. Other options might be overexpressing the *acn* gene encoding aconitase, as realized by Okamoto et al. (2014) to improve itaconate production with *E. coli*, or mutating the isocitrate lyase gene *icl* to reduce flux in the glyoxylate cycle. Besides carbon fluxes, itaconate transport across the cell wall is another point of optimization. Otten et al (2015) found that intracellular itaconate levels started to surpass the extracellular itaconate concentration after 24.0 – 48.0 h of production with *C. glutamicum* and related this to transport limitation at higher productivities. This limitation could be released by expression of itaconate transporters from *A. terreus*. For industrial application genomic integration of *cad* or promotor exchange to a constitutive promoter might be promising to reduce cost for supplements like IPTG needed for gene expression.

From a process engineering standpoint, overall productivity can potentially be increased further by optimizing the starting concentration of ammonium (effects μ_{max}) and the biomass concentration at the start of the production phase. With a C-N ratio of 10 mol/mole a biomass concentration of up to 69.8 g/L can potentially be achieved, as shown in a previous study (Kiefer et al., 2021a). The total process time can be extended by optimizing the C-N ratio of the feeds during production phase. Probably a C-N ratio between 20 and 40 mol/mole is more optimal for maintaining cellular activity without active cell growth. As changes in these points also relate to other parameters, a DOE or model-based approach for optimization might be most promising. Regarding downstream processing, as *C. glutamicum* is known for a broad pH optimum between a pH of 6 to 9 (Follmann et al., 2009), stepwise reducing pH coupled to DO instead of addition of Na-acetate might further decrease salt waste.

4. Conclusion

In this work, the high potential of *C. glutamicum* as a model organism for bioproduction of itaconate using acetate as alternative carbon source was demonstrated. $Y_{P,S}$ was increased from 0.03 g/g in shake flasks to 0.16 g/g in bioreactors using a two-step fed-batch strategy that combines pH and DO-coupled feeding of acetate without the need for titration of a base for pH control. With this feeding strategy a peak volumetric productivity of 1.01 g $L^{-1}h^{-1}$ resulting in an itaconate titer of 29.2 g/L was achieved.

CRediT authorship contribution statement

Manuel Merkel: Conceptualization, Methodology, Formal analysis, Validation, Investigation, Writing – original draft, Writing – review & editing, Visualization. **Dirk Kiefer:** Conceptualization, Methodology, Formal analysis, Investigation, Writing – review & editing. **Marc Schmollack:** Conceptualization, Methodology, Investigation, Writing – review & editing. **Bastian Blombach:** Conceptualization, Resources, Writing – review & editing, Supervision, Project administration, Funding acquisition. **Lars Lilge:** Conceptualization, Validation, Formal analysis, Writing – review & editing. **Marius Henkel:** Conceptualization, Validation, Methodology, Formal analysis, Writing – review & editing, Supervision, Funding acquisition. **Rudolf Hausmann:**

Conceptualization, Validation, Formal analysis, Writing – review & editing, Supervision, Project administration, Funding acquisition.

Declaration of Competing Interest

The authors declare that they have no known competing financial interests or personal relationships that could have appeared to influence the work reported in this paper.

Acknowledgements

The authors would like to thank Prof. Dr. Michael Bott and his group from IBG-1: Biotechnology, Institute of Bio- and Geosciences, Forschungszentrum Juelich (Juelich, Germany) for kindly providing the plasmid pEKEx2-*malEcad*$_{opt}$.

Funding sources

This study was partially funded by the Federal Ministry of Education and Research, Germany (BMBF, funding codes: 031B0673B and 031B0673C). MM is a member of the " BBW ForWerts " graduate program funded by the Ministry of Science, Research and the Arts of Baden-Wuerttemberg (MWK).

Appendix A. Supplementary data

Supplementary data to this article can be found online at https://doi.org/10.1016/j.biortech.2022.126994.

References

Ali, M.A., Kaneko, T., 2022. High-Performance bionylons from itaconic and amino acids with pepsin degradability. Adv. Sustainable Syst. 6 (2), 2100052.
Arnold, S., Moss, K., Henkel, M., Hausmann, R., 2017. Biotechnological perspectives of pyrolysis oil for a bio-based economy. Trends Biotechnol. 35 (10), 925–936.
Arnold, S., Tews, T., Kiefer, M., Henkel, M., Hausmann, R., 2019. Evaluation of small organic acids present in fast pyrolysis bio-oil from lignocellulose as feedstocks for bacterial bioconversion. GCB Bioenergy 11 (10), 1159–1172.
Becker, J., Tehrani, H.H., Ernst, P., Blank, L.M., Wierckx, N., 2020. An Optimized *Ustilago maydis* for itaconic acid production at maximal theoretical yield. J. fungi, 20.
Blombach, B., Grünberger, A., Centler, F., Wierckx, N., Schmid, J., 2022. Exploiting unconventional prokaryotic hosts for industrial biotechnology. Trends Biotechnol. 40 (4), 385–397.
Boondaeng, A., Suwanruji, P., Vaithanomsat, P., Apiwatanapiwat, W., Trakunjae, C., Janchai, P., Apipatpapha, T., Chanka, N., Chollakup, R., 2021. Bio-synthesis of itaconic acid as an anti-crease finish for cellulosic fiber fabric. RSC Adv. 11 (42), 25943–25950.
Burkovski, A., 2007. Nitrogen control in *Corynebacterium glutamicum*: proteins, mechanisms, signals. J. Microbiol. Biotechnol. 187–194.
Chiloeches, A., Funes, A., Cuervo-Rodríguez, R., López-Fabal, F., Fernández-García, M., Echeverría, C., Muñoz-Bonilla, A., 2021. Biobased polymers derived from itaconic acid bearing clickable groups with potent antibacterial activity and negligible hemolytic activity. Polym. Chem. 12 (21), 3190–3200.
Demir, H.T., Bezirci, E., Becker, J., Tehrani, H.H., Nikerel, E., Wierck, N., Türker, M., 2021. High level production of itaconic acid at low pH by *Ustilago maydis* with fed-batch fermentation. Bioprocess and biosystems engineering 44 (4), 749–758.
Eggeling, L., Reyes, O., 2005. In: Handbook of *Corynebacterium glutamicum*. CRC Press, pp. 535–566.
Follmann, M., Ochrombel, I., Krämer, R., Trötschel, C., Poetsch, A., Rückert, C., Hüser, A., Persicke, M., Seiferling, D., Kalinowski, J., Marin, K., 2009. Functional genomics of pH homeostasis in *Corynebacterium glutamicum* revealed novel links between pH response, oxidative stress, iron homeostasis and methionine synthesis. BMC Genomics 10 (1).
Garcia-Gonzalez, L., De Wever, H., 2018. Acetic acid as an indirect sink of CO_2 for the synthesis of polyhydroxyalkanoates (PHA): comparison with PHA production processes directly using CO_2 as feedstock. Appl. Sci. 8 (9), 1416.
Gerstmeir, R., Wendisch, V.F., Schnicke, S., Ruan, H., Farwick, M., Reinscheid, D., Eikmanns, B.J., 2003. Acetate metabolism and its regulation in *Corynebacterium glutamicum*. Journal of Biotechnology 104 (1-3), 99–122.
Gong, Z., Zhou, W., Shen, H., Yang, Z., Wang, G., Zuo, Z., Hou, Y., Zhao, Z.K., 2016. Co-fermentation of acetate and sugars facilitating microbial lipid production on acetate-rich biomass hydrolysates. Bioresource technology 207, 102–108.
Green, M.R., Sambrook, J., 2012. Molecular cloning: A laboratory manual, 4th ed. Cold Spring Harbor Laboratory Press, New York.
Hanahan, D., 1983. Studies on transformation of *Escherichia coli* with plasmids. Journal of molecular biology 166 (4), 557–580.
Harder, B.-J., Bettenbrock, K., Klamt, S., 2016. Model-based metabolic engineering enables high yield itaconic acid production by *Escherichia coli*. Metabolic engineering 38, 29–37.
Harder, B.-J., Bettenbrock, K., Klamt, S., 2018. Temperature-dependent dynamic control of the TCA cycle increases volumetric productivity of itaconic acid production by *Escherichia coli*. Biotechnology and bioengineering 115 (1), 156–164.
Hartford, C.G., 1962. Rapid spectrophotometric method for the determination of itaconic, citric, aconitic, and fumaric acids. Analytical Chemistry 34 (3), 426–428.
Hoffmann, M., Fernandez Cano Luna, Xiao, S., Stegemüller, L., Rief, K., Heravi, K.M., Lilge, L., Henkel, M., Hausmann, R., 2020. Towards the anaerobic production of surfactin using *Bacillus subtilis*. Front. Bioeng. Biotechnol. 8.
Hosseinpour Tehrani, H., Becker, J., Bator, I., Saur, K., Meyer, S., Rodrigues Lóia, A.C., Blank, L.M., Wierckx, N., 2019. Integrated strain- and process design enable production of 220 g L-1 itaconic acid with *Ustilago maydis*. Biotechnology for biofuels 263.
Hu, P., Rismani-Yazdi, H., Stephanopoulos, G., 2013. Anaerobic CO_2 fixation by the acetogenic bacterium *Moorella thermoacetica*. AIChE J. 59 (9), 3176–3183.
Huang, B., Yang, H., Fang, G., Zhang, X., Wu, H., Li, Z., Ye, Q., 2018. Central pathway engineering for enhanced succinate biosynthesis from acetate in *Escherichia coli*. Biotechnol. Bioeng. 115 (4), 943–954.
Keilhauer, C., Eggeling, L., Sahm, H., 1993. Isoleucine synthesis in *Corynebacterium glutamicum*: molecular analysis of the ilvB-ilvN-ilvC operon. Journal of bacteriology 175 (17), 5595–5603.
Kiefer, D., Merkel, M., Lilge, L., Hausmann, R., Henkel, M., 2021a. High cell density cultivation of *Corynebacterium glutamicum* on bio-based lignocellulosic acetate using pH-coupled online feeding control. Bioresource technology 340, 125666.
Kiefer, D., Merkel, M., Lilge, L., Henkel, M., Hausmann, R., 2021b. From acetate to bio-based products: underexploited potential for industrial biotechnology. Trends in biotechnology 39 (4), 397–411.
Klement, T., Büchs, J., 2013. Itaconic acid–a biotechnological process in change. Bioresource technology 135, 422–431.
Krull, S., Hevekerl, A., Kuenz, A., Prüße, U., 2017. Process development of itaconic acid production by a natural wild type strain of *Aspergillus terreus* to reach industrially relevant final titers. Applied microbiology and biotechnology 101 (10), 4063–4072.
López-Garzón, C.S., Straathof, A.J.J., 2014. Recovery of carboxylic acids produced by fermentation. Biotechnology Advances 32 (5), 873–904.
Noh, M.H., Lim, H.G., Woo, S.H., Song, J., Jung, G.Y., 2018. Production of itaconic acid from acetate by engineering acid-tolerant *Escherichia coli* W. Biotechnology and bioengineering 115 (3), 729–738.
Novak, K., Pflügl, S., 2018. Towards biobased industry: acetate as a promising feedstock to enhance the potential of microbial cell factories. FEMS microbiology letters.
Okamoto, S., Chin, T., Hiratsuka, K., Aso, Y., Tanaka, Y., Takahashi, T., Ohara, H., 2014. Production of itaconic acid using metabolically engineered *Escherichia coli*. The Journal of general and applied microbiology 60 (5), 191–197.
Otten, A., Brocker, M., Bott, M., 2015. Metabolic engineering of *Corynebacterium glutamicum* for the production of itaconate. Metabolic engineering 30, 156–165.
Philp, J., 2018. The bioeconomy, the challenge of the century for policy makers. New biotechnology 40, 11–19.
Robert, T., Friebel, S., 2016. Itaconic acid – a versatile building block for renewable polyesters with enhanced functionality. Green Chem. 18 (10), 2922–2934.
Saha, B.C., 2017. Emerging biotechnologies for production of itaconic acid and its applications as a platform chemical. Journal of industrial microbiology & biotechnology 44 (2), 303–315.
Schäfer, A., Tauch, A., Jäger, W., Kalinowski, J., Thierbach, G., Pühler, A., 1994. Small mobilizable multi-purpose cloning vectors derived from the *Escherichia coli* plasmids pK18 and pK19: selection of defined deletions in the chromosome of *Corynebacterium glutamicum*. Gene 145 (1), 69–73.
Schlembach, I., Hosseinpour Tehrani, H., Blank, L.M., Büchs, J., Wierckx, N., Regestein, L., Rosenbaum, M.A., 2020. Consolidated bioprocessing of cellulose to itaconic acid by a co-culture of *Trichoderma reesei* and *Ustilago maydis*. Biotechnology for biofuels 207.
Schwentner, A., Feith, A., Münch, E., Busche, T., Rückert, C., Kalinowski, J., Takors, R., Blombach, B., 2018. Metabolic engineering to guide evolution - Creating a novel mode for L-valine production with *Corynebacterium glutamicum*. Metabolic engineering 47, 31–41.
Silberbach, M., Hüser, A., Kalinowski, J., Pühler, A., Walter, B., Krämer, R., Burkovski, A., 2005. DNA microarray analysis of the nitrogen starvation response of *Corynebacterium glutamicum*. Journal of Biotechnology 119 (4), 357–367.
Tauch, A., Kirchner, O., Löffler, B., Götker, S., Pühler, A., Kalinowski, J., 2002. Efficient electrotransformation of *Corynebacterium diphtheriae* with a mini-replicon derived from the *Corynebacterium glutamicum* plasmid pGA1. Current microbiology 45 (5), 362–367.
Trček, J., Mira, N.P., Jarboe, L.R., 2015. Adaptation and tolerance of bacteria against acetic acid. Applied microbiology and biotechnology 99 (15), 6215–6229.
Trotta, J.T., Watts, A., Wong, A.R., LaPointe, A.M., Hillmyer, M.A., Fors, B.P., 2019. Renewable thermosets and thermoplastics from itaconic acid. ACS Sustainable Chem. Eng. 7 (2), 2691–2701.
van der Rest, M.E., Lange, C., Molenaar, D., 1999. A heat shock following electroporation induces highly efficient transformation of *Corynebacterium glutamicum* with xenogeneic plasmid DNA. Applied microbiology and biotechnology 52 (4), 541–545.
Wendisch, V.F., de Graaf, A.A., Sahm, H., Eikmanns, B.J., 2000. Quantitative determination of metabolic fluxes during coutilization of two carbon sources: Comparative analyses with *Corynebacterium glutamicum* during growth on acetate and/or glucose. Journal of bacteriology 182 (11), 3088–3096.
Werpy, T., Petersen, G., 2004. Top value added chemicals from biomass: volume I – Results of screening for potential candidates from sugars and synthesis gas.

Yoneda, N., Kusano, S., Yasui, M., Pujado, P., Wilcher, S., 2001. Recent advances in processes and catalysts for the production of acetic acid. Applied Catalysis A: General 221 (1-2), 253–265.

Liu, Y., Wu, H., Li, Q., Tang, X., Li, Z., Ye, Q., 2011. Process development of succinic acid production by *Escherichia coli* NZN111 using acetate as an aerobic carbon source. Enzyme and Microbial Technology 49 (5), 459–464.

Zhang, X.-X., Ma, F., Lee, D.-J., 2009. Recovery of itaconic acid from supersaturated waste fermentation liquor. Journal of the Taiwan Institute of Chemical Engineers 40 (5), 583–585.

2.2 Design and evaluation of a 3D-printed, lab-scale perfusion bioreactor for novel biotechnological applications

This article is published as original article:

Merkel, Manuel; Noll, Philipp; Lilge, Lars; Hausmann, Rudolf; Henkel, Marius (2023):

Design and evaluation of a 3D-printed, lab-scale perfusion bioreactor for novel biotechnological applications.

In: Biotechnology Journal, e2200554
DOI: 10.1002/biot.202200554

This publication contains supplemental material which can be found at: https://onlinelibrary.wiley.com/doi/full/10.1002/biot.202200554 Additionally, the supplemental material and the CAD-files are included on the disc provided with this dissertation as a pdf-file "Supplementary Materials Publication 2" and a zip-folder "CAD-stl-files".

Received: 24 November 2022 | Revised: 5 June 2023 | Accepted: 21 June 2023

DOI: 10.1002/biot.202200554

Biotechnology Journal

RESEARCH ARTICLE

Design and evaluation of a 3D-printed, lab-scale perfusion bioreactor for novel biotechnological applications

Manuel Merkel[1] | **Philipp Noll**[2] | **Lars Lilge**[1,3] | **Rudolf Hausmann**[1] | **Marius Henkel**[2]

[1]Department of Bioprocess Engineering (150k), University of Hohenheim, Stuttgart, Germany

[2]Cellular Agriculture, TUM School of Life Sciences, Technical University of Munich, Freising, Germany

[3]Department of Molecular Genetics, University of Groningen, AG, Groningen, The Netherlands

Correspondence
Marius Henkel, Cellular Agriculture, TUM School of Life Sciences, Technical University of Munich, Freising, Germany.
Email: marius.henkel@tum.de

Funding information
Ministerium für Wissenschaft, Forschung und Kunst Baden-Württemberg, Grant/Award Number: MM is a member of the "BBW ForWerts" graduate program; Bundesministerium für Bildung und Forschung, Grant/Award Number: 031B0673C

Abstract

3D-printing increased in significance for biotechnological research as new applications like lab-on-a-chip systems, cell culture devices or 3D-printed foods were uncovered. Besides mammalian cell culture, only few of those applications focus on the cultivation of microorganisms and none of these make use of the advantages of perfusion systems. One example for applying 3D-printing for bioreactor development is the microbial utilization of alternative substrates derived from lignocellulose, where dilute carbon concentrations and harmful substances present a major challenge. Furthermore, quickly manufactured and affordable 3D-printed bioreactors can accelerate early development phases through parallelization. In this work, a novel perfusion bioreactor system consisting of parts manufactured by fused filament fabrication (FFF) is presented and evaluated. Hydrophilic membranes are used for cell retention to allow the application of dilute substrates. Oxygen supply is provided by membrane diffusion via hydrophobic polytetrafluoroethylene membranes. An exemplary cultivation of *Corynebacterium glutamicum* ATCC 13032 supports the theoretical design by achieving competitive biomass concentrations of 18.4 g L^{-1} after 52 h. As a proof-of-concept for cultivation of microorganisms in perfusion mode, the described bioreactor system has application potential for bioconversion of multi-component substrate-streams in a lignocellulose-based bioeconomy, for in-situ product removal or design considerations of future applications for tissue cultures. Furthermore, this work provides a template-based toolbox with instructions for creating reference systems in different application scenarios or tailor-made bioreactor systems.

KEYWORDS
3D-printing, bioeconomy, *Corynebacterium glutamicum*, membrane bioreactor, perfusion bioreactor process

Abbreviations: ABS, acrylonitrile butadiene styrene; CAD, computer-aided design; CPE, co-polyester; DO, dissolved oxygen; FFF, fused filament fabrication; iD, inner diameter; MOPS, morpholino propanesulfonic acid; oD, outer diameter; OD_{600nm}, optical density; PTFE, polytetrafluoroethylene; PVDF, polyvinylidene difluoride; TES, trace element solution.

1 | INTRODUCTION

Additive manufacturing or 3D-printing is a novel manufacturing technique that has advanced from a tool for creation of demonstration models to real world industrial applications.[1] Its main benefits in comparison to conventional manufacturing methods are high flexibility regarding design choices and short manufacturing times.[2] There are different 3D-printing technologies available like laser sintering,[3] stereolithography or fused filament fabrication (FFF).[2] This work focused on the FFF technology, which describes the manufacturing of objects by applying layers of molten plastic through a heated extrusion nozzle. In comparison to the other mentioned 3D-printing methods, FFF printing is less expensive, and a wide range of different materials are available.[4,5]

Recently, the technological advancement of 3D-printing has led to increased interest of research for applications in the biotechnological context. The development of cultivation devices for mammalian cell cultures, where special geometries are necessary to induce cell differentiation and tissue formation is an example.[6–8] It is also applied for manufacturing of lab-on-a-chip systems,[9,10] cell immobilization devices or individualized labware.[11,12] The most recent applications even include 3D-printed foods or artificial organs for clinical studies.[13–16] Nevertheless, there are only a few studies available on 3D-printed bioreactors for bacterial cultivation. They either focus on microbioreactors or combine commercially available glass vessels with 3D-printed holders and components, which limits design freedom.[17,18] Nowadays, research on utilization of alternative substrates for sustainable bioproduction is increasing and 3D-printing can be used to develop new reactor concepts for tailor-made applications.[19,20] The major challenges for bacterial cultivation, however, is the high content of non-fermentable, potentially harmful substances that inhibit bacterial growth as reported by Arnold et al.[21] Using perfusion systems is a possible solution to utilize such substrates, since the continuous flow of the medium through the bioreactor prevents the accumulation of inhibitors.[6,21] Additionally, the retention with membranes reduces the risk to wash-out the bacterial cells, allowing dilute concentrations to be used at higher flow rates. 3D-printed perfusion bioreactors also offer benefits for optimization experiments or kinetic studies through parallelization. Because of the low manufacturing times and the affordable price, multiple bioreactors can easily be produced by 3D-printing and operated in parallel.[6,22] This enables simultaneous examination of different parameters, thus speeding up process development times.

With these applications in mind, a new concept for a 3D-printed perfusion bioreactor system is presented in this study. The bioreactor system with a volume of ~50 mL utilizes a hydrophilic flat sheet membrane for cell retention. It includes a circulation line for diffusive transfer of oxygen to the medium via a module that includes hydrophobic membranes for separation of gaseous and liquid phases. An electric heat exchanger combined with a PID-controller is used for temperature control. To evaluate the suitability of the system for bacterial cultivation, the mixing times and oxygen transfer coefficient were determined. Finally, a cultivation with *Corynebacterium glutamicum* ATCC 13032 on glucose was performed as proof-of-concept, which showed that the cultivation process can be maintained for at least 52 h up to a biomass concentration of 18.4 g L^{-1} without membrane blockage. In this way, this study provides a template of a 3D-printed perfusion bioreactor that facilitates the exploitation of alternative substrates without the need for expensive commercial equipment.

2 | MATERIALS AND METHODS

2.1 | Analytics and chemicals

If not stated otherwise, the chemicals used in this work were obtained from Carl Roth GmbH (Karlsruhe, Germany). Morpholino propanesulfonic acid (MOPS, order number 1081) as buffering agent was obtained from GERBU Biotechnik GmbH (Heidelberg, Germany). Enzymatic assay kits from R-biopharm AG (Darmstadt, Germany) were obtained for analysis of glucose (Cat No. 10716251035) and lactate (Cat. No. 11112821035).

2.2 | The 3D-printed perfusion bioreactor system and its operating conditions

The main flow through the system is generated by two syringe pumps (Cetoni neMESYS 290N, Cetoni GmbH, Corbussen, Germany) with 10 mL single-use syringes (Omnifix 10 mL with Luer Lock, B.Braun AG, Melsungen, Germany). A 1-to-10 valve module (Cetoni Qmix V Ex, Cetoni GmbH, Corbussen, Germany) allows switching between different feeding or sterilization solutions (Figure 1A). In front of the main entrance to the bioreactor a pressure probe and a 3-2-way valve were installed to monitor the pressure of the system followed by the main bioreactor module (Figure 1B) with ports for different probes, a sample port and the cell retention membrane as described in detail in Section 2.1.1. With the latter, the permeate leaves the bioreactor and is collected in a bottle. Stirring is used for mixing the reactor content (Figure 1C). Besides the main flow through the reactor, a six-channel peristaltic pump (Peristaltic Pump peRISYS-S, Cetoni GmbH, Corbussen, Germany) in combination with two 2-stopper flexible tubing (2.7 mm iD) is used to generate a circulation flow. The circulation flow is used for oxygen supply via membrane diffusion by an oxygen transfer module (Figure 1D) as well as for temperature control via a heat exchanger module (Figure 1E). Polytetrafluoroethylene (PTFE)-tubing with 1.6 mm inner diameter (iD) and 3.3 mm outer diameter (oD) in combination with corresponding ¼″−28 flat bottom fittings and ferrules were used to connect most modules of the system. To connect the PTFE-tubing to flexible tubing female Luer to ¼″−28 male adapters were used. All pumps, valves and pressure probes were controlled and monitored via the software Qmix elements (Cetoni GmbH, Korbussen, Germany). The corresponding 3D-models are provided in the supplementary information as .stl-files. A flow diagram and render pictures of the different modules are shown in Figure 1.

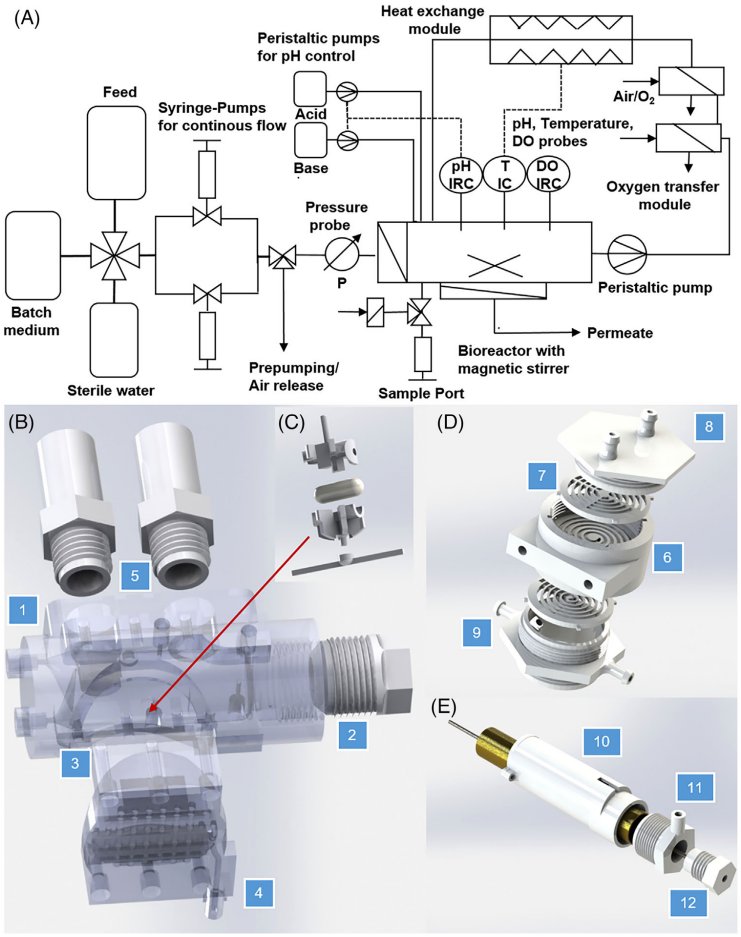

FIGURE 1 Layout and render pictures of the perfusion bioreactor system. (A) Flow chart of the bioreactor system. (B) Render picture of the bioreactor main body (1), the cap (2), cell retention membrane support (3 + 4) and probe connectors (5); (C) render picture of the 3D-printed stirrer frame; (D) render picture of half of the oxygen transfer module with connectors for gas tubing (8), a stabilizer (7), the liquid compartment, that has spiral flow channels on both sides which are covered by circular membranes (6), and a middle compartment with connectors for gas tubing (9). (E) Render of half of the heat exchange module, consisting of an encasing (10), a fitting with connections to fill the outer tube (11) and a cap for connection to the flow system of the culture broth (12). The brass tubing as well as the thin capillary in the middle are not 3D-printed.

2.2.1 | The main bioreactor module

The main component of the system is the bioreactor module shown in the exploded view in Figure 1B. The main bioreactor module has an oD of 41 mm and an iD of 24 mm. The lower half of the tube is horizontal, while the upper half has an outward slope with an angle of 4.4° (Figure S1, supporting information). At the reactor end, the tube splits and narrows into two 2-mm channels with two tap holes for ¼″−28 threading (Figure 1B1). At this point the circulation flow starts. The main inlet into the reactor (Figure 1B2) consists of a socket with M27 threading, in which a hydrophilic polyvinylidene difluoride (PVDF) membrane (Durapore, 0.22 μm pore size, 47 mm oD, Merck KGaA, Darmstadt, Germany), with 24 mm diameter, and a stabilizing grid are placed. The inlet is closed by the reactor cap with two tap holes for ¼″−28 threading. Starting from the inlet-membrane the inner tube of the bioreactor module has a height of 7.7 mm. Together with the iD of 2.4 mm this results in height-to-diameter ratio of 3.2 which is close to the typical ratio of ~3 for microbial bioreactors allowing best

mixing conditions.[23] Figure 1B3 shows the cavity, in which another hydrophilic PVDF membrane (diameter = 47 mm) with wide bearing area of 4 mm (effective membrane area of 12 cm^2) is placed for cell retention. The membrane is kept in place by the membrane support (Figure 1B4), which is fixed with six M3.5 screws and nuts. It was incorporated into the bioreactor's mantle to offer a high enough surface area to keep the pressure in the system caused by the transmembrane pressure low and to lower the risk of pressure spikes caused by membrane fouling as shown by Darcy's law: [24]

$$Q = \frac{k * A}{\eta} * \frac{dP}{L} \quad (1)$$

Q = flow rate in mL min^{-1}, k = permeability in Darcy, A = membrane area in cm^2, dP = pressure difference in bar, η = dynamic viscosity in kg m^{-1} s^{-1}, L = membrane/filter thickness in m.

The stirrer (Figure 1C) consists of a 3D-printed frame covering a magnetic stirrer bar (7 mm diameter, 20 mm long) and is placed above the membrane. In addition, Figure 1B5 marks two ports for pH or DO probes. The probe adapters are connected via M20 threading. Furthermore, on the sides of the reactor module five connections for ¼″−28 threading are placed. Another connection with a 3 mm channel is reserved for a Pt100 temperature probe. Three connections are used for the sample port and the pH-correction solutions (1 M HCl and 4 M NaOH), the last one as inlet for the circulation flow. For the pH-correction solutions, PTFE tubing with an oD of 1.6 mm was used, which could be pushed through the channels directly into the interior of the bioreactor to prevent contact between NaOH and the 3D-printing material. For the sample port, a Luer 3-2 way valve was added with a sterile filter at one end and a syringe on the other. In total, the reactor contains a volume of 39 mL. All probes, the bioreactor cap and the membrane support were sealed with o-ring gaskets.

2.2.2 | Liquid-gas membrane contactors for oxygen supply

For the reactor setup chosen in this work bubble aeration is not suitable, as the gas flow would have to be strictly controlled to prevent liquid expulsion from the reactor. Additionally, bubble aeration could cause foam formation, which leads to the same problem. Accordingly, oxygen supply via diffusion was chosen and an oxygen transfer module was constructed (Figure 1D), relying on hydrophobic PTFE membranes for separation of liquid and gaseous phases. One module consists of several compartments. The liquid compartment (Figure 1D6) with flow channels for the culture broth is equipped with two tap holes for ¼″−28 threading. The liquid follows spiral patterns on each side of the module, which are connected in the middle. The rectangular channels (1 mm deep and 2.3 mm wide) are covered by hydrophobic PTFE-membranes with an oD of 47 mm, a pore size of 0.22 μm and 85% porosity (Fluoropore membrane filter, Merck KGaA, Darmstadt, Germany) resulting in an effective membrane area of 8.7–9.0 cm^2. To seal the liquid compartment, a ring socket with 42 mm iD and 47.5 mm oD surrounds the spiral flow pattern, in which silicone gaskets with a strength of 2 mm are placed beneath the membrane. A plastic grid (Figure 1D7) that mimics the flow channels is placed on top of the membrane to prevent it from warping outwards. The module was set up in a way that allows increasing the membrane area by stacking multiple liquid and gas compartments (Figure 1D8 and D9) onto each other. Each liquid compartment contains a volume of ∼1 mL.

2.2.3 | Heating module for temperature control

The heat exchange module follows the principle of a double pipe heat exchanger. The outside pipe is a brass pipe (19 mm length, 25 mm oD, 1 mm strong) that is covered by an electric heating element (Thermo Tech Polyester heating foil, 30 W, 24 V). It is filled with water as heat transfer medium. The inner pipe is a stainless-steel pipe (21 mm length, 0.5 mm strength) with 2.1 mm iD, through which the culture broth is pumped. Brass was chosen as metal for the outer pipe, due to its superior thermal conductivity compared to stainless steel. The heating element as well as a PT100 temperature probe were connected to a PID controller (ITC-100VL PID Temperature Controller 12–24 V, Inkbird, China) for temperature control. The temperature probe was placed into the bioreactor to measure the temperature at the main reaction compartment. 3D-printed holders (Figure 1E10) and a 3D-printed encasing (Figure 1E11) were used to separate the tubes and isolate the heating element from external factors. The heat exchange module adds 0.8 mL to the total reactor volume.

2.3 | Design and fabrication of the 3D-printed components

All 3D-printed components were constructed using the computer-aided design (CAD) software Solidworks 2018 (Dassault Systèmes SolidWorks Corporation, Waltham, USA). The designed CAD-files were then exported to .stl files (see supporting information for a list and description of included models) that could be imported and converted by the slicing-application for 3D-printers Cura (Ultimaker BV, Utrecht, Netherlands). Cura is an open-source software that converts 3D-objects into layer-based files, which can be used by most 3D-printers for manufacturing real objects. In this study, the FFF 3D-printers Ultimaker 3 and Ultimaker 3 extended (Ultimaker BV, Utrecht, Netherlands) outfitted with AA 0.4 mm brass nozzles were used. The Ultimaker 3 is equipped with a dual extrusion print head allowing the use of two different filament types at the same time. Additionally, the printing chambers of both printers were encased. This allowed higher temperatures on the inside of the printer and prevented disturbances from the outside, which is necessary for printing with most technical filaments. The 3D-printing filaments acrylonitrile butadiene styrene (ABS), CPE+, CPE from Ultimaker and nGen flex from ColorFabb (ColorFabb B.V., Belfeld, Netherlands) were used in this study. For

the Ultimaker materials, printing profiles were available in Cura, which were used as templates with some modifications. For nGen flex, the profile of CPE+ was used as template. The settings used for printing the different materials are given as part of the supporting information (Table S1).

Only threading with a size of M20 or higher could be printed when the tap hole had a vertical orientation. For all other threading-types special cutting tools (taps) were used. Since 3D-printing using the FFF principle often produces rough and porous surfaces, but clean surfaces are needed for sealing and waterproof prints, two methods were applied for smoothing. The first method is only applicable for ABS-prints, for which acetone vapor was used.[25] In detail, the objects to be treated were placed into a 1 L glass beaker filled with 30–50 mL of acetone, which was then heated to a temperature of 80°C for 25 min to generate the vapor. A glass inlet was used to prevent the objects from touching the liquid acetone. The top of the beaker was closed with aluminum foil. The second method was material independent and contained treatment of sealing surfaces with a two-component epoxy resin (XTC-3D, Smooth-On, Inc, Macungie, Pennsylvania).

2.4 | Determination of mixing time

Typically, the t_{95} value is determined to characterize the mixing efficiency (time to reach 95% of complete homogenization). In this work, a decolorization method based on iodometry was used.[26] Therefore, a 0.05 g L^{-1} starch solution colored by addition of 12 mL L^{-1} 1% iodine/potassium iodide solution was filled into the bioreactor system. After a stable circulation flow was achieved, 4 mL L^{-1} 0.1 M sodium thiosulfate heptahydrate solution was added via syringe for decolorization. The time until complete decolorization of the starch solution is then defined as t_{95}. A camera was used to document the mixing experiments.

2.5 | Determination of oxygen transfer rates

The dynamic gassing-out method according to Van't Riet was used for determination of oxygen transfer rates.[27] First, oxygen was removed from the solution by nitrogen aeration. Subsequently, aeration was switched to pure oxygen and the dissolved oxygen (DO) was measured with a probe. The oxygen transfer rate was calculated from the slope of the DO curve according to equation 1:

$$\dot{M}_{O2} = V_R * \frac{c_{O2}(t) - c_{O2}(t_0)}{t - t_0} \quad (2)$$

$\dot{M}_{O2}$ = oxygen mass transfer in mg h^{-1}, $c_{O2}(t)$ = oxygen concentration and $c_{O2,s}$ = oxygen solubility in mg L^{-1}, V_R = Reactor volume in L, t = time in h.

A 35 g L^{-1} NaCl-solution was used as substitute for typical media, since solubilities for this solution are available.[28]

2.6 | Cultivation conditions

2.6.1 | Bacterial strain and cultivation medium

The bacterial wildtype strain *C. glutamicum* ATCC 13032 was used for all cultivations performed in this study. The inoculum and media were prepared as described in an earlier publication, with the difference that glucose instead of acetate was used as the sole carbon source.[29] The medium composition $CGXII_F$ was used for shake flask cultivations and as batch medium for cultivations in the perfusion bioreactor with a pH value of 7.[29] For experiments with the perfusion bioreactor, $CGXII_{Perfusion}$ was used as feed medium during the continuous phase:

5 g L^{-1} glucose, 0.5 g L^{-1} KH_2PO_4, 0.5 g L^{-1} K_2HPO_4, 0.13 g L^{-1} $MgSO_4 \times 7\,H_2O$, 0.01 g L^{-1} $CaCl_2 \times 2\,H_2O$, 21 g L^{-1} MOPS, 0.2 mg L^{-1} D-biotin and 0.5 mL L^{-1} trace element solution (TES).

In comparison to the medium composition $CGXII_F$ most concentrations (besides $CaCl_2$ and D-biotin) were halved to prevent precipitation.

2.6.2 | Determining the effects of 3D-printed filaments on cell growth

Shake flask cultivations were performed to determine potential effects on the cell growth of *C. glutamicum* caused by the presence of 3D-printing materials. Therefore, the different 3D-printing filaments used during this study, ABS, CPE+, nGen flex, were cut to 1–2 cm pieces, sterilized by autoclaving and added to 500 mL shake flasks containing 50 mL $CGXII_F$ medium. For each filament, 10 g of pieces were added to one shake flask. Additionally, the experiment was also performed with pieces of CPE+ covered in epoxy resin. As control, a cultivation without filaments was performed. All cultures were inoculated to a starting optical density (OD_{600nm}) of 1.

2.6.3 | Cultivation in the perfusion bioreactor

For bioreactor cultivations, the 3D-printed perfusion bioreactor system described before was used. For measurement of DO and for pH-control, the reactor was equipped with a DO (VisiFerm DO 225; Hamilton Hamilton Company, Reno, USA) and a pH probe (EasyFerm Bio K8224; Hamilton Company, Reno, USA), which were connected to a data station of a 2 L bioreactor (Labfors 4, Infors AG, Bottmingen, Switzerland). The pumps and the pH controller of the Labfors were used for addition of pH-control solutions. At the beginning of the cultivation, air was used for oxygen transfer. When the DO concentration became limiting, pure oxygen was used instead. The cultivation temperature was controlled at 30°C by using a PID controller connected to a temperature probe and to the heating module described before. To start a cultivation, the culture broth was inoculated to a starting OD_{600nm} of 1 using the sample port. The pH control was set to a value of 7.0 with the pH control solutions 1 M HCl and 4 M NaOH.

Sterilisation of the main bioreactor compartment and the fluidic control system was performed with 70% ethanol using the peristaltic pump of the circulation line. After filling, the ethanol solution was connected to the syringe pumps and pumped through the perfusion system at a flow rate of 1 mL min^{-1}. At the same time, the peristaltic pump was set to 30 mL min^{-1} for distributing the ethanol through the system. After 1 h of sterilization, the bioreactor module was disconnected from the pumps, manually rinsed, and filled again with sterile water beneath the laminar flow. After reconnecting, an additional volume of 400 mL sterile water was pumped through the system to rinse off all remaining traces of ethanol at a flow rate of 0.5 mL min^{-1}. The oxygen transfer module was sterilized separately from the remaining bioreactor system. For sterilization of the oxygen transfer module, 1 M NaOH was used and incubated for 1 h at room temperature beneath the laminar flow, followed by careful rinsing with 50 mL of sterile water.

After both modules were sterilized, they were reconnected beneath the laminar flow cabinet and the pH and DO probes were installed. Finally, the whole system was flushed and filled with medium at a flow rate of 3 mL min^{-1} for 1 h using the syringe pumps.

2.7 | Sampling and offline analytics

During cultivations, samples were taken every 2 h. The OD_{600nm} was determined using a spectrophotometer (Biochrom WPA CO8000, Biochrom Ltd., Cambrigde, United Kingdom) to monitor the cell growth. The biomass concentration was determined with a OD_{600nm} correlation factor of 4.3, determined in a previous study.[29] A volume of 0.5 mL of cell-free supernatant was prepared by centrifugation of each sample for 10 min at 14,000 rpm and 4°C (5430 R, Eppendorf AG, Hamburg, Germany). The supernatants were stored at −20°C. Glucose and lactate concentrations were determined using a spectrometer (Genesys 150 UV/Vis, Thermo Fisher Scientific GmbH, Braunschweig, Germany) and enzymatic assays from R-biopharm AG (Darmstadt, Germany), according to the manufacturer's protocols.

2.8 | Data analysis

Data analysis was performed using Microsoft Office Excel (Microsoft Corporation, Redmont). Maximum specific growth rates μ_{max} [h^{-1}] were determined by linear regression of a semi-logarithmic plot of OD_{600nm} against time with at least four sample points and a R^2 higher than 0.99. Biomass yields $Y_{X,S}$ [$g_{biomass}/g_{glucose}$] were calculated by linear regression of the accumulated biomass (dm_x) and the mass of glucose consumed during the same time (dm_s). At least four sample points were included with a R^2 higher than 0.95. Linear regression was also used for determining oxygen transfer rates by plotting DO against time as described in Section 2.5. During the experiment DO was recorded every 5 s until saturation. R^2 was higher than 0.99 for all conditions tested. Standard deviations were calculated using the "STDEV" function of Microsoft Excel.

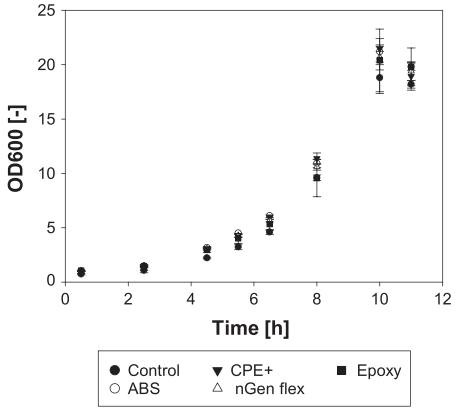

FIGURE 2 Time course of optical densities for *C. glutamicum* ATCC 13032 grown in the presence of 3D-printing filament pieces. 10 g of filament pieces were added to 50 mL of CGXIIF-medium using 10 g L^{-1} glucose as carbon source.

3 | RESULTS

3.1 | Selection of 3D-printing filaments

Different types of plastic filaments are available for 3D-printers following the FFF-principle. The filaments used in this work were chosen based on their chemical resistance and thermal stability according to the manufacturers' technical data sheets. Accordingly, the following materials were chosen for manufacturing the bioreactor: Ultimaker ABS (deformation temperature (T_D) of 87°C) and Ultimaker CPE+ (T_D of 100°C). Colorfabbs nGen flex was also considered as an additional material because it is autoclavable. But since printed objects were not waterproof, it was not used for the final bioreactor.

Instead, CPE+ was used as 3D-printing material for the bioreactor's main body and for smaller parts like Y- or T-connectors due to its superior mechanical stability, when compared to ABS. The main body was exposed to increased tension because of the high number of connections via threading. One drawback of CPE+ was its intolerance for NaOH, which was intended to be used as sterilization agent because heat sterilization was not applicable. Ethanol, as alternative, wets the hydrophobic PTFE membranes of the oxygen transfer modules, making them permeable for aqueous solutions. Accordingly, ABS was used for manufacturing the oxygen transfer module, as it proved to be tolerant for contact with 1 M NaOH even for extended periods of time (over 24 h). The different modules were sterilized independently from each other according to Section 2.8 and reconnected aseptically.

To examine the impact of the 3D-printing materials on bacterial growth, shake flask cultivations with *C. glutamicum* ATCC 13032 were performed with pieces of the different filaments (CPE+, ABS, nGen flex or CPE+ covered with hardened epoxy resin, see Figure 2). Compared to the control all cultures with filaments showed a reduction of 10% in

μ_{max} (from $0.42 \pm 0.01\ 1\ h^{-1}$ to $0.36 \pm 0.01\ 1\ h^{-1}$), while the maximum biomass concentration was unaffected (4.9 ± 0.4 g L^{-1}). Altogether, even though a small reduction in cell growth was determined, sufficient μ_{max} of $0.36 \pm 0.01\ 1\ h^{-1}$ was achieved.

3.2 | Evaluation of oxygen transfer

The construction of the oxygen transfer module was based on model equations for diffusive mass transfer of oxygen into a moving liquid based on Fick's law.[30] In this study, a hydrophobic, non-wettable PTFE membrane was used. A high solubility of oxygen in PTFE, a porosity of 85% and the low solubility of oxygen in water (8.3 mg L^{-1} at 25°C) led to the assumption that the mass-transfer-resistance on the liquid side is limiting for oxygen supply.[30–32] Accordingly, Equation (3) was used for calculating the mass transfer of oxygen into a flowing medium $\dot{M}_{O2}$, considering only the mass transfer coefficient on the liquid side β_L:

$$\dot{M}_{O2} = \beta_L * A * c_{O2,s} \tag{3}$$

β_L = liquid mass transfer coefficient in cm/s.

β_L can be calculated from the Sherwood number *Sh*, a dimensionless number describing the ratio of convective to diffusive mass transfer according to Equation (4):

$$Sh = \frac{d_h * \beta_L}{D} \tag{4}$$

Sh = dimensionless Sherwood number, d_h = characteristic diameter in m, *D* = diffusion coefficient in cm^2/s.

The analogy between heat and mass transfer was used for calculation of *Sh*, Thus, dimensionless Nusselt-numbers were replaced with Sherwood-numbers and Prandtl-numbers with Schmidt-numbers. As no equations for heat transfer with forced convection in non-circular channels were available, heat transfer in a narrow slit was used as an approximation.[33]

The Reynold's number *Re* and the characteristic diameter for a narrow slit d_h were calculated to determine the flow pattern of the medium in the channels according to Equations (5–7). The flow is considered laminar for $Re < 2300$ and turbulent for $Re > 10^5$. The flow pattern strongly influences substance transfer as it effects the thickness of boundary layers, the degree of radial mixing between flow layers as well as the distribution of flow speed.

$$d_h = 2 * s \tag{5}$$

$$Re = \frac{d_h * u}{\vartheta} \tag{6}$$

$$u = \frac{Q}{A_{cross}} = \frac{Q}{60 * s * b} \tag{7}$$

s = channel height in cm, *Re* = dimensionless Reynolds number, *u* = flow velocity in cm/s, ϑ = kinematic viscosity in cm^2/s, A_{cross} = channel cross area in cm^2, *b* = channel width in cm.

Restrictions caused by the 3D-printer and pumping equipment used in this work limited the range of flow rates and channel sizes to ranges where a laminar flow pattern is achieved. Thus, Equations (8–11) for the laminar flow through a narrow slit were used for calculating the mean *Sh*.

$$Sh = \left(Sh_1^3 + Sh_2^3\right)^{1/3} \tag{8}$$

$$Sh_1 = 4.861 \tag{9}$$

$$Sh_2 = 1.841 * \left(Re * Sc * \frac{d_h}{l}\right)^{1/3} \tag{10}$$

$$Sc = \vartheta / D \tag{11}$$

Sc = dimensionless Schmidt number, *l* = channel length in cm.

Equation (8) is valid in case that mass transfer only takes place from one side of the rift. This is true for the oxygen transfer module since oxygen can only be transferred from the membrane side but not from the channel bottom. Combining Equations (3–11) allows estimation of the oxygen mass transfer rate. Solubilities of oxygen can be found in literature.[34] Figure 3A shows a comparison between measured values of the oxygen permeability for the module as described in Section 2 and the values calculated with the equations above for different flow rates (10, 20, 30, 40, and 50 mL min^{-1}). For this experiment 3.5% NaCl-solution in water was chosen to mimic typical medium osmolarity. Two liquid compartments with an effective membrane area of 35.7 cm^2 were used. Pure oxygen was used for the gaseous phase and the temperature was controlled to 30°C, which is the typical cultivation temperature for *C. glutamicum*.[35] The experimentally determined mass flow coefficients correlated well with the coefficients calculated. This proves that the Sherwood correlation for thin channels was suited as a first approximation, when using rectangular channels. As expected, the highest mass transfer coefficient of 2.1 g h^{-1} m^{-2} bar^{-1} was determined with the highest flow rate of 50 mL min^{-1}. This resulted in a maximum oxygen transfer rate (OTR) of 161.6 mg L^{-1} h^{-1}. As expected for diffusion-based aeration, this is lower than the OTR achieved with typical stirred tank bioreactors, which can be as high as 9000 mg L^{-1} h^{-1} at maximum stirring and aeration rate (1200 rpm, 4 vvm).[36] Ways to increase the OTR are to increase the membrane area or the flow rate. With the pump used in this work, the maximum possible flow rate was 50 mL min^{-1}. Switching, for example, to a membrane pump would allow application of higher flow rates. For the test cultivations with *C. glutamicum* ATCC 13032, it was planned to use two of the oxygen transfer modules in series to increase the oxygen transfer rate to 236.0 mg L^{-1} h^{-1}.

3.3 | Determination of the perfusion bioreactor's mixing time

Table 1 shows a summary of important process parameters of the perfusion process, including mixing time t_{95}. Mixing time refers to the time

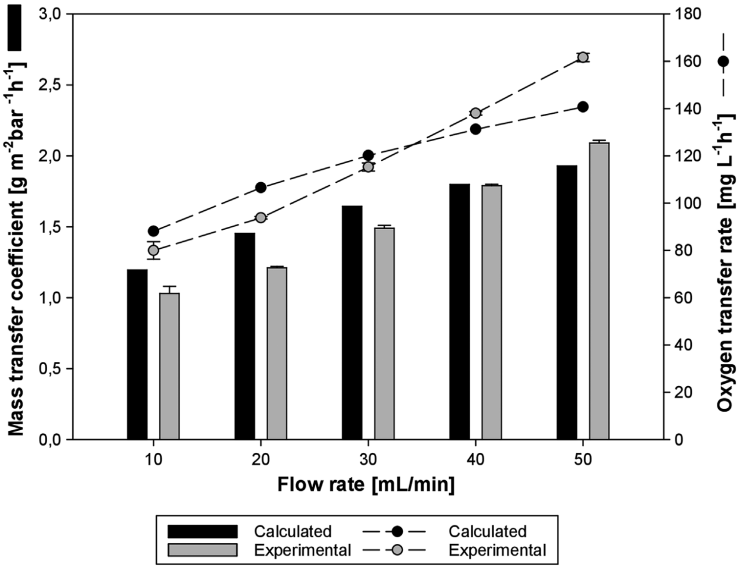

FIGURE 3 Summary of important process parameter. Comparison of oxygen transfer coefficients and rates experimentally obtained to mathematically estimated versions at different flow rates. Experimental conditions were 30°C, 35 g L^{-1} NaCl-solution as liquid medium and aeration with pure oxygen.

TABLE 1 Summary of important process parameters of the 3D-printed perfusion bioreactor.

Parameter	Unit	Value
Total volume[a]	mL	~50
Circulation flow rate	mL min^{-1}	30–50
Main flow rate	mL min^{-1}	0.25
t_{95}	s	63.3 ± 6.4
$t_{95,\ stirrer}$[b]	s	3.5 ± 0.6
Oxygen transfer rate[c]	mg/h	6.3–7.4
Oxygen mass transfer coefficient	g m^{-2} $bar^{-1}h^{-1}$	1.5–2.1
Membrane area, oxygen transfer[c]	cm^2	35.4
Membrane area, cell retention	cm^2	12.0
μ_{max}[d]	1 h^{-1}	0.34
Max. biomass concentration[d]	g L^{-1}	18.4

[a]Final volume depending on tubing length.
[b]With 300 rpm stirring speed.
[c]Determined with two liquid module parts.
[d]Determined with *C. glutamicum* ATCC 13032.

until 95% of total homogeneity is achieved. It was determined with the decolorization method described in Section 2.7. In a first configuration of the bioreactor system without stirrer, where mixing was achieved by circulation of the medium, a high mixing time of 63.3 ± 6.4 s was determined. This was due to the laminar flow conditions in the bioreactor at a circulation flow rate of 30 mL min^{-1}. To improve mixing, the magnetic stirrer and 3D-printed stirrer frame (see Figure 1C) were implemented into the bioreactor system, leading to a strongly reduced mixing time of 3.5 ± 0.6 s. The design of the stirrer resembles a plate impeller, a type of stirrer which is known to cause strong turbulences. It was placed directly above the membrane, as early perfusion experiments resulted in cells depositing on the membrane and forming a biofilm. The stirrer placement as well as the turbulences caused by it, prevented this effect. The unusual direction of the rotary axis (90°) was necessary to position the magnetic stirrer close enough to the stirring plate.

3.4 | Cultivation of *C. glutamicum* as proof-of-principle

To evaluate the suitability of the perfusion system for bacterial cultivation, a test cultivation was performed with the bacterial wildtype strain *C. glutamicum* ATCC 13032 on glucose as carbon source. In the beginning, a batch phase with 10 g L^{-1} of glucose was performed until a biomass concentration of 2.8 g L^{-1} was reached and 55% of the available glucose was consumed. At that point, a continuous feed with a flow rate of 0.25 mL min^{-1} was started, containing 5 g L^{-1} of glucose. Regarding oxygen transfer, pressurized air was initially used for diffusive oxygen transfer to prevent oxygen stress for the bacteria during the early growth phase. The circulation flow was set to 30 mL min^{-1} and the magnetic stirrer to 300 rpm. For pH control, 4 M NaOH and HCl

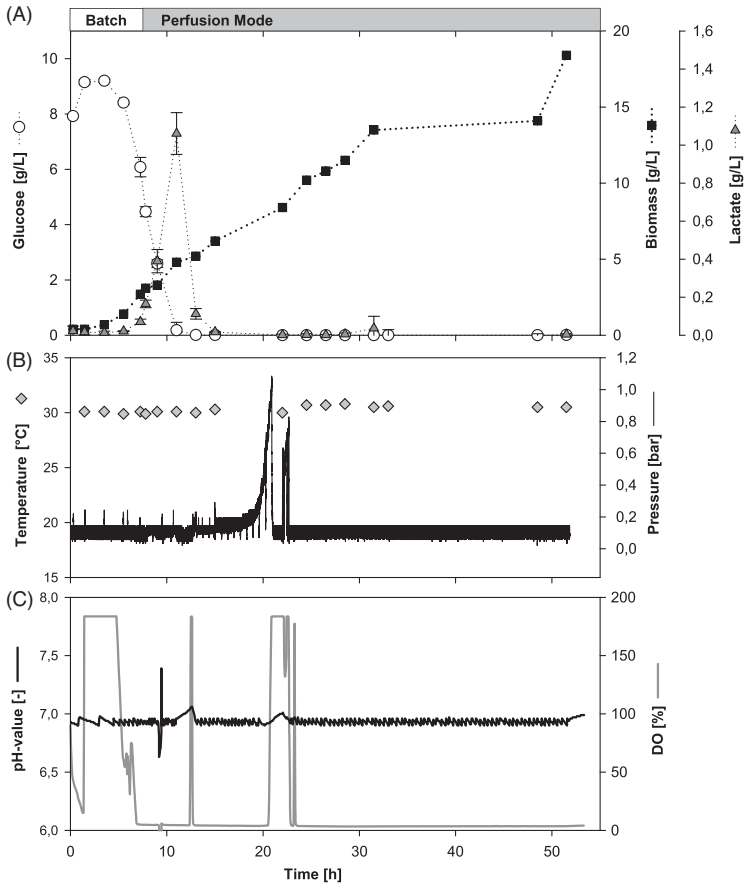

FIGURE 4 Cultivation data of a batch-perfusion hybrid cultivation of *C. glutamicum* ATCC 13032 performed in the 3D-printed perfusion bioreactor. The batch phase started with an initial glucose concentration of 10 g L^{-1}. At a biomass concentration of 3.1 g L^{-1}, the continuous feed containing 5 g L^{-1} glucose was started with a flow rate of 0.25 mL min^{-1}. Temperature was set to 30°C and pH to 7. (A) Time courses of glucose, biomass, and lactate concentration. Error bars show the standard deviation for a technical triplicate. (B) Time courses of temperature and pressure at the entrance to the bioreactor system. C) Time courses of the pH-value and DO.

were used to adjust the pH to 7.0. The time course of the cultivation data is provided in Figure 4.

While the bacteria were still adapting to the new medium composition, the air was sufficient for diffusive oxygen supply. When cell growth started after 1.4 h, the DO was quickly decreasing (Figure 4C). At a DO of 15.0%, pure oxygen was used for oxygen transfer, resulting in a DO-peak. After 4.8 h of cultivation, the DO started to decrease again and was depleted about 3.0 h later. During the time until oxygen depletion, the biomass concentration increased exponentially to 2.7 g L^{-1} (Figure 4A) with a μ_{max} of 0.34 1 h^{-1}. Overall, the oxygen supply was sufficient to allow an exponential growth until a biomass concentration of 3.3 g L^{-1} was reached after 9 h of cultivation. As quick consumption of the remaining glucose was expected after this time point, continuous feed was started with a flow rate of 0.25 mL min^{-1}. To allow strong mixing and turbulent flow conditions inside the main bioreactor module, the stirring rate was increased to 400 rpm. Growth of *C. glutamicum* continued with a gradual decrease to 0.05 1 h^{-1} until the process was stopped at a biomass concentration of 18.4 g L^{-1} after 51.5 h.

During the batch phase, growth of *C. glutamicum* resulted in a maximum biomass yield of 0.51 g g^{-1} glucose. After the feeding phase was started, the biomass yield decreased to 0.24 g g^{-1}, as oxygen depletion led to partially anaerobic conditions. This is shown by the drop in DO close to 0%. Nevertheless, the added glucose was completely consumed, as can be seen in Figure 4. Besides biomass, glucose was transformed to lactate, a side product which is typically produced

by *C. glutamicum* under anaerobic conditions.[37] In literature it was stated that *C. glutamicum* shows neglectable growth under anaerobic conditions and instead converted glucose to lactate, acetate and succinate.[38,39] While lactate was produced at the end of the batch phase during this cultivation, cell growth continued at a reduced rate of 0.05 1 h^{-1}. This suggests that cell growth was not completely under anaerobic conditions, as the oxygen transfer module still supplied the medium with oxygen, resulting in micro-aerobic conditions.

The pressure in the system is another important parameter especially for perfusion processes. During cultivations, it is a direct indicator for the degree of clogging of the cell retention membrane and thus of process stability. During the first 15 h after starting the continuous feed the pressure was stable at 0.2 bar. Subsequently, the pressure increased and peaked at 1 bar after 21 h. This peak was caused by clogging of the inlet membrane, potentially because of precipitated medium components and entrapped air bubbles. By removing the inlet membrane, the pressure could be reduced to 0.2 bar, proving that the main cell retention membrane was still free of blockage. Following this, the pressure remained constant until the end of the process after 44 h of feeding.

4 | DISCUSSION

In this work, a novel perfusion bioreactor system based on membrane diffusion for aeration and on hydrophilic flat sheet membranes for cell retention was developed using 3D-printing as manufacturing method. As described in Section 3.1 the 3D-printing materials CPE+ and ABS were selected for manufacturing different parts of the bioreactor, due to their respective mechanical stability and chemical resistances. The 10% reduction in specific growth rate μ_{max} observed in shake flask cultivations of *C. glutamicum* ATCC 13032 in presence of the different materials, was either caused by volatile additives of the plastic filaments,[40,41] or by the presence of solids and potentially hydrophobic surfaces, which is likely as all materials tested showed the same effect. Still, an observed μ_{max} of 0.36 1 h^{-1} allows for acquisition of data in a meaningful range, and the materials thus considered suitable for manufacturing the reactor.

Following the material selection, the oxygen transfer rate was evaluated, and the bioreactor's mixing time determined. For construction of the oxygen transfer module a combination of model equations for diffusive mass transfer into a moving liquid based on Fick's law and Sherwood correlations for thin channels were used. In an experiment the actual oxygen transfer rates at flow rates from 10 to 50 mL min^{-1} were determined and compared to the expected transfer rates, based on the model equations. Experimentally determined oxygen transfer rates of 80.0–161.6 mg L^{-1} h^{-1} aligned well with calculated values, showing that the model equations offer an accurate representation (Figure 3).

Regarding the mixing time, without a stirrer the mixing time t_{95} was 67 s and thus not efficient for providing a homogenous medium. To improve mixing, a magnetic stirrer encased in a 3D-printed frame was added, which reduced the mixing time to 3.5 ± 0.6 s at 300 rpm. This was comparable to commercial small scale bioreactors, which can achieve a mixing time between 5–20 s. [42] Besides a strong reduction of $t_{95,}$ the addition of the magnetic stirrer also reduced cell sedimentation and membrane fouling, as the stirrer was placed directly above the membrane. Consequently, this contributes to the ability to sustain longer process times.

The final step of the perfusion bioreactor's evaluation was a batch/perfusion hybrid cultivation of *C. glutamicum* ATCC 13032. During the batch phase, the specific growth rate μ_{max} of 0.34 1 h^{-1} was comparable to shake flask cultivations with the same medium composition in presence of 3D-printing materials (Section 3.1). Although oxygen became limiting after 7.3 h, growth continued at a reduced rate and a final biomass concentration of 18.4 g L^{-1} could be achieved after 51 h of cultivation. Furthermore, there was no clogging of the main cell retention membrane, while the pressure in the system remained constant at 0.2 bar for at least 44 h of feeding, indicating no or only limited clogging of the membrane system.

While bacterial cell growth continued even after oxygen depletion, depending on the intended application, it might be required to improve the oxygen transfer rate. This can be done by increasing the membrane area available for oxygen diffusion either by increasing the number of oxygen transfer modules or by upscaling the module and membrane size. In this respect, upscaling the module size and the size of the membrane circles used seems to be more efficient, as the increase in volume would be lower than for the other approach. Another option would be to switch to hollow fiber membranes. It should be considered however, that the use of hollow fibers would likely be more cost intensive.

In summary, a novel 3D-printed perfusion bioreactor system was presented, and its functionality demonstrated. Using a magnetic stirrer with a 3D-printed frame, homogenous medium conditions could be guaranteed in the main bioreactor, as shown by the mixing time of only 3.6 s. While a mass transfer coefficient for oxygen of 2.1 g h^{-1} m^{-2} bar^{-1} at a circulation flow rate of 50 mL min^{-1} was not enough to offer aerobic conditions above a biomass concentration of 2.7 g L^{-1}, it was still sufficient to support cell growth up to a biomass concentration of 18.4 g L^{-1} using *C. glutamicum* ATCC 13032 as model organism in a continuous cultivation experiment. Furthermore, pressure in the bioreactor remained constant at 0.2 bar even after 44 h of feeding in perfusion mode. This shows that only minor membrane fouling occurred, offering the potential for prolonged cultivation times. It should be considered however that perfusion processes come with innate disadvantages, which should be taken into account during the planning and design stage of a bioreactor system and process layout. These disadvantages include high amounts of perfused liquid and consequently diluted (extracellular) products, a potentially higher risk of contamination and a lack of data and comparable processes during the design stage of new processes. The described perfusion bioreactor system has broad application potential, from multi-component substrate-stream in a lignocellulose-based bioeconomy to in-situ product removal of potentially high-value products or even considerations of future applications for cultured meat by perfusion tissue cultures. As such, this work offers researchers a low-cost template for perfusion systems as well as a toolbox (all CAD files used or referred to in this

study are included as .stl files and described in the supporting information) with instructions for creating reference systems in different application scenarios or tailor-made bioreactor systems.

AUTHOR CONTRIBUTIONS

Manuel Merkel: Conceptualization, Methodology, Formal analysis, Validation, Investigation, Writing—Original Draft, Writing—Review & Editing, Visualization. Philipp Noll: Conceptualization, Methodology, Formal analysis, Investigation, Writing—Review & Editing. Lars Lilge: Conceptualization, Validation, Formal analysis, Writing—Review & Editing. Rudolf Hausmann: Conceptualization, Validation, Formal analysis, Writing—Review & Editing, Supervision, Funding acquisition. Marius Henkel: Conceptualization, Validation, Methodology, Formal analysis, Writing—Review & Editing, Supervision, Project administration, Funding acquisition.

ACKNOWLEDGMENTS

This study was partially funded by the Federal Ministry of Education and Research, Germany (BMBF, funding codes: 031B0673C). MM is a member of the "BBW ForWerts" graduate program funded by the Ministry of Science, Research and the Arts of Baden-Wuerttemberg (MWK).

Open access funding enabled and organized by Projekt DEAL.

CONFLICTS OF INTEREST STATEMENT

The authors declare no commercial or financial conflict of interest.

DATA AVAILABILITY STATEMENT

The data that supports the findings of this study are available in the supplementary material of this article.

ORCID

Marius Henkel https://orcid.org/0000-0002-5343-9661

REFERENCES

1. Schniederjans, D. G. (2017). Adoption of 3D-printing technologies in manufacturing: A survey analysis. *International Journal of Production Economics*, *183*, 287.
2. Melchels, F. P. W., Feijen, J., & Grijpma, D. W. (2010). A review on stereolithography and its applications in biomedical engineering. *Biomaterials*, *24*, 6121.
3. Kruth, J.-P., Levy, G., Klocke, F., & Childs, T. (2007). Consolidation phenomena in laser and powder-bed based layered manufacturing. *Cirp Annals*, *2*, 730.
4. Capel, A. J., Edmondson, S., Christie, S. D. R., Goodridge, R. D., Bibb, R. J., & Thurstans, M. (2013). Design and additive manufacture for flow chemistry. *Lab on A Chip*, *23*, 4583.
5. Gensler, M., Leikeim, A., Möllmann, M., Komma, M., Heid, S., Müller, C., Boccaccini, A. R., Salehi, S., Groeber-Becker, F., & Hansmann, J. (2020). 3D printing of bioreactors in tissue engineering: A generalised approach. *PLoS ONE*, *11*, e0242615.
6. Schmid, J., Schwarz, S., Meier-Staude, R., Sudhop, S., Clausen-Schaumann, H., Schieker, M., & Huber, R. (2018). A perfusion bioreactor system for cell seeding and oxygen-controlled cultivation of three-dimensional cell cultures. *Tissue Engineering Part C: Methods*, *10*, 585.
7. Balakrishnan, S., Suma, M. S., Raju, S. R., Bhargav, S. D. B., Arunima, S., Das, S., & Ananthasuresh, G. K. (2015). A scalable perfusion culture system with miniature peristaltic pumps for live-cell imaging assays with provision for microfabricated scaffolds. *BioRes. Open Access*, *1*, 343.
8. Smith, L. J., Li, P., Holland, M. R., & Ekser, B. (2018). FABRICA: A Bioreactor Platform for Printing, Perfusing, Observing, & Stimulating 3D Tissues. *Scientific Reports*, *1*, 7561.
9. Monaghan, T., Harding, M. J., Harris, R. A., Friel, R. J., & Christie, S. D. R. (2016). Customisable 3D printed microfluidics for integrated analysis and optimisation. *Lab on A Chip*, *17*, 3362.
10. Lockwood, S. Y., Meisel, J. E., Monsma, F. J., & Spence, D. M. (2016). A diffusion-based and dynamic 3D-printed device that enables parallel in vitro pharmacokinetic profiling of molecules. *Analytical Chemistry*, *3*, 1864.
11. Lücking, T. H., Sambale, F., Beutel, S., & Scheper, T. (2015). 3D-printed individual labware in biosciences by rapid prototyping: A proof of principle. *Engineering in Life Sciences*, *1*, 51.
12. Pantazis, A. K., Papadakis, G., Parasyris, K., Stavrinidis, A., & Gizeli, E. (2020). 3D-printed bioreactors for DNA amplification: Application to companion diagnostics. *Sensors & Actuators*, *B*, *319*, 128161.
13. Park, J., Wetzel, I., Dréau, D., & Cho, H. (2018). 3D Miniaturization of Human Organs for Drug Discovery. *Advanced Healthcare Materials*, *7*(2), https://doi.org/10.1002/adhm.201700551
14. Johnson, B. N., Lancaster, K. Z., Hogue, I. B., Meng, F., Kong, Y. L., Enquist, L. W., & McAlpine, M. C. (2016). 3D printed nervous system on a chip. *Lab on A Chip*, *8*, 1393.
15. Johansson, M., Nilsson, K., Knab, F., & Langton, M. (2022). Faba bean fractions for 3D printing of protein-, starch- and fibre-rich foods. *Processes*, *3*, 466.
16. Tejada-Ortigoza, V., & Cuan-Urquizo, E. (2022). Towards the development of 3D-printed food: A rheological and mechanical approach. *Foods*, *9*, 1191.
17. Guarino, A., Shannon, B., Marucci, L., Grierson, C., & Savery, N. (2019). A low-cost, open-source Turbidostat design for in-vivo control experiments in Synthetic Biology. *M. Di Bernardo*, *IFAC-PapersOnLine*, *26*, 244.
18. Hoffmann, S. A., Wohltat, C., Müller, K. M., & Arndt, K. M. (2017). A user-friendly, low-cost turbidostat with versatile growth rate estimation based on an extended Kalman filter. *PLoS ONE*, *7*, e0181923.
19. Zhang, B., Jiang, Y., Li, Z., Wang, F., & Wu, X.-Y. (2020). Recent progress on chemical production from non-food renewable feedstocks using Corynebacterium glutamicum. *Frontiers in Bioengineering and Biotechnology*, *8*, 606047.
20. Yaguchi, A., Spagnuolo, M., & Blenner, M. (2018). Engineering yeast for utilization of altiernative feedstocks. *Current Opinion in Biotechnology*, 122.
21. Arnold, S., Moss, K., Henkel, M., & Hausmann, R. (2017). Biotechnological perspectives of pyrolysis oil for a bio-based economy. *Trends in Biotechnology*, *10*, 925.
22. Kotz, F., Risch, P., Helmer, D., & Rapp, B. E. (2019). High-performance materials for 3D printing in chemical synthesis applications. *Advanced Materials*, *26*, e1805982.
23. Clapp, K. P., Castan, A., & Lindskog In, E. K. *Biopharmaceutical processing* (Eds: J, Günter, L, Eva, Ł, Karol, G, Parrish), Elsevier 2018, 457.
24. Whitaker, S. (1986). Flow in porous media I: A theoretical derivation of Darcy's law. *Transport in Porous Media*, *1*, 3.
25. Raveling, A. R., Theodossiou, S. K., & Schiele, N. R. (2018). A 3D printed mechanical bioreactor for investigating mechanobiology and soft tissue mechanics. *MethodsX*, 924.
26. Löffelholz, C., Husemann, U., Greller, G., Meusel, W., Kauling, J., Ay, P., Kraume, M., Eibl, R., & Eibl, D. (2013). Bioengineering parameters for single-use bioreactors: Overview and evaluation of suitable methods. *Chemie Ingenieur Technik*, *1-2*, 40.

27. Van't Riet, K. (1979). Review of measuring methods and results in nonviscous gas-liquid mass transfer in stirred vessels. *Industrial & Engineering Chemistry Process Design and Development*, *3*, 357.
28. Ramsing, N., & Gundersen, J., Seawater and Gases Tabulated physical parameters of interest to people working with microsensors in marine systems.
29. Kiefer, D., Merkel, M., Lilge, L., Hausmann, R., & Henkel, M. (2021). High cell density cultivation of *Corynebacterium glutamicum* on bio-based lignocellulosic acetate using pH-coupled online feeding control. *Bioresource Technology*, 125666.
30. Schneider, M., Reymond, F., Marison, I. W., & von Stockar, U. (1995). Bubble-free oxygenation by means of hydrophobic porous membranes. *Enzyme and Microbial Technology*, *9*, 839.
31. Ahmed, T., & Semmens, M. J. (1992). Use of sealed end hollow fibers for bubbleless membrane aeration: experimental studies. *Journal of Membrane Science*, *1–2*, 1.
32. Kreulen, H., Smolders, C. A., Versteeg, G. F., & van Swaaij, W. (1993). Microporous hollow fibre membrane modules as gas-liquid contactors. Part 1. Physical mass transfer processes. *Journal of Membrane Science*, *3*, 197.
33. Gnielinski, V.. In: Stephan, P., Mewes, D., Kabelac, S., Kind, M., Schaber, K., Wetzel, T. (eds) *VDI-Wärmeatlas*, 1.
34. Ramsing, N., & Gundersen, J. (2011). Seawater and gases tabulated physical parameters of interest to people working with microsensors in marine systems. *Unisense*, https://unisense.com/wp-content/uploads/2021/10/Seawater-Gases-table.pdf (accessed 21 February 2020)
35. Eikmanns, B. J., Metzger, M., Reinscheid, D., Kircher, M., & Sahm, H. (1991). Amplification of three threonine biosynthesis genes in *Corynebacterium glutamicum* and its influence on carbon flux in different strains. *Applied Microbiology and Biotechnology*, *5*, 617.
36. Schaepe, S., Kuprijanov, A., Sieblist, C., Jenzsch, M., Simutis, R., & Lübbert, A. (2013). kLa of stirred tank bioreactors revisited. *Journal of Biotechnology*, *4*, 576.
37. Takeno, S., Ohnishi, J., Komatsu, T., Masaki, T., Sen, K., & Ikeda, M. (2007). Anaerobic growth and potential for amino acid production by nitrate respiration in *Corynebacterium glutamicum*. *Applied Microbiology and Biotechnology*, *5*, 1173.
38. Michel, A., Koch-Koerfges, A., Krumbach, K., Brocker, M., & Bott, M. (2015). Anaerobic growth of *Corynebacterium glutamicum* via mixed-acid fermentation. *Applied and Environmental Microbiology*, *21*, 7496.
39. Nishimura, T., Vertès, A. A., Shinoda, Y., Inui, M., & Yukawa, H. (2007). Anaerobic growth of *Corynebacterium glutamicum* using nitrate as a terminal electron acceptor. *Applied Microbiology and Biotechnology*, *4*, 889.
40. Thompson, M. S. (2022). Current status and future roles of additives in 3D printing—A perspective. *Vinyl Additive Technology*, *1*, 3.
41. Min, K., Li, Y., Wang, D., Chen, B., Ma, M., Hu, L., Liu, Q., & Jiang, G. (2021). 3D printing-induced fine particle and volatile organic compound emission: An emerging health risk. *Environmental Science and Technology Letters*, *8*, 616.
42. Nienow, A. W., Rielly, C. D., Brosnan, K., Bargh, N., Lee, K., Coopman, K., & Hewitt, C. J. (2013). The physical characterisation of a microscale parallel bioreactor platform with an industrial CHO cell line expressing an IgG4. *Biochemical Engineering Journal*, *76*, 25.

SUPPORTING INFORMATION

Additional supporting information can be found online in the Supporting Information section at the end of this article.

How to cite this article: Merkel, M., Noll, P., Lilge, L., Hausmann, R., & Henkel, M. (2023). Design and evaluation of a 3D-printed, lab-scale perfusion bioreactor for novel biotechnological applications. *Biotechnology Journal*, 2200554. https://doi.org/10.1002/biot.202200554

Chapter

3 General Discussion

3.1 Introductory remarks

The topic of this work was the development of suitable process strategies and technologies for bacterial conversion of acetate as alternative, potentially more sustainable carbon source in comparison to glucose. The industrial producer *C. glutamicum* was used as model organism for utilization of acetate, because of its well-researched acetate metabolism and its capability for efficient utilization of acetate as energy source. Still, no study was available that considered *C. glutamicum* as production organism in combination with acetate as sole carbon source. Furthermore, only few studies reporting high-titer production processes with bacteria grown on acetate were available in literature, probably due to the difficulties that the inhibiting and acidic nature of acetate brings for process development (see Table 2). As such, one approach was to examine the production capability of *C. glutamicum* with acetate as sole carbon source and to develop a process strategy for efficient production using itaconic acid as exemplary product. A pH-coupled fed-batch process for feeding of glacial acetic acid, which was reported by Kiefer et al. (2021b), served as starting point and was expanded further for the specific production requirements of itaconic acid. The results for this approach are presented in chapter 2.1.

Another approach was the development of a perfusion bioreactor manufactured with the additive manufacturing method 3D-printing. Sustainable biobased production methods for acetate like electrosynthesis, C1-gas fixation or conversion of lignocellulose biomass often result in dilute concentrations, which are not suited for conventional process strategies like fed-batch, as they would lead to strong product dilution and process limitations due to the high feed volume (Kantzow et al. 2015; Marshall et al. 2013; Xinhua Shi et al. 2014). Furthermore, especially lignocellulose-based substrates often contain organic components that are harmful for bacteria (Arnold et al. 2017). A perfusion bioreactor allows utilization of dilute and inhibitor containing substrates, as the continuous flow-through in combination with cell retention allows the application of high feeding rates and prevents the accumulation of inhibitors. The results regarding the characterization of the developed perfusion bioreactor as well as a proof-of-concept study are presented in chapter 2.2.

3.2 Acetate as promising alternative carbon source

Acetate is a promising alternative to sugar-based carbon sources like glucose, which recently has gained increased attention in research as shown by several reviews (Kiefer et al. 2021a; Novak et al. 2018a). Additionally to its low cost (461 – 1019 $ per ton in the second quarter of 2023, Chemanalyst 2023) and estimated high market size of 17.9 million tons in 2023 (Mordor Intelligence 2023), it does not compete with the food and feed sector (Martín-Espejo et al. 2022), thus evading moral problems. While its production still relies mostly on petrochemical production pathways like methanol carbonylation or direct oxidation of ethane, the share of sustainably produced acetate via fermentation was already at 10% in 2015 and is expected to increase with novel sustainable production methods like syngas fermentation, conversion of lignocellulose biomass or electrosynthesis being under research (Martín-Espejo et al. 2022; Spekreijse et al. 2021).
Still, the utilization of acetate as microbial carbon source offers several challenges. The first being its inhibitory nature for most bacteria at a concentration of 5 g/L (Trček et al. 2015), which is mostly caused by unhindered diffusion of acetic acid through the cell membrane and consequential dissociation in the cytoplasm causing an uncoupling of the proton gradient necessary for generating ATP and changes of the intracellular pH (Roe et al. 2002; Herrero et al. 1985; Axe et al. 1995). This necessitates using specialised bacteria able to tolerate and grow under these conditions for bioproduction with acetate as sole carbon source.
In literature several suitable bacteria already have been identified, with *Cupriavidus necator* being an example for an efficient producer of the bioplastic PHB using acetate as sole carbon source (Vlaeminck et al. 2022; Garcia-Gonzalez et al. 2018). Another bacterium, that was shown to be able to achieve high growth rates of up to 0.52 1/h on acetate as sole carbon source is the gram-negative *Pseudomonas putida*, a model organism for bacterial PHA and rhamnolipid production (Arnold et al. 2019b). Also, the well-known industrial producer *E. coli* has been genetically enhanced for growth and production with acetate as sole carbon source in several studies, demonstrating a broad spectrum of products from organic acids to organic solvents like 2,3-butanediol or acetone (H. Yang et al. 2019; Novak et al. 2020; Huang et al. 2018). This broad array of products that can be produced with acetate as sole carbon source, is an important argument for its potential.
Still, the final titers of most production processes with acetate as sole carbon source are rather low, with only few cases that achieved titers higher than 10 g/L (see Table 2). This can partially be explained by a lack of optimized process strategies. Due to its acidic nature, conventional strategies like linear or exponential feeding are not applicable as the pH would be strongly affected. Solubility of acetate salt on the other side is rather low. Conventional feeding strategies with this solution would lead to saltification, osmotic

stress and strong dilution, which lowers growth and limits feeding capacity. An efficient strategy to feed acetate as carbon source, is to directly couple the addition of acetic acid to pH-control (Kiefer et al. 2021b). This strategy is based on the increase in pH due to the consumption of acetic acid in the protonated form and has been successfully applied for example for production of PHB by Garcia-Gonzalez und Wever (2018), for production of biomass in a high cell density process with *C. glutamicum* by Kiefer et al. (2021b) and for itaconate production with *C. glutamicum* as shown in chapter 2.1. In all these cases high product titers could be achieved, proving the efficiency of this type of feeding strategy. Further adaptations to other products combined with enhanced genetic optimization attempts will potentially help to further increase the competitiveness of acetate as carbon source in comparison to glucose.

3.3 Acetate-based production of itaconic acid with *Corynebacterium glutamicum* using an integrated pH-coupled feeding control

C. glutamicum is a bacterium that was shown to be able to utilize acetate nearly equally well for growth as glucose but has not been considered for bioproduction with acetate as sole carbon source before the start of this work (Arnold et al. 2019a). *C. glutamicum* is a gram-positive soil bacterium, that is established as industrial producer of amino acids like glutamate or lysine, but also for organic acids like lactate (J.-Y. Lee et al. 2016). Furthermore, while not possessing the GRAS status, it is generally considered as non-pathogenic save bacterium. The acetate metabolism of *C. glutamicum* is well researched (Wendisch et al. 2000; Gerstmeir et al. 2004; Cramer et al. 2007) and the bacterium has been shown to be free of inhibition at acetate concentrations of up to 10 g/L and to be able to tolerate even higher acetate concentrations in an earlier study by Arnold et al. (2019a). This observation was confirmed by a study from Kiefer et al. (2021b) where high μ_{max} of up to 0.47 1/h were determined, which was similar to μ_{max} achieved with glucose as sole carbon source. Furthermore, growth was not completely inhibited even at a concentration of 60 g/L. Besides examining growth of *C. glutamicum* on acetate, the study also presented a process strategy for feeding of acetate, where the addition of glacial acetic acid was directly coupled to pH-control. Urea as nitrogen source as well as the phosphate source were added via a secondary feed solution. With this feeding strategy, a biomass concentration of 80 g/L could be achieved. These results already demonstrate the strong capability of *C. glutamicum* for utilizing acetate as sole carbon source and its potential as model organism for production with acetate. The next step was to adapt this process strategy and utilize it for production of itaconate to evaluate *C. glutamicum*'s production capability with acetate as sole carbon source. This was the objective of the first publication (see section 2.1 for results).

In this study the strain *C. glutamicum* ICD^{R453C} (pEKEx2-*malE*cad$_{opt}$) was used for production of itaconic acid. As a first step growth and itaconic acid production was examined at different C-N ratios (2 (standard), 10, 20, 40 and 60 mole/mole) in shaking flask cultivations. From a study from Otten et al. (2015) in which a similar strain was used for production of itaconic acid on glucose, it was known that nitrogen limitation is necessary to achieve itaconic acid production with *C. glutamicum*. With the insights on how the C-N ratio effects growth and production, the earlier published pH-coupled fed-batch process for glacial acetic acid (Kiefer et al. 2021b) was expanded by a DO-coupled feeding strategy for sodium acetate and adapted to the conditions needed for growth decoupled itaconate production in a 42 L bioreactor.

The production strain *C. glutamicum* ICD^{R453C} (pEKEx2-*malE*cad$_{opt}$) was able to grow at all C-N ratios tested. At standard conditions with a C-N ratio of 2 mole/mole μ_{max} was reduced from 0.45 1/h for the wildtype strain to 0.34 1/h and further to 0.20 1/h at strong nitrogen limitation with a C-N ratio of 60 mole/mole. The reduction in μ_{max} in comparison to the wildtype strain was probably caused by the mutation of the gene *icd* and the consequentially reduced activity of the enzyme. While the glyoxylate circle is active during growth on acetate as sole carbon source, most of the carbon flux is still metabolized via the TCA-cycle to provide building blocks for growth (Wendisch et al. 2000). As expected, no itaconic acid was produced at standard conditions without nitrogen limitation. With increasing C-N ratio the $Y_{P,S}$ did also increase to a maximum of 0.03 g/g at C-N 60 mole/mole, but volumetric productivity and titer did not continue to increase at higher C-N ratios than 20 mole/mole. In the end it was decided to go for a C-N ratio of 40 mole/mole for production of itaconate in the fed-batch process, as productivity and titer were already at maximum under this condition. Furthermore, it was observed that at a C-N ratio of 60 mole/mole remaining acetate in the medium was left unconsumed, which could be a result of low viability due to the strong nitrogen limitation. The C-N ratio of 40 mole/mole was selected to prevent this effect during the fed-batch experiment, while still achieving high productivity and itaconic acid yields.

After the shake flask cultivations, the next step was to perform a fed-batch process in the 42 L bioreactor with pH-coupled feeding of acetic acid and high C-N ratios between the feeds. But consumption of the ammonium supplied at the start of the cultivation counteracted the pH increase caused by acetate consumption leading to acetate depletion, a short production phase and only low titer.

Therefore, the process strategy was expanded by a DO-coupled feeding strategy for sodium acetate, which was started once acetate got depleted for the first time leading to a rise in DO above 80%. The DO-coupled feeding of sodium acetate allowed it to supply acetate to the medium without directly effecting the pH. The continued consumption then led again to a rise in pH-value and thus continued pH-coupled feeding of glacial acetic acid. This combined pH and DO-coupled feeding strategy led to a high itaconic acid titer of 29 g/L, a high overall volumetric productivity of 0.63 g $L^{-1}h^{-1}$ and final product yield of 0.16 g/g. These results surpassed the only other bacterial itaconic acid production process with acetate as sole carbon source, which used a strain of *E. coli* as production organism (3.6 g/L itaconic acid, $Y_{P,S}$ 0.09 g/g and overall productivity of 0.04 g $L^{-1}h^{-1}$, (Noh et al. 2018)) and was even comparable to glucose-based bacterial production processes in regards to volumetric productivity (B.-J. Harder et al. 2018; Demir et al. 2021) and partially also titer (B. Harder et al. 2016). This again shows the huge potential of *C. glutamicum* as model organism for bioproduction using acetate as sole carbon source.

While productivity and titer were comparable, most production processes that used glu-

cose as sole carbon source managed to achieve 2 - 3-fold higher product yields (B. Harder et al. 2016; B.-J. Harder et al. 2018; Demir et al. 2021; Otten et al. 2015). This was partially explained by the activity of the glyoxylate shunt, that is active during growth on acetate but not on glucose as sole carbon source and represents an additional sink for isocitrate (Wendisch et al. 2000). The result is a lowered availability of aconitate, the precursor for itaconic acid production. Furthermore, the strain itself was not yet optimised genetically at this point. More recently Schmollack et al. (2022) reported an genetically optimised itaconic acid production strain for *C. glutamicum* based on the strain used in this work. The new strain *C. glutamicum* Δ*ramB* Δ*gdh* ICD^{R453C} (pEKEx2-*malE*cad$_{opt}$) included a deletion of the regulator ramB, which according to the authors led to decreased activity of the glyoxylate shunt, and deletion of the gene *gdh* which is part of the main nitrogen assimilation pathway. As a result the maximum specific growth rate of the optimized strain was strongly reduced, but the product yield increased to 0.18 g/g in shaking flask cultivations. Thus, applying the process strategy presented in this work for the new strain might lead to even more competitive results. From a process development point of view, the integrated DO and pH-coupled itaconic acid production process offers a few points of optimisation, with probably the most important being the C-N ratios in the biomass formation and production phases. By adjusting the C-N ratios depletion of acetate could be prevented and the process efficiency improved. A model-based approach in combination with a feeding program would even allow to adjust the C-N ratio during the process and adapt it to changes in the bacteria's metabolism.

In summary, while the itaconic acid yield on acetate as sole carbon source was lower than for glucose-based itaconic acid production processes, the volumetric productivity and final titer were comparable, especially since the maximum volumetric productivity was constant at 1.0 g $L^{-1}h^{-1}$ for more than 22 h of production. This shows that *C. glutamicum* has great potential as producer for itaconic acid on acetate as the sole carbon source, but also as general production organism on this carbon source. This conclusion is further supported by a recent publication that achieved production of eYFP as example for recombinant protein production on acetate (Kiefer et al. 2022). The authors even observed 83% higher biomass specific production of eYFP for acetate as carbon source in comparison to glucose.

3.4 Design and evaluation of a 3D-printed, lab-scale perfusion bioreactor for novel biotechnological applications

Most sustainable production methods for acetic acid result in rather dilute acetate concentrations of up to 59 g/L (Arnold et al. 2017; Kantzow et al. 2015). Substrates like this are not applicable for fed-batch processes like the one presented in chapter 2.1, as the low nutrient concentration would make it necessary to add high volumes of feed to the process. Furthermore, in case of lignocellulose-based acetate, the substrate solutions even contain harmful substances to varying degrees that would accumulate in the process and eventually lead to an early process end (Arnold et al. 2017). As such, it is necessary to rely on process strategies that are less commonly applied for bacterial bioproduction, namely perfusion processes. Therefore, in this study a 3D-printed perfusion bioreactor was developed, characterized and its applicability for dilute feed solutions evaluated.
As a first step, the compatibility of the materials selected for 3D-printing with cultures of *C. glutamicum* was evaluated in shaking flask cultivations on glucose as carbon source. As all materials led to the same reduction of μ_{max} to 0.36 1/h in comparison to the 0.42 1/h observed for the control, the selected materials Ultimaker CPE+ and ABS as well as the epoxy resin used for sealing the bioreactor system were considered suitable. The reduction of growth was referred to the presence of hydrophobic surfaces or to volatile 3D-printing additives (Min et al. 2021; Thompson 2022). Besides biological compatibility, the materials were also selected due to their chemical properties. Both materials were described by the manufacturer to show good chemical resistance. To be sure compatibility with a pyrolysis oil won from straw and provided by the Bioliq pilot plant in Karlsruhe was tested, by placing 3D-printed objects into the pyrolysis oil for one week and observing changes in colour, size, weight, and consistency (see supplementary materials). Besides other organic and non-organic components, the pyrolysis oil contained around 30 g/L acetate. While a change in colour was observed, changes in weight of the testobjects were between 0.1 – 0.4 g and in size below 0.5 mm. No degradation of the objects structure was visible, which was showing that the materials were suited for usage with this kind of pyrolysis oil, but also for acetate concentrations in a similar range.
Next step was the development and characterisation of the perfusion bioreactor, which consisted of a main bioreactor module that included hydrophilic PVDF membranes for cell retention, multiple connectors for pH, temperature and DO-probes as well as for sampling. Further modules of the perfusion system were an oxygen transfer system using hydrophobic PTFE membranes and a heat transfer module connected to a PID controller for temperature control. These were connected to the main bioreactor module by a circu-

lation flow. A magnetic stirrer with 3D-printed frame was placed in the main bioreactor module, with which a fast mixing time of 3.5 s could be achieved. This was sufficient to achieve a homogenously mixed medium and comparable to other small-scale bioreactors (Nienow et al. 2013).

The last step was a proof-of-concept cultivation with *C. glutamicum* and glucose as carbon source. The perfusion process was separated into two phases, a first batch phase that started at a glucose concentration of 10 g/L and a second perfusion phase, during which CGXII-medium with halved concentrations and 5 g/L glucose were used as dilute feed with a rate of 0.25 mL/min. During the batch-phase a μ_{max} comparable to the shaking flask cultivations with 3D-printing filaments was achieved. Furthermore, besides a technical failure of the syringe pumps that could be resolved, the pressure in the bioreactor was rather stable at 0.2 bar over 52 h of cultivation. This shows that only minor fouling occurred and no blockage of the membrane, even at the final cell density of 18.4 g/L. From this it could be concluded that the proof of concept was successful.

One down-side of the presented bioreactor was a rather low oxygen transfer rate, which led to oxygen limitation and micro-aerobic conditions already at a biomass concentration of 2.7 g/L. This caused formation of lactate, a typical side-product of *C. glutamicum* produced under anaerobic conditions (Michel et al. 2015), and a gradual reduction of the specific growth rate to 0.05 1/h. Thus, a next step for a follow-up project would be to optimize the oxygen transfer either by scaling up the module size and thus the membrane area or by replacing the flat-sheet membranes with hollow fibers. They offer the advantage of a high surface to volume ratio at the disadvantage of higher cost.

Regarding the application of sustainable acetate solutions, the range of expected acetate concentration is up to 59 g/L for acetate solutions produced through syngas fermentation or pyrolysis (Arnold et al. 2017; Kantzow et al. 2015). In case of hydrolysis the expected concentration is up to 15 g/L (Ko et al. 2020). All these concentrations are considered dilute. While not with acetate, the capability of the perfusion system presented here to be used with dilute substrate concentrations was demonstrated with the feed solution containing only 5 g/L glucose. The application was possible due to the successful retention of the bacterial cells inside the reactor by the hydrophilic membrane. This allowed to apply a dilution rate of 0.3 1/h (the flow rate of 0.25 mL/min divided by the total reactor volume of 50 mL), which was multiple times higher than the specific growth rate of the bacteria at the time (0.05 – 0.1 1/h). In a typical continuous bioreactor without cell retention, the cells would have been washed out of the reactor at this rate. Since the glucose concentration was at 0 g/L during the perfusion phase, the flow rate or the glucose concentration could still be increased, as all supplied glucose was completely consumed. Regarding the flow rate, care must be taken, that a higher flow rate leads to a higher back pressure caused by the cell retention membrane. To reduce the back pressure, the

membrane area must be increased.

Besides optimisation of the oxygen transfer rate, a next step would be the development of actual production processes. Preferably intracellular products should be selected since the continuous feeding would lead to strong dilution of extracellular products. Examples would be intracellular proteins or bioplastics like PHA (Kiefer et al. 2022; Garcia-Gonzalez et al. 2018). Since the 3D-printed perfusion bioreactor can be produced rather easily and fast, an interesting application would be a consecutive process, where in a first step acetate is produced either through anaerobic fermentation with acetogenic bacteria or by syngas fermentation and in a second step the produced acetate is continuously converted to a valuable product. An example for such a consecutive process would be a process reported by Oswald et al. (2016), who used acetogenic mixed culture to convert syngas to acetate and then in a follow up fermentation produced malic acid from acetate with the filamentous fungus *A. oryzae* reaching a malic acid yield of 0.22 g/g syngas.

Overall, a 3D-printed perfusion bioreactor was successfully developed, and its functionality demonstrated in a proof-of-concept cultivation with *C. glutamicum*. Although oxygen transfer was limiting and needs to be improved in future, a high biomass concentration of 18.4 g/L could be achieved. The process could be run for 52 h without the main cell retention membrane getting blocked. Instead, the pressure inside the bioreactor was stable at 0.2 bar. The CAD-files and instruction on how to create such systems, were published (Merkel et al. 2023) and should enable researchers to create reference systems in different applications by using this bioreactor system as template.

Chapter

4 Concluding remarks

This study aimed at evaluating the suitability of the industrial production organism *C. glutamicum* for bioproduction with acetate as alternative carbons source and at developing suitable process strategies for utilization of acetate. As such a novel integrated pH and DO-coupled fed-batch process for production of itaconic acid with *C. glutamicum* on acetate as sole carbon source was presented. A high titer and volumetric productivity comparable to glucose-based production processes for itaconic acid could be achieved. Still, one downside was a comparably low product yield, that should be the target for future optimization for example through genetic engineering targeting acetate uptake and the glyoxylate cycle, an additional sink for the precursor of itaconic acid. Nonetheless, the potential of *C. glutamicum* for bioproduction with acetate as sole carbon source was demonstrated for the first time and an efficient process strategy was developed.
While the fed-batch process presented was suitable for highly concentrated acetic acid, it was not suited for most cases of sustainably produced acetate due to their low concentration. To utilize those solutions, without using energy-demanding concentration steps, a perfusion bioreactor was successfully developed. The additive manufacturing method 3D-printing with the advantages of fast prototyping and design freedom was successfully used for manufacturing the perfusion reactor. While the oxygen transfer rate was leading to oxygen limitation and needs to be optimized in future, the suitability of the perfusion bioreactor for applying dilute substrate concentrations and its general functionality could be demonstrated in a proof-of-concept cultivation with *C. glutamicum* on glucose as carbon source. Future studies should focus on developing actual production processes for example in consecutive cultivations with different organisms.

References

Ahmed, Tariq and Michael J. Semmens (1992). "Use of sealed end hollow fibers for bubbleless membrane aeration: experimental studies". In: *Journal of Membrane Science* 69.1-2, pp. 1–10. DOI: 10.1016/0376-7388(92)80162-D.

Ahn, Woo Suk, Si Jae Park, and Sang Yup Lee (2001). "Production of poly(3-hydroxybutyrate) from whey by cell recycle fed-batch culture of recombinant *Escherichia coli*". In: *Biotechnology Letters* 23.3, pp. 235–240. DOI: 10.1023/A:1005633418161.

Akkoyunlu, Burcu, Sorcha Daly, and Eoin Casey (2021). "Membrane bioreactors for the production of value-added products: Recent developments, challenges and perspectives". In: *Bioresource Technology* 341, p. 125793. DOI: 10.1016/j.biortech.2021.125793.

Aloui, Hajer et al. (2022). "Enhanced co-production of medium-chain-length polyhydroxyalkanoates and phenazines from crude glycerol by high cell density cultivation of *Pseudomonas chlororaphis* in membrane bioreactor". In: *International Journal of Biological Macromolecules* 211, pp. 545–555. DOI: 10.1016/j.ijbiomac.2022.05.089.

Andrés-Barrao, Cristina et al. (2012). "Proteome analysis of *Acetobacter pasteurianus* during acetic acid fermentation". In: *Journal of Proteomics* 75.6, pp. 1701–1717. DOI: 10.1016/j.jprot.2011.11.027.

Andrés-Barrao, Cristina et al. (2016). "Metaproteomics and ultrastructure characterization of *Komagataeibacter* spp. involved in high-acid spirit vinegar production". eng. In: *Food Microbiology* 55, pp. 112–122. DOI: 10.1016/j.fm.2015.10.012.

Arnold, Stefanie et al. (2017). "Biotechnological Perspectives of Pyrolysis Oil for a Bio-Based Economy". In: *Trends in Biotechnology* 35.10, pp. 925–936. DOI: 10.1016/j.tibtech.2017.06.003.

Arnold, Stefanie et al. (2019a). "Evaluation of small organic acids present in fast pyrolysis bio–oil from lignocellulose as feedstocks for bacterial bioconversion". In: *GCB Bioenergy* 11.10, pp. 1159–1172. DOI: 10.1111/gcbb.12623.

Arnold, Stefanie et al. (2019b). "Heterologous rhamnolipid biosynthesis by *P. putida* KT2440 on bio-oil derived small organic acids and fractions". eng. In: *AMB Express* 9.1, p. 80. DOI: 10.1186/s13568-019-0804-7.

Aryal, Nabin et al. (2018). "Highly Conductive Poly(3,4-ethylenedioxythiophene) Polystyrene Sulfonate Polymer Coated Cathode for the Microbial Electrosynthesis of Acetate From Carbon Dioxide". In: *Frontiers in Energy Research* 6. DOI: 10.3389/fenrg.2018.00072.

Al-Asheh, Sameer, Marzieh Bagheri, and Ahmed Aidan (2021). "Membrane bioreactor for wastewater treatment: A review". In: *Case Studies in Chemical and Environmental Engineering* 4, p. 100109. DOI: 10.1016/j.cscee.2021.100109.

Axe, Douglas D. and James E. Bailey (1995). "Transport of lactate and acetate through the energized cytoplasmic membrane of *Escherichia coli*". In: *Biotechnology and Bioengineering* 47.1, pp. 8–19. DOI: 10.1002/bit.260470103.

Becker, Judith et al. (2011). "From zero to hero–design-based systems metabolic engineering of *Corynebacterium glutamicum* for L-lysine production". In: *Metabolic Engineering* 13.2, pp. 159–168. DOI: 10.1016/j.ymben.2011.01.003.

Bell, John et al. (2018). "EU ambition to build the world's leading bioeconomy-Uncertain times demand innovative and sustainable solutions". In: *New Biotechnology* 40.Pt A, pp. 25–30. DOI: 10.1016/j.nbt.2017.06.010.

Bertanza, Giorgio et al. (2017). "A comparison between two full-scale MBR and CAS municipal wastewater treatment plants: techno-economic-environmental assessment". In: *Environmental Science and Pollution Research International* 24.21, pp. 17383–17393. DOI: 10.1007/s11356-017-9409-3.

Blombach, Bastian and Bernhard Eikmanns (2014). "*Corynebacterium glutamicum* als Produzent von Pyruvat-abgeleiteten Produkten". In: *BIOspektrum* 20.6. PII: 504, pp. 696–699. DOI: 10.1007/s12268-014-0504-4.

Booth, Ian R. (1985). "Regulation of cytoplasmic pH in bacteria". In: *Microbiological Reviews* 49.4, pp. 359–378. DOI: 10.1128/mr.49.4.359-378.1985.

Braun, M., Frank Mayer, and Gerhard Gottschalk (1981). "*Clostridium aceticum* (Wieringa), a microorganism producing acetic acid from molecular hydrogen and carbon dioxide". In: *Archives of Microbiology* 128.3, pp. 288–293. DOI: 10.1007/BF00422532.

Brennan, Andrew J., Jerry Shevitz, and James D. Macmillan (1987). "A perfusion system for antibody production by shear-sensitive hybridoma cells in a stirred reactor". In: *Biotechnology Techniques* 1.3. DOI: 10.1007/BF00227555.

Bridgwater, Anthony V. (2012). "Review of fast pyrolysis of biomass and product upgrading". In: *Biomass and Bioenergy* 38, pp. 68–94. DOI: 10.1016/j.biombioe.2011.01.048.

Briki, Amani et al. (2020). "*Corynebacterium glutamicum*, a natural overproducer of succinic acid?" In: *Engineering in life sciences* 20.5-6, pp. 205–215. DOI: 10.1002/elsc.201900141.

Castanie-Cornet, Marie-Pierre and John W. Foster (2001). "*Escherichia coli* acid resistance: cAMP receptor protein and a 20 bp cis-acting sequence control pH and stationary phase expression of the gadA and gadBC glutamate decarboxylase genes". In:

Microbiology (Reading, England) 147.Pt 3, pp. 709–715. DOI: 10.1099/00221287-147-3-709.

Castaño-Cerezo, Sara et al. (2015). "Regulation of acetate metabolism in *Escherichia coli* BL21 by protein lysine acetylation". In: *Applied Microbiology and Biotechnology* 99.8, pp. 3533–3545. DOI: 10.1007/s00253-014-6280-8.

Chemanalyst, ed. (2023). *Acetic Acid Price Trend and Forecast*. URL: https://www.chemanalyst.com/Pricing-data/acetic-acid-9 (visited on 08/11/2023).

Chmiel, Horst, ed. (2011). *Bioprozesstechnik*. Heidelberg: Spektrum Akademischer Verlag. ISBN: 978-3-8274-2476-1. DOI: 10.1007/978-3-8274-2477-8.

Chong, Huiqing et al. (2013). "Improving acetate tolerance of *Escherichia coli* by rewiring its global regulator cAMP receptor protein (CRP)". In: *PloS One* 8.10, e77422. DOI: 10.1371/journal.pone.0077422.

Choo, Chiou-Yu et al. (2007). "High-level production of a monoclonal antibody in murine myeloma cells by perfusion culture using a gravity settler". In: *Biotechnology Progress* 23.1, pp. 225–231. DOI: 10.1021/bp060231v.

Coronel, Juliana et al. (2020). "Application of an Inclined Settler for Cell Culture-Based Influenza A Virus Production in Perfusion Mode". In: *Frontiers in Bioengineering and Biotechnology* 8, p. 672. DOI: 10.3389/fbioe.2020.00672.

Coutte, F. et al. (2017). "Recent Trends in Membrane Bioreactors". In: *Current developments in biotechnology and bioengineering. Bioprocesses, bioreactors and controls*. Amsterdam [i pozostałe]: Elsevier, pp. 279–311. ISBN: 9780444636638. DOI: 10.1016/B978-0-444-63663-8.00010-0.

Cramer, Annette and Bernhard J. Eikmanns (2007). "RamA, the transcriptional regulator of acetate metabolism in *Corynebacterium glutamicum*, is subject to negative autoregulation". In: *Journal of Molecular Microbiology and Biotechnology* 12.1-2, pp. 51–59. DOI: 10.1159/000096459.

Demir, Hatice Taşpınar et al. (2021). "High level production of itaconic acid at low pH by *Ustilago maydis* with fed-batch fermentation". In: *Bioprocess and Biosystems Engineering* 44.4, pp. 749–758. DOI: 10.1007/s00449-020-02483-6.

Demirbas, Ayhan (2007). "The influence of temperature on the yields of compounds existing in bio-oils obtained from biomass samples via pyrolysis". In: *Fuel Processing Technology* 88.6, pp. 591–597. DOI: 10.1016/j.fuproc.2007.01.010.

Deo, Yashwant M., Mina D. Mahadevan, and Renato Fuchs (1996). "Practical considerations in operation and scale-up of spin-filter based bioreactors for monoclonal antibody production". In: *Biotechnology Progress* 12.1, pp. 57–64. DOI: 10.1021/bp950079p.

Deshmukh, Gunjan and Haresh Manyar (2021). "Production Pathways of Acetic Acid and Its Versatile Applications in the Food Industry". In: *Biotechnological Applications of*

Biomass. Ed. by Thalita Peixoto Basso, Thiago Olitta Basso, and Luiz Carlos Basso. IntechOpen. ISBN: 978-1-83881-180-8. DOI: 10.5772/intechopen.92289.

Dieken, Sophia and Sandra Venghaus (2020). "Potential Pathways to the German Bioeconomy. A Media Discourse Analysis of Public Perceptions". In: *Sustainability* 12.19, p. 7987. DOI: 10.3390/su12197987.

Diekert, Gabriele and Gert Wohlfarth (1994). "Metabolism of homoacetogens". In: *Antonie van Leeuwenhoek* 66.1, pp. 209–221. DOI: 10.1007/BF00871640.

Ercan, Duygu and Ali Demirci (2015). "Current and future trends for biofilm reactors for fermentation processes". In: *Critical Reviews in Biotechnology* 35.1, pp. 1–14. DOI: 10.3109/07388551.2013.793170.

Esclade, Laurent R., Stéphane Carrel, and Paul Péringer (1991). "Influence of the screen material on the fouling of spin filters". In: *Biotechnology and Bioengineering* 38.2, pp. 159–168. DOI: 10.1002/bit.260380208.

Freeman, Cassandra A., Premsingh S. D. Samuel, and Dhinakar S. Kompala (2017). "Compact Cell Settlers for Perfusion Cultures of Microbial (and Mammalian) Cells". In: *Biotechnology Progress* 33.4, pp. 913–922. DOI: 10.1002/btpr.2533.

Gagnon, Matthew et al. (2018). "Shift to high-intensity, low-volume perfusion cell culture enabling a continuous, integrated bioprocess". In: *Biotechnology Progress* 34.6, pp. 1472–1481. DOI: 10.1002/btpr.2723.

Garcia-Gonzalez, Linsey and Heleen de Wever (2018). "Acetic Acid as an Indirect Sink of CO_2 for the Synthesis of Polyhydroxyalkanoates (PHA): Comparison with PHA Production Processes Directly Using CO_2 as Feedstock". In: *Applied Sciences* 8.9, p. 1416. DOI: 10.3390/app8091416.

Gerstmeir, Robert et al. (2003). "Acetate metabolism and its regulation in *Corynebacterium glutamicum*". In: *Journal of Biotechnology* 104.1-3, pp. 99–122. DOI: 10.1016/S0168-1656(03)00167-6.

Gerstmeir, Robert et al. (2004). "RamB, a novel transcriptional regulator of genes involved in acetate metabolism of *Corynebacterium glutamicum*". In: *Journal of Bacteriology* 186.9, pp. 2798–2809. DOI: 10.1128/JB.186.9.27982809.2004.

Ghodake, Gajanan Sampatrao et al. (2021). "Review on biomass feedstocks, pyrolysis mechanism and physicochemical properties of biochar: State-of-the-art framework to speed up vision of circular bioeconomy". In: *Journal of Cleaner Production* 297, p. 126645. DOI: 10.1016/j.jclepro.2021.126645.

Gupta, Sanjeev K. (2017). "Upstream Continuous Process Development". In: *Continuous Biomanufacturing - Innovative Technologies and Methods*. Ed. by Ganapathy Subramanian. Weinheim, Germany: Wiley-VCH Verlag GmbH & Co. KGaA, pp. 201–232. ISBN: 9783527699902. DOI: 10.1002/9783527699902.ch8.

Haas, Cornelia et al. (2017). "High cell-density production of poly(3-hydroxybutyrate) in a membrane bioreactor". In: *New Biotechnology* 37.Pt A, pp. 117–122. DOI: 10.1016/j.nbt.2016.06.1461.

Haghighi Mood, Sohrab et al. (2013). "Lignocellulosic biomass to bioethanol, a comprehensive review with a focus on pretreatment". In: *Renewable and Sustainable Energy Reviews* 27, pp. 77–93. DOI: 10.1016/j.rser.2013.06.033.

Han, Keehyun, Juan Hong, and Henry C. Lim (1993). "Relieving effects of glycine and methionine from acetic acid inhibition in *Escherichia coli* fermentation". In: *Biotechnology and Bioengineering* 41.3, pp. 316–324. DOI: 10.1002/bit.260410305.

Harder, Björn-Johannes, Katja Bettenbrock, and Steffen Klamt (2016). "Model-based metabolic engineering enables high yield itaconic acid production by *Escherichia coli*". In: *Metabolic Engineering* 38, pp. 29–37. DOI: 10.1016/j.ymben.2016.05.008.

Harder, Björn-Johannes, Katja Bettenbrock, and Steffen Klamt (2018). "Temperature-dependent dynamic control of the TCA cycle increases volumetric productivity of itaconic acid production by *Escherichia coli*". In: *Biotechnology and Bioengineering* 115.1, pp. 156–164. DOI: 10.1002/bit.26446.

Herrero, Alejandro A. et al. (1985). "Growth inhibition of *Clostridium thermocellum* by carboxylic acids: A mechanism based on uncoupling by weak acids". In: *Applied Microbiology and Biotechnology* 22.1. DOI: 10.1007/BF00252157.

Himmel, Michael E. et al. (2007). "Biomass recalcitrance: engineering plants and enzymes for biofuels production". In: *Science (New York, N.Y.)* 315.5813, pp. 804–807. DOI: 10.1126/science.1137016.

Horlamus, Felix et al. (2019). "Potential of biotechnological conversion of lignocellulose hydrolyzates by *Pseudomonas putida* KT2440 as a model organism for a bio–based economy". In: *GCB Bioenergy* 11.12, pp. 1421–1434. DOI: 10.1111/gcbb.12647.

Huang, Bing et al. (2018). "Central pathway engineering for enhanced succinate biosynthesis from acetate in *Escherichia coli*". In: *Biotechnology and Bioengineering* 115.4, pp. 943–954. DOI: 10.1002/bit.26528.

Hutkins, Robert W., ed. (2007a). *Microbiology and technology of fermented foods*. Hutkins, Robert W., (ed.) Chichester, West Sussex: John Wiley & Sons. 473 pp. ISBN: 9780470277515. DOI: 10.1002/9780470277515.

"Vinegar Fermentation" (2007b). In: *Microbiology and Technology of Fermented Foods*. Ed. by Robert W. Hutkins. Chichester, West Sussex: John Wiley & Sons, pp. 397–417. ISBN: 9780470277515. DOI: 10.1002/9780470277515.ch11.

Jo, Minji et al. (2019). "Precise tuning of the glyoxylate cycle in *Escherichia coli* for efficient tyrosine production from acetate". In: *Microbial Cell Factories* 18.1, p. 57. DOI: 10.1186/s12934-019-1106-0.

Johnson, Mark et al. (1996). "Use of the Centritech Lab centrifuge for perfusion culture of hybridoma cells in protein-free medium". In: *Biotechnology Progress* 12.6, pp. 855–864. DOI: 10.1021/bp960072n.

Jolkver, Elena et al. (2009). "Identification and characterization of a bacterial transport system for the uptake of pyruvate, propionate, and acetate in *Corynebacterium glutamicum*". In: *Journal of Bacteriology* 191.3, pp. 940–948. DOI: 10.1128/JB.01155-08.

Jönsson, Leif J. and Carlos Martín (2016). "Pretreatment of lignocellulose: Formation of inhibitory by-products and strategies for minimizing their effects". In: *Bioresource Technology* 199, pp. 103–112. DOI: 10.1016/j.biortech.2015.10.009.

Jourdin, Ludovic et al. (2015). "High Acetic acid production rate obtained by microbial electrosynthesis from carbon dioxide". In: *Environmental Science & Technology* 49.22, pp. 13566–13574. DOI: 10.1021/acs.est.5b03821.

Jung, Ilseon and Robert W. Lovitt (2010). "A comparative study of the growth of lactic acid bacteria in a pilot scale membrane bioreactor". In: *Journal of Chemical Technology & Biotechnology* 85.9, pp. 1250–1259. DOI: 10.1002/jctb.2424.

Kabisch, Johannes et al. (2013). "Metabolic engineering of *Bacillus subtilis* for growth on overflow metabolites". In: *Microbial Cell Factories* 12, p. 72. DOI: 10.1186/1475-2859-12-72.

Kacanski, Milos et al. (2022). "Cell retention as a viable strategy for PHA production from diluted VFAs with *Bacillus megaterium*". In: *Bioengineering (Basel, Switzerland)* 9.3. DOI: 10.3390/bioengineering9030122.

Kalinowski, Jörn et al. (2003). "The complete *Corynebacterium glutamicum* ATCC 13032 genome sequence and its impact on the production of l-aspartate-derived amino acids and vitamins". In: *Journal of Biotechnology* 104.1-3, pp. 5–25. DOI: 10.1016/S0168-1656(03)00154-8.

Kantzow, Christina, Alexander Mayer, and Dirk Weuster-Botz (2015). "Continuous gas fermentation by *Acetobacterium woodii* in a submerged membrane reactor with full cell retention". In: *Journal of Biotechnology* 212, pp. 11–18. DOI: 10.1016/j.jbiotec.2015.07.020.

Khomlaem, Chanin et al. (2023). "Production of polyhydroxyalkanoates and astaxanthin from lignocellulosic biomass in high cell density membrane bioreactor". In: *Chemical Engineering Journal* 451, p. 138641. DOI: 10.1016/j.cej.2022.138641.

Kiefer, Dirk et al. (2021a). "From Acetate to Bio-Based Products: Underexploited Potential for Industrial Biotechnology". In: *Trends in Biotechnology* 39.4, pp. 397–411. DOI: 10.1016/j.tibtech.2020.09.004.

Kiefer, Dirk et al. (2021b). "High cell density cultivation of *Corynebacterium glutamicum* on bio-based lignocellulosic acetate using pH-coupled online feeding control". In: *Bioresource Technology* 340, p. 125666. DOI: 10.1016/j.biortech.2021.125666.

Kiefer, Dirk et al. (2022). "High-level recombinant protein production with *Corynebacterium glutamicum* using acetate as carbon source". In: *Microbial Biotechnology* 15.11, pp. 2744–2757. DOI: 10.1111/1751-7915.14138.

Kim, Byoung Jin, Ho Nam Chang, and Duk Jae Oh (2007). "Application of a cell-once-through perfusion strategy for production of recombinant antibody from rCHO cells in a Centritech Lab II centrifuge system". In: *Biotechnology Progress* 23.5, pp. 1186–1197. DOI: 10.1021/bp0700861.

Kinoshita, Shukuo, Shigezo Udaka, and Masakazu Shimono (1957). "Studies on the amino acid fermentation". In: *The Journal of General and Applied Microbiology* 3.3, pp. 193–205. DOI: 10.2323/jgam.3.193.

Ko, Ja Kyong et al. (2020). "Improved bioconversion of lignocellulosic biomass by *Saccharomyces cerevisiae* engineered for tolerance to acetic acid". In: *GCB Bioenergy* 12.1, pp. 90–100. DOI: 10.1111/gcbb.12656.

Kornberg, Hans L. and Hans A. Krebs (1957). "Synthesis of cell constituents from C2-units by a modified tricarboxylic acid cycle". In: *Nature* 179.4568, pp. 988–991. DOI: 10.1038/179988a0.

Kövilein, Aline, Julia Umpfenbach, and Katrin Ochsenreither (2021). "Acetate as substrate for L-malic acid production with *Aspergillus oryzae* DSM 1863". In: *Biotechnology for Biofuels* 14.1, p. 48. DOI: 10.1186/s13068-021-01901-5.

Lai, Ningyu et al. (2021). "One stone two birds: Biosynthesis of 3-hydroxypropionic acid from CO_2 and syngas-derived acetic acid in *Escherichia coli*". In: *Synthetic and Systems Biotechnology* 6.3, pp. 144–152. DOI: 10.1016/j.synbio.2021.06.003.

Lange, Jean-Paul (2007). "Lignocellulose conversion: an introduction to chemistry, process and economics". In: *Biofuels, Bioproducts and Biorefining* 1.1, pp. 39–48. DOI: 10.1002/bbb.7.

Lee, Ji et al. (2018). "Efficient conversion of acetate to 3-Hydroxypropionic acid by engineered *Escherichia coli*". In: *Catalysts* 8.11, p. 525. DOI: 10.3390/catal8110525.

Lee, Joo-Young et al. (2016). "The Actinobacterium *Corynebacterium glutamicum*, an industrial workhorse". In: *Journal of microbiology and biotechnology* 26.5, pp. 807–822. DOI: 10.4014/jmb.1601.01053.

Lee, Min Ju and Pil Kim (2018). "Recombinant protein expression system in *Corynebacterium glutamicum* and its application". In: *Frontiers in Microbiology* 9, p. 2523. DOI: 10.3389/fmicb.2018.02523.

Li, Yunjie et al. (2016). "Production of succinate from acetate by metabolically engineered *Escherichia coli*". In: *ACS Synthetic Biology* 5.11, pp. 1299–1307. DOI: 10.1021/acssynbio.6b00052.

Lin, Henry et al. (2006). "Acetyl-CoA synthetase overexpression in *Escherichia coli* demonstrates more efficient acetate assimilation and lower acetate accumulation: a potential tool in metabolic engineering". In: *Applied Microbiology and Biotechnology* 71.6, pp. 870–874. DOI: 10.1007/s00253-005-0230-4.

Lokko, Yvonne et al. (2018). "Biotechnology and the bioeconomy-Towards inclusive and sustainable industrial development". In: *New Biotechnology* 40.Pt A, pp. 5–10. DOI: 10.1016/j.nbt.2017.06.005.

Lu, Peilong et al. (2013). "L-glutamine provides acid resistance for *Escherichia coli* through enzymatic release of ammonia". In: *Cell Research* 23.5, pp. 635–644. DOI: 10.1038/cr.2013.13.

Luo, Jingyang, Yinguang Chen, and Leiyu Feng (2016). "Polycyclic aromatic hydrocarbon affects acetic acid production during anaerobic fermentation of waste activated sludge by altering activity and viability of acetogen". In: *Environmental Science & Technology* 50.13, pp. 6921–6929. DOI: 10.1021/acs.est.6b00003.

Ma, Xin et al. (2021). "Boosting the microbial electrosynthesis of acetate from CO_2 by hydrogen evolution catalysts of Pt nanoparticles/rGO". In: *Catalysis Letters* 151.10, pp. 2939–2949. DOI: 10.1007/s10562-021-03537-4.

Marshall, Christopher W. et al. (2013). "Long-term operation of microbial electrosynthesis systems improves acetate production by autotrophic microbiomes". In: *Environmental Science & Technology* 47.11, pp. 6023–6029. DOI: 10.1021/es400341b.

Martín-Espejo, Juan Luis et al. (2022). "Sustainable routes for acetic acid production: Traditional processes vs a low-carbon, biogas-based strategy". In: *The Science of the Total Environment* 840, p. 156663. DOI: 10.1016/j.scitotenv.2022.156663.

Matsushita, Kazunobu et al. (2005). "*Acetobacter aceti* possesses a proton motive force-dependent efflux system for acetic acid". In: *Journal of Bacteriology* 187.13, pp. 4346–4352. DOI: 10.1128/JB.187.13.4346-4352.2005.

Merkel, Manuel et al. (2022). "Acetate-based production of itaconic acid with *Corynebacterium glutamicum* using an integrated pH-coupled feeding control". In: *Bioresource Technology* 351, p. 126994. DOI: 10.1016/j.biortech.2022.126994.

Merkel, Manuel et al. (2023). "Design and evaluation of a 3D-printed, lab-scale perfusion bioreactor for novel biotechnological applications". In: *Biotechnology Journal* 00, p. 2200554. DOI: 10.1002/biot.202200554.

Michel, Andrea et al. (2015). "Anaerobic growth of *Corynebacterium glutamicum* via mixed-acid fermentation". In: *Applied and Environmental Microbiology* 81.21, pp. 7496–7508. DOI: 10.1128/AEM.02413-15.

Min, Ke et al. (2021). "3D printing-induced fine particle and volatile organic compound emission: An emerging health risk". In: *Environmental Science & Technology Letters* 8.8, pp. 616–625. DOI: 10.1021/acs.estlett.1c00311.

Mordor Intelligence, ed. (2023). *Acetic Acid Market Size & Share Analysis - Growth Trends & Forecasts (2023 - 2028)*. URL: https://www.mordorintelligence.com/industry-reports/acetic-acid-market (visited on 08/11/2023).

Mordukhova, Elena A., Hee-Soon Lee, and Jae-Gu Pan (2008). "Improved thermostability and acetic acid tolerance of *Escherichia coli* via directed evolution of homoserine o-succinyltransferase". In: *Applied and Environmental Microbiology* 74.24, pp. 7660–7668. DOI: 10.1128/AEM.00654-08.

Mordukhova, Elena A. and Jae-Gu Pan (2013). "Evolved cobalamin-independent methionine synthase (MetE) improves the acetate and thermal tolerance of *Escherichia coli*". In: *Applied and Environmental Microbiology* 79.24, pp. 7905–7915. DOI: 10.1128/AEM.01952-13.

Mosier, Nathan et al. (2005). "Features of promising technologies for pretreatment of lignocellulosic biomass". In: *Bioresource Technology* 96.6, pp. 673–686. DOI: 10.1016/j.biortech.2004.06.025.

Mullins, Elwood A. and T. Joseph Kappock (2013). "Functional analysis of the acetic acid resistance (*aar*) gene cluster in *Acetobacter aceti* strain 1023". In: *Acetic Acid Bacteria* 2.1s, p. 3. DOI: 10.4081/aab.2013.s1.e3.

Nakano, Shigeru and Masahiro Fukaya (2008). "Analysis of proteins responsive to acetic acid in *Acetobacter*. Molecular mechanisms conferring acetic acid resistance in acetic acid bacteria". In: *International Journal of Food Microbiology* 125.1, pp. 54–59. DOI: 10.1016/j.ijfoodmicro.2007.05.015.

Nakano, Shigeru, Masahiro Fukaya, and Sueharu Horinouchi (2006). "Putative ABC transporter responsible for acetic acid resistance in *Acetobacter aceti*". In: *Applied and Environmental Microbiology* 72.1, pp. 497–505. DOI: 10.1128/AEM.72.1.497505.2006.

Napoli, Ilaria E. de et al. (2014). "Transport modeling of convection-enhanced hollow fiber membrane bioreactors for therapeutic applications". In: *Journal of Membrane Science* 471, pp. 347–361. DOI: 10.1016/j.memsci.2014.08.026.

Netzer, Roman et al. (2004). "Roles of pyruvate kinase and malic enzyme in *Corynebacterium glutamicum* for growth on carbon sources requiring gluconeogenesis". In: *Archives of Microbiology* 182.5, pp. 354–363. DOI: 10.1007/s00203-004-0710-4.

Nevin, Kelly P. et al. (2010). "Microbial electrosynthesis: feeding microbes electricity to convert carbon dioxide and water to multicarbon extracellular organic compounds". In: *mBio* 1.2. DOI: 10.1128/mBio.00103-10.

Nevin, Kelly P. et al. (2011). "Electrosynthesis of organic compounds from carbon dioxide is catalyzed by a diversity of acetogenic microorganisms". In: *Applied and Environmental Microbiology* 77.9, pp. 2882–2886. DOI: 10.1128/AEM.02642-10.

Nienow, Alvin W. et al. (2013). "The physical characterisation of a microscale parallel bioreactor platform with an industrial CHO cell line expressing an IgG4". In: *Biochemical Engineering Journal* 76, pp. 25–36. DOI: 10.1016/j.bej.2013.04.011.

Noh, Myung Hyun et al. (2018). "Production of itaconic acid from acetate by engineering acid-tolerant *Escherichia coli* W". In: *Biotechnology and Bioengineering* 115.3, pp. 729–738. DOI: 10.1002/bit.26508.

Novak, Katharina, Regina Kutscha, and Stefan Pflügl (2020). "Microbial upgrading of acetate into 2,3-butanediol and acetoin by *E. coli* W". In: *Biotechnology for Biofuels* 13, p. 177. DOI: 10.1186/s13068-020-01816-7.

Novak, Katharina and Stefan Pflügl (2018a). "Towards biobased industry: acetate as a promising feedstock to enhance the potential of microbial cell factories". In: *FEMS Microbiology Letters* 365.20. DOI: 10.1093/femsle/fny226.

Novak, Katharina et al. (2018b). "Characterizing the effect of expression of an acetyl-CoA synthetase insensitive to acetylation on co-utilization of glucose and acetate in batch and continuous cultures of *E. coli* W". In: *Microbial Cell Factories* 17.1, p. 109. DOI: 10.1186/s12934-018-0955-2.

Oasmaa, Anja et al. (2010). "Fast pyrolysis bio-oils from wood and agricultural residues". In: *Energy & Fuels* 24.2, pp. 1380–1388. DOI: 10.1021/ef901107f.

Okamoto-Kainuma, Akiko et al. (2011). "Characterization of rpoH in *Acetobacter pasteurianus* NBRC3283". In: *Journal of Bioscience and Bioengineering* 111.4, pp. 429–432. DOI: 10.1016/j.jbiosc.2010.12.016.

Okino, Shohei, Masayuki Inui, and Hideaki Yukawa (2005). "Production of organic acids by *Corynebacterium glutamicum* under oxygen deprivation". In: *Applied Microbiology and Biotechnology* 68.4, pp. 475–480. DOI: 10.1007/s00253-005-1900-y.

Oswald, Florian et al. (2016). "Sequential mixed cultures: From syngas to malic acid". In: *Frontiers in Microbiology* 7, p. 891. DOI: 10.3389/fmicb.2016.00891.

Otten, Andreas, Melanie Brocker, and Michael Bott (2015). "Metabolic engineering of *Corynebacterium glutamicum* for the production of itaconate". In: *Metabolic Engineering* 30, pp. 156–165. DOI: 10.1016/j.ymben.2015.06.003.

Pal, Parimal and Jayato Nayak (2017). "Acetic acid production and purification: Critical review towards process intensification". In: *Separation & Purification Reviews* 46.1, pp. 44–61. DOI: 10.1080/15422119.2016.1185017.

Peebo, Karl et al. (2014). "Coordinated activation of PTA-ACS and TCA cycles strongly reduces overflow metabolism of acetate in *Escherichia coli*". In: *Applied Microbiology and Biotechnology* 98.11, pp. 5131–5143. DOI: 10.1007/s00253-014-5613-y.

Price, Stuart B. et al. (2000). "Role of *rpoS* in acid resistance and fecal shedding of *Escherichia coli* O157:H7". In: *Applied and Environmental Microbiology* 66.2, pp. 632–637. DOI: 10.1128/AEM.66.2.632-637.2000.

Rajaraman, Eashwar et al. (2016). "Transcriptional analysis and adaptive evolution of *Escherichia coli* strains growing on acetate". In: *Applied Microbiology and Biotechnology* 100.17, pp. 7777–7785. DOI: 10.1007/s00253-016-7724-0.

Renilla, Sergio et al. (2012). "Acetate scavenging activity in *Escherichia coli*: interplay of acetyl-CoA synthetase and the PEP-glyoxylate cycle in chemostat cultures". In: *Applied Microbiology and Biotechnology* 93.5, pp. 2109–2124. DOI: 10.1007/s00253-011-3536-4.

Roe, Andrew J. et al. (1998). "Perturbation of anion balance during inhibition of growth of *Escherichia coli* by weak acids". In: *Journal of Bacteriology* 180.4, pp. 767–772. DOI: 10.1128/JB.180.4.767-772.1998.

Roe, Andrew J. et al. (2002). "Inhibition of *Escherichia coli* growth by acetic acid: a problem with methionine biosynthesis and homocysteine toxicity". In: *Microbiology (Reading, England)* 148.Pt 7, pp. 2215–2222. DOI: 10.1099/00221287-148-7-2215.

Salsabila, R. and M. Ilmi (2021). "Lipid production from *Zygosaccharomyces siamensis* AP1 using sequencing batch method with acetic acid as carbon source". In: *IOP Conference Series: Earth and Environmental Science* 743.1, p. 012096. DOI: 10.1088/1755-1315/743/1/012096.

Sandoval, Nicholas R. et al. (2011). "Elucidating acetate tolerance in *E. coli* using a genome-wide approach". In: *Metabolic Engineering* 13.2, pp. 214–224. DOI: 10.1016/j.ymben.2010.12.001.

Sarchami, Tahereh, Neha Batta, and Franco Berruti (2021). "Production and separation of acetic acid from pyrolysis oil of lignocellulosic biomass: a review". In: *Biofuels, Bioproducts and Biorefining* 15.6, pp. 1912–1937. DOI: 10.1002/bbb.2273.

Sauer, Uwe and Bernhard J. Eikmanns (2005). "The PEP-pyruvate-oxaloacetate node as the switch point for carbon flux distribution in bacteria". In: *FEMS Microbiology Reviews* 29.4, pp. 765–794. DOI: 10.1016/j.femsre.2004.11.002.

Schmidt, Mélodi et al. (2016). "Poly(3-hydroxybutyrate- co -3-hydroxyvalerate) production in a system with external cell recycle and limited nitrogen feeding during the production phase". In: *Biochemical Engineering Journal* 112, pp. 130–135. DOI: 10.1016/j.bej.2016.04.013.

Schmollack, Marc et al. (2022). "Metabolic engineering of *Corynebacterium glutamicum* for acetate-based itaconic acid production". In: *Biotechnology for Biofuels and Bioproducts* 15.1, p. 139. DOI: 10.1186/s13068-022-02238-3.

Senouci-Rezkallah, Khadidja, Philippe Schmitt, and Michel P. Jobin (2011). "Amino acids improve acid tolerance and internal pH maintenance in *Bacillus cereus* ATCC14579 strain". In: *Food Microbiology* 28.3, pp. 364–372. DOI: 10.1016/j.fm.2010.09.003.

Shen, Xi-Hui, Ning-Yi Zhou, and Shuang-Jiang Liu (2012). "Degradation and assimilation of aromatic compounds by *Corynebacterium glutamicum*: another potential for applications for this bacterium?" In: *Applied Microbiology and Biotechnology* 95.1, pp. 77–89. DOI: 10.1007/s00253-012-4139-4.

Shi, Xiafu et al. (2014). "Fouling and cleaning of ultrafiltration membranes: A review". In: *Journal of Water Process Engineering* 1, pp. 121–138. DOI: 10.1016/j.jwpe.2014.04.003.

Shi, Xinhua and Jie Wang (2014). "A comparative investigation into the formation behaviors of char, liquids and gases during pyrolysis of pinewood and lignocellulosic components". In: *Bioresource Technology* 170, pp. 262–269. DOI: 10.1016/j.biortech.2014.07.110.

Sieck, Jochen B., Christian Schild, and Jörg von Hagen (2017). "Perfusion formats and their specific medium requirements". In: *Continuous Biomanufacturing - Innovative Technologies and Methods*. Ed. by Ganapathy Subramanian. Weinheim, Germany: Wiley-VCH Verlag GmbH & Co. KGaA, pp. 171–200. ISBN: 9783527699902. DOI: 10.1002/9783527699902.ch7.

Singh, Nisha et al. (2022). "Global status of lignocellulosic biorefinery: Challenges and perspectives". In: *Bioresource Technology* 344, Part B, p. 126415. DOI: 10.1016/j.biortech.2021.126415.

Sleat, Robert, Robert A. Mah, and Ralph Robinson (1985). "*Acetoanaerobium noterae* gen. nov., sp. nov.: an anaerobic bacterium that forms acetate from H_2 and CO_2". In: *International Journal of Systematic Bacteriology* 35.1, pp. 10–15. DOI: 10.1099/00207713-35-1-10.

Slimane, Fatma Zohra, Fatma Ellouze, and Nihel Ben Amar (2019). "Fouling mechanism and screening of backwash parameters: Seawater ultrafiltration case". In: *Environmental Engineering Research* 24.2, pp. 298–308. DOI: 10.4491/eer.2018.165.

Song, Hun-Suk et al. (2018). "Enhanced isobutanol production from acetate by combinatorial overexpression of acetyl-CoA synthetase and anaplerotic enzymes in engineered *Escherichia coli*". In: *Biotechnology and Bioengineering* 115.8, pp. 1971–1978. DOI: 10.1002/bit.26710.

Song, Tian-Shun et al. (2017). "High efficiency microbial electrosynthesis of acetate from carbon dioxide by a self-assembled electroactive biofilm". In: *Bioresource Technology* 243, pp. 573–582. DOI: 10.1016/j.biortech.2017.06.164.

Spekreijse, Jurjen et al. (2021). *Bio-based value chains for chemicals, plastics and pharmaceuticals. A comparison of bio-based and fossil-based value chains*. Vol. 30653. EUR.

Luxembourg: Publications Office of the European Union. 1 online resource. ISBN: 978-92-76-32459-1.

Starai, Vincent J. and Jorge C. Escalante-Semerena (2004). "Identification of the protein acetyltransferase (Pat) enzyme that acetylates acetyl-CoA synthetase in *Salmonella enterica*". In: *Journal of Molecular Biology* 340.5, pp. 1005–1012. DOI: 10.1016/j.jmb.2004.05.010.

Stark, Christina et al. (2022). "The potential of sequential fermentations in converting C1 substrates to higher-value products". In: *Frontiers in Microbiology* 13, p. 907577. DOI: 10.3389/fmicb.2022.907577.

Stefanidis, Stylianos D. et al. (2014). "A study of lignocellulosic biomass pyrolysis via the pyrolysis of cellulose, hemicellulose and lignin". In: *Journal of Analytical and Applied Pyrolysis* 105, pp. 143–150. DOI: 10.1016/j.jaap.2013.10.013.

Steiner, P. and U. Sauer (2003). "Overexpression of the ATP-dependent helicase RecG improves resistance to weak organic acids in *Escherichia coli*". In: *Applied Microbiology and Biotechnology* 63.3, pp. 293–299. DOI: 10.1007/s00253-003-1405-5.

Su, Yuning et al. (2021). "Optimized process operations reduce product retention and column clogging in ATF-based perfusion cell cultures". In: *Applied Microbiology and Biotechnology* 105.24, pp. 9125–9136. DOI: 10.1007/s00253-021-11662-8.

Sun, Yirong et al. (2011). "ATP requirement for acidic resistance in *Escherichia coli*". In: *Journal of Bacteriology* 193.12, pp. 3072–3077. DOI: 10.1128/JB.00091-11.

Tajarudin, Husnul et al. (2018). "Intensive production of carboxylic acids using *C. butyricum* in a membrane bioreactor (MBR)". In: *Fermentation* 4.4, p. 81. DOI: 10.3390/fermentation4040081.

Tanaka, Y. et al. (2008). "Lysine decarboxylase of *Vibrio parahaemolyticus*: kinetics of transcription and role in acid resistance". In: *Journal of Applied Microbiology* 104.5, pp. 1283–1293. DOI: 10.1111/j.1365-2672.2007.03652.x.

Thompson, Matthew S. (2022). "Current status and future roles of additives in 3D printing—A perspective". In: *Journal of Vinyl and Additive Technology* 28.1, pp. 3–16. DOI: 10.1002/vnl.21887.

Trampler, Felix et al. (1994). "Acoustic cell filter for high density perfusion culture of hybridoma cells". In: *Bio/technology (Nature Publishing Company)* 12.3, pp. 281–284. DOI: 10.1038/nbt0394-281.

Trcek, Janja, Katarina Jernejc, and Kazunobu Matsushita (2007). "The highly tolerant acetic acid bacterium *Gluconacetobacter europaeus* adapts to the presence of acetic acid by changes in lipid composition, morphological properties and PQQ-dependent ADH expression". In: *Extremophiles : Life under extreme conditions* 11.4, pp. 627–635. DOI: 10.1007/s00792-007-0077-y.

Trcek, Janja et al. (2006). "Correlation between acetic acid resistance and characteristics of PQQ-dependent ADH in acetic acid bacteria". In: *Applied Microbiology and Biotechnology* 70.3, pp. 366–373. DOI: 10.1007/s00253-005-0073-z.

Trček, Janja, Nuno Pereira Mira, and Laura R. Jarboe (2015). "Adaptation and tolerance of bacteria against acetic acid". In: *Applied Microbiology and Biotechnology* 99.15, pp. 6215–6229. DOI: 10.1007/s00253-015-6762-3.

Vallez-Chetreanu, F. et al. (2007). "An on-line method for the reduction of fouling of spin-filters for animal cell perfusion cultures". In: *Journal of Biotechnology* 130.3, pp. 265–273. DOI: 10.1016/j.jbiotec.2007.04.007.

Veit, Andrea et al. (2009). "Pathway identification combining metabolic flux and functional genomics analyses: acetate and propionate activation by *Corynebacterium glutamicum*". In: *Journal of Biotechnology* 140.1-2, pp. 75–83. DOI: 10.1016/j.jbiotec.2008.12.014.

Vlaeminck, Elodie et al. (2022). "Advanced PHB fermentation strategies with CO_2-derived organic acids". In: *Journal of Biotechnology* 343, pp. 102–109. DOI: 10.1016/j.jbiotec.2021.11.010.

Voisard, D. et al. (2003). "Potential of cell retention techniques for large-scale high-density perfusion culture of suspended mammalian cells". In: *Biotechnology and Bioengineering* 82.7, pp. 751–765. DOI: 10.1002/bit.10629.

Walther, Jason et al. (2019). "Perfusion cell culture decreases process and product heterogeneity in a head-to-head comparison with fed-batch". In: *Biotechnology Journal* 14.2, e1700733. DOI: 10.1002/biot.201700733.

Wang, Bin, Yanchun Shao, and Fusheng Chen (2015a). "Overview on mechanisms of acetic acid resistance in acetic acid bacteria". In: *World Journal of Microbiology & Biotechnology* 31.2, pp. 255–263. DOI: 10.1007/s11274-015-1799-0.

Wang, Bin et al. (2015b). "Global insights into acetic acid resistance mechanisms and genetic stability of *Acetobacter pasteurianus* strains by comparative genomics". In: *Scientific Reports* 5, p. 18330. DOI: 10.1038/srep18330.

Wang, Pan et al. (2019). "Metabolomic insights into polyhydroxyalkanoates production by halophilic bacteria with acetic acid as carbon source". In: *Bioscience, Biotechnology, and Biochemistry* 83.10, pp. 1955–1963. DOI: 10.1080/09168451.2019.1630252.

Wang, Shurong et al. (2017). "Lignocellulosic biomass pyrolysis mechanism: A state-of-the-art review". In: *Progress in Energy and Combustion Science* 62, pp. 33–86. DOI: 10.1016/j.pecs.2017.05.004.

Wang, Yingying et al. (2007). "Quantification of the filterability of freshwater bacteria through 0.45, 0.22, and 0.1 microm pore size filters and shape-dependent enrichment of filterable bacterial communities". In: *Environmental Science & Technology* 41.20, pp. 7080–7086. DOI: 10.1021/es0707198.

Weinberger, Maria E. and Ulrich Kulozik (2022). "Understanding the fouling mitigation mechanisms of alternating crossflow during cell-protein fractionation by microfiltration". In: *Food and Bioproducts Processing* 131, pp. 136–143. DOI: 10.1016/j.fbp.2021.11.003.

Wendisch, Volker F. et al. (2000). "Quantitative determination of metabolic fluxes during coutilization of two carbon sources: comparative analyses with *Corynebacterium glutamicum* during growth on acetate and/or glucose". In: *Journal of Bacteriology* 182.11, pp. 3088–3096. DOI: 10.1128/jb.182.11.3088-3096.2000.

Wendisch, Volker F. et al. (2016). "The flexible feedstock concept in Industrial Biotechnology. Metabolic engineering of *Escherichia coli*, *Corynebacterium glutamicum*, *Pseudomonas*, *Bacillus* and yeast strains for access to alternative carbon sources". In: *Journal of Biotechnology* 234, pp. 139–157. DOI: 10.1016/j.jbiotec.2016.07.022.

Wilks, Jessica C. and Joan L. Slonczewski (2007). "pH of the cytoplasm and periplasm of *Escherichia coli*: rapid measurement by green fluorescent protein fluorimetry". In: *Journal of Bacteriology* 189.15, pp. 5601–5607. DOI: 10.1128/JB.00615-07.

Wolfe, Alan J. (2005). "The acetate switch". In: *Microbiology and Molecular Biology Reviews* 69.1, pp. 12–50. DOI: 10.1128/MMBR.69.1.1250.2005.

Wong, H. Edward et al. (2022). "From chemostats to high-density perfusion: the progression of continuous mammalian cell cultivation". In: *Journal of Chemical Technology & Biotechnology* 97.9, pp. 2297–2304. DOI: 10.1002/jctb.6841.

Woźniak, Ewa, Agata Tyczewska, and Tomasz Twardowski (2021). "Bioeconomy development factors in the European Union and Poland". In: *New Biotechnology* 60, pp. 2–8. DOI: 10.1016/j.nbt.2020.07.004.

Xiao, Yi et al. (2013). "Engineering *Escherichia coli* to convert acetic acid to free fatty acids". In: *Biochemical Engineering Journal* 76, pp. 60–69. ISSN: 1369703X. DOI: 10.1016/j.bej.2013.04.013.

Xu, Hao et al. (2020). "A Simple method to identify the dominant fouling mechanisms during membrane filtration based on piecewise multiple linear regression". In: *Membranes* 10.8. ISSN: 2077-0375. DOI: 10.3390/membranes10080171.

Xu, Xin, Mo Xian, and Huizhou Liu (2017). "Efficient conversion of acetate into phloroglucinol by recombinant *Escherichia coli*". In: *RSC Advances* 7.80, pp. 50942–50948. DOI: 10.1039/c7ra09519h.

Xu, Xin et al. (2018). "Microbial production of mevalonate by recombinant *Escherichia coli* using acetic acid as a carbon source". In: *Bioengineered* 9.1, pp. 116–123. DOI: 10.1080/21655979.2017.1323592.

Yabannavar, V. M., V. Singh, and N. V. Connelly (1992). "Mammalian cell retention in a spinfilter perfusion bioreactor". In: *Biotechnology and Bioengineering* 40.8, pp. 925–933. DOI: 10.1002/bit.260400809.

Yang, Hao et al. (2019). "Metabolic engineering of *Escherichia coli* carrying the hybrid acetone-biosynthesis pathway for efficient acetone biosynthesis from acetate". In: *Microbial Cell Factories* 18.1, p. 6. DOI: 10.1186/s12934-019-1054-8.

Yang, Jianming and Qingjuan Nie (2016). "Engineering *Escherichia coli* to convert acetic acid to caryophyllene". In: *Microbial Cell Factories* 15, p. 74. DOI: 10.1186/s12934-016-0475-x.

Yang, Songyuan, Suhang Li, and Xiaoqiang Jia (2019). "Production of medium chain length polyhydroxyalkanoate from acetate by engineered *Pseudomonas putida* KT2440". In: *Journal of Industrial Microbiology & Biotechnology* 46.6, pp. 793–800. DOI: 10.1007/s10295-019-02159-5.

Yu, Linpeng et al. (2017). "Thermophilic *Moorella thermoautotrophica*-immobilized cathode enhanced microbial electrosynthesis of acetate and formate from CO_2". In: *Bioelectrochemistry (Amsterdam, Netherlands)* 117, pp. 23–28. DOI: 10.1016/j.bioelechem.2017.05.001.

Zhang, Dalong et al. (2014). "Reducing lactate secretion by *ldhA* Deletion in L-glutamate-producing strain *Corynebacterium glutamicum* GDK-9". In: *Brazilian Journal of Microbiology : [Publication of the Brazilian Society for Microbiology]* 45.4, pp. 1477–1483. DOI: 10.1590/s1517-83822014000400044.

Zhang, Jing et al. (2022). "Adaptive Laboratory Evolution of *Halomonas bluephagenesis* Enhances Acetate Tolerance and Utilization to Produce Poly(3-hydroxybutyrate)". In: *Molecules (Basel, Switzerland)* 27.9. DOI: 10.3390/molecules27093022.

Zhang, Shasha et al. (2019). "Metabolic engineering for efficient supply of acetyl-CoA from different carbon sources in *Escherichia coli*". In: *Microbial Cell Factories* 18.1, p. 130. DOI: 10.1186/s12934-019-1177-y.

Zhang, Wei et al. (2013). "Three lignocellulose features that distinctively affect biomass enzymatic digestibility under NaOH and H_2SO_4 pretreatments in Miscanthus". In: *Bioresource Technology* 130, pp. 30–37. DOI: 10.1016/j.biortech.2012.12.029.

Zhao, Hanjun et al. (2018). "The soluble transhydrogenase UdhA affecting the glutamate-dependent acid resistance system of *Escherichia coli* under acetate stress". In: *Biology Open* 7.9. DOI: 10.1242/bio.031856.

Appendix

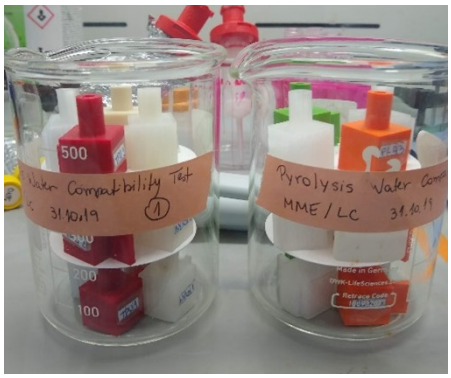

Figure S1: Arrangement of a set of 3D-printed objects for examining compatibility with an aqueous fraction of a pyrolysis oil.

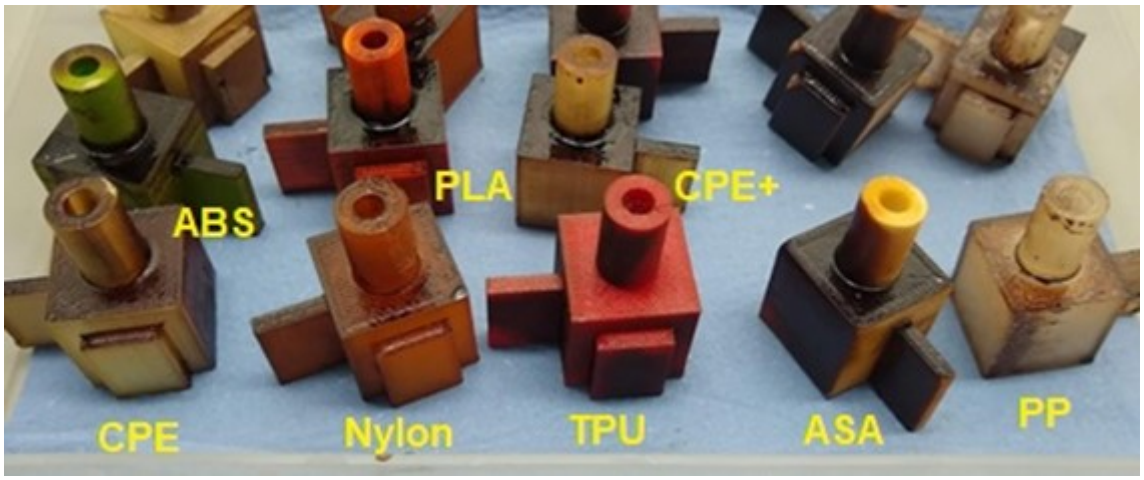

Figure S2: 3D-printed objects consisting of different materials after immersion in an aqueous condensate of a pyrolysis oil for one week at room temperature (RT). The tested 3D-printing materials were Ultimaker ABS, polylactidacid (PLA), CPE+, CPE, Nylon, thermoplastic polyurethane (TPU), polypropylene (PP) (Ultimaker BV, Utrecht, The Netherlands)and BASF Ultrafuse acrylonitrile styrene acrylate (ASA) (BASF 3D Printing Solutions GmbH, Heidelberg, Germany). After drying the objects were examined optically, weighted and their sizes measured.

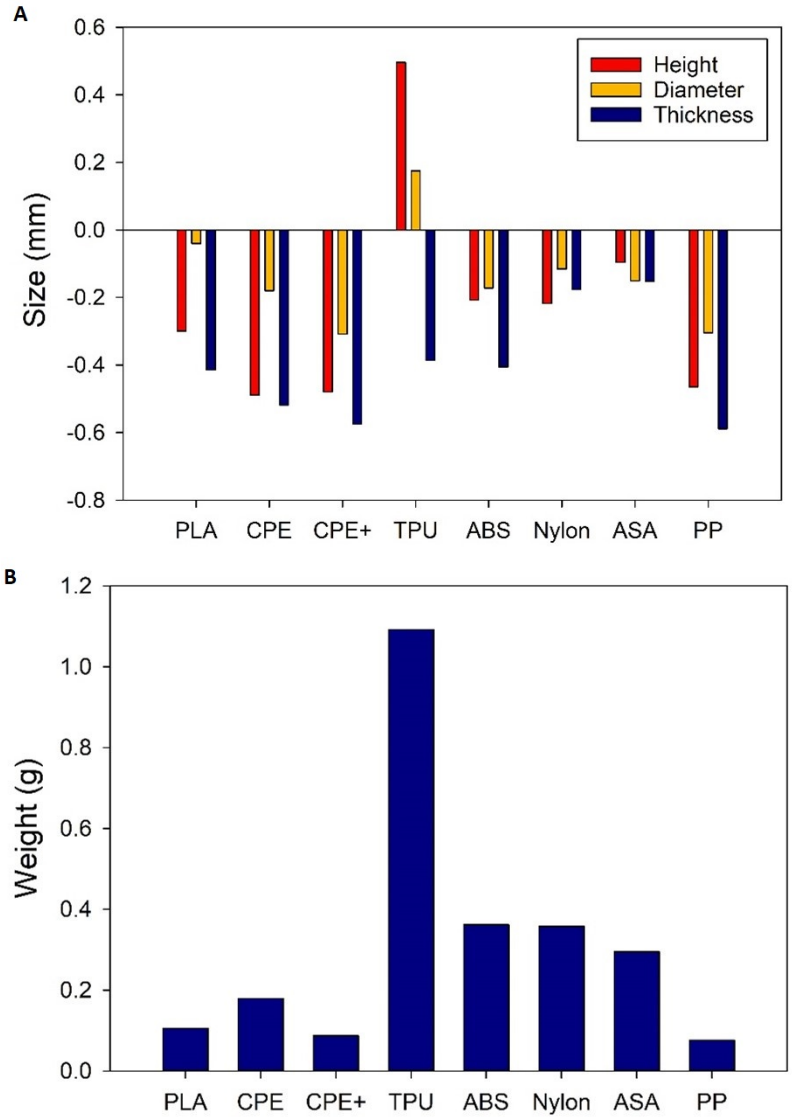

Figure S3: Graphs showing the change in size (**A**) and weight (**B**) of 3D-printed objects after immersion in the aqueous condensate of a pyrolysis oil for one week at RT. The objects are shown in figure S1 (before immersion) and S2 (after immersion). The changes were determined after drying the objects at RT.